



Universität für Bodenkultur Wien

FLOOD RISK ANALYSIS: RESIDUAL RISKS AND UNCERTAINTIES IN AN AUSTRIAN CONTEXT

Rudolf Faber

Dissertation
for obtaining a doctorate degree
at the University of Natural Resources and Applied Life
Sciences, Vienna

Advisor: Prof Dr Hans-Peter Nachtnebel

Department of Water, Atmosphere and Environment
Institute of Water Management, Hydrology and Hydraulic
Engineering

Vienna, December 2006

Acknowledgements

First, let me thank Prof Nachtnebel for giving me the chance to join the Institute of Water Management, Hydrology and Hydraulic Engineering at the University of Natural Resources and Applied Life Sciences, Vienna. He has encouraged my research on flood risks, which turned into a major issue a year after my commencement. His scientific advice and his willingness to let me take a time-out enabled me to complete this dissertation.

I would then like to recognise numerous colleagues at the Institute for their technical advice, good talks and plentiful outdoor and after-work activities that I will keep in mind. I give big credit to Alexander Debene, Christoph Hauer, Michael Heufelder, Roland Herndler, Sonja Hofbauer, Hubert Holzmann, Harald Kling, Klaus Lerach and Matthias Weissgram, just to name a few.

I would also like to acknowledge IIASA's Keith Compton and Joanne Linnerooth-Bayer for the interesting and collegial partnership in a multidisciplinary study that extended my understanding of risk and at last let me travel to Japan.

My research over the last five years was funded by numerous organisations, which I am grateful to. These are the Austrian Science Fund FWF, the European Union, the Austrian Federal Ministry of Transport, Innovation and Technology, the Austrian Federal Ministry of Agriculture, Forestry, Environment and Water Management and the Governments of the provinces of Styria and Upper Austria.

A special thanks goes to Ross Woods at the National Institute of Water and Atmospheric Research in Christchurch, New Zealand for his interest in my work and for being a kind host. Within his group, I highly appreciate the help of my office mates Gaby Turek and Jordy Hendrix.

I also thank Suzanne Ebert and Ross Woods for their corrections.

And of course, I acknowledge the support of my parents. It was my mother, who told me to enjoy some spare time today, as everyday working life might not offer this chance tomorrow.

Finally, I am deeply obliged to my partner Sonja Ebner for her advice in scientific writing, for her help in managing the references and for sharing good and hard times while I wrote this dissertation.

Abstract

Since technical flood protection systems are limited in their resistance, the sensible values in protected areas are exposed to a residual flood risk. This dissertation aimed to demonstrate by means of two case studies how such flood events can be evaluated by scenarios and how the consequences can be analysed.

The first case study focused on the former floodplain of the Raab River in the Gleisdorf region, located in the Austrian province of Styria. The analysis based on a set of rainfall-runoff scenarios, on two dimensional inundation flow-simulations and other hydraulic models and on the estimation of monetary flood losses. At the largest of the computed flood scenarios the damage costs to buildings ranged up to several tens of Million Euros. But since such extreme scenarios were assigned with low probabilities, the expected annual losses were estimated by a magnitude of 0.1 percent of the maximum losses.

The second case study analysed the flash flood risk to a particular open subway stretch at the Wien River bank, located in the City of Vienna. Here, the hydrologic and hydraulic loads as well as the system resistance were modelled as stochastic parameters. The statistical spread in the peak flow frequency was considerably exceeding the variability in the channel flow processes. But the largest data scattering was associated with the loss estimation. The computations showed that the recently completed upgrades of the flood retention schemes reduced the probability of failure by a factor of approximately two. In the current system, the probability of failure was about 0.1 percent per year. Finally, the mobile flood barriers were most important for preventing large financial losses, as their reliability significantly reduced the expected annual damage costs.

Finally, suggestions on the future analysis of flood risks and residual risks were derived from the elaboration of the methodology and the findings of the case studies.

Keywords: Flood risk analysis, residual risk, flood hazard, flood losses

Kurzfassung (Abstract, German)

Da die Belastbarkeit von technischen Hochwasserschutzmaßnahmen begrenzt ist, besteht für sensible Nutzungen in geschützten Gebieten ein von Überflutungen ausgehendes Restrisiko. Die gegenständliche Arbeit zeigt anhand von zwei Fallstudien auf wie Überlastungsfälle in Form von Szenarien formuliert, und wie die Folgen beurteilt werden können.

Die erste Fallstudie untersuchte jene Bereiche um die Stadt Gleisdorf in der Steiermark, die durch Hochwässer der Raab betroffen sein können. Die Analyse basierte auf der Definition von Niederschlag-Abfluss-Szenarien, der zweidimensionalen Überflutungsberechnung und anderen hydraulischen Beurteilungsmethoden, sowie der Abschätzung von monetären Hochwasserschäden. Für das größte modellierte Szenario ergab die Berechnung eine Schadenssumme an Gebäuden in zweistelliger Euro-Millionenhöhe. Durch die geringe Wahrscheinlichkeit solcher Ereignisse lagen die mittleren jährlichen Schadenskosten im Bereich eines Tausendstels der größten errechneten Verluste.

Die zweite Fallstudie widmete sich dem Überflutungsrisiko eines U-Bahn Abschnittes am Ufer des Wienflusses in Wien, wobei sowohl die hydrologisch-hydraulische Belastung als auch die Hochwasser-Abfuhrkapazität mittels wahrscheinlichkeitsverteilten Größen modelliert wurden. Die Schwankungsbreite der Hochwasser-Häufigkeit lag dabei wesentlich über jener der Abflusskapazität des Flusslaufes. Die größten Unsicherheiten brachte jedoch die Schadensschätzung mit sich. Die Berechnungen zeigten, dass die neulich abgeschlossene Adaptierung der Hochwasser-Rückhalteinrichtungen die Versagenswahrscheinlichkeit etwa um die Hälfte reduzierte. Sie lag für den derzeitigen Systemzustand im Bereich eines Tausendstels pro Jahr. Letztlich stellten sich die mobilen Sperren im U-Bahn System als wesentlich für die Verhinderung großer Schäden heraus. Deren Wirksamkeit konnte den Schadensersparungswert erheblich verringern.

Aus der Erarbeitung der Methode und den Erkenntnissen beider Fallstudien wurden abschließend Anregungen zur Analyse des Hochwasserrisikos und im Besonderen des Restrisikos abgeleitet.

Schlüsselwörter: Hochwasserrisikoanalyse, Restrisiko, Hochwassergefährdung, Hochwasserschäden

Table of contents

1	Introduction	11
1.1	Structure of the dissertation	11
1.2	Definition of terms	12
1.3	Background	15
1.3.1	Hazard analysis	15
1.3.2	Loss analysis	16
1.3.3	Risk quantification	18
1.3.4	Design procedures for flood protection schemes	20
1.3.5	Uncertainties	22
1.4	Problem statement	24
1.5	Aims and objectives	25
1.5.1	Defining the scope	27
2	Methodology	29
2.1	Hazard identification	29
2.2	Scenario definition	29
2.3	Loss analysis	30
2.4	Modelling approaches	30
2.4.1	Deterministic approach	31
2.4.2	Stochastic approach	31
3	Case study 1: Application	35
3.1	System description	35
3.2	Hazard identification	37
3.3	Scenario definition	38
3.4	Hydrologic analysis	39
3.4.1	Analysis of extreme rainfall patterns	39
3.4.2	Design rainfall	39
3.4.3	Rainfall runoff modelling	42
3.4.4	Probability estimation of peak flows	42
3.4.5	Selection of hydrographs	43
3.5	Hydraulic analysis	44
3.5.1	Scenarios without technical or operational failure	44
3.5.2	Bridge jam scenario	46
3.5.3	Levee failure scenario	47
3.5.4	Failure scenario of weirs	47
3.5.5	Bank vegetation scenarios	48
3.5.6	Flood retention basin failure scenarios	49

3.5.7	Hinterland inundation scenarios	50
3.6	Loss analysis	51
3.6.1	Direct loss analysis	51
3.6.2	Loss analysis for the industrial and the commercial sector	54
3.7	Risk quantification	55
4	Case study 1: Results	57
4.1	Hydrologic analysis	57
4.1.1	Analysis of extreme rainfall patterns	57
4.1.2	Design rainfall	59
4.1.3	Rainfall runoff modelling	61
4.1.4	Probability estimation of peak flows	63
4.2	Hydraulic analysis	65
4.2.1	Scenarios without technical and operational failure	65
4.2.2	Bridge jam scenario	67
4.2.3	Levee failure scenario	67
4.2.4	Failure scenario of weirs	67
4.2.5	Bank vegetation scenarios	68
4.2.6	Flood retention basin failure scenarios	70
4.2.7	Hinterland inundation scenarios	71
4.2.8	Conclusions on the hydraulic analysis	71
4.3	Loss analysis	72
4.3.1	Direct loss analysis	72
4.3.2	Loss analysis for the industrial and the commercial sector	74
4.4	Risk quantification	76
4.4.1	Risk quantification for scenarios without technical and operational failure	76
4.4.2	Risk quantification considering structural and operational failure	78
5	Case study 2: Application	81
5.1	System description	81
5.2	Hazard identification	84
5.3	Definition of scenarios	86
5.3.1	Stochastic modelling algorithm	87
5.4	Hydrologic analysis	89
5.4.1	Design rainfall	89
5.4.2	Rainfall runoff modelling	91
5.4.3	Flow statistics	92
5.5	Hydraulic analysis	93
5.5.1	Deterministic 1D water surface model	93
5.5.2	Hydraulic basic random parameters	96

5.5.3	Reliability and probability of failure	96
5.6	Loss analysis	98
5.6.1	Direct loss analysis	98
5.7	Risk quantification	100
6	Case study 2: Results	101
6.1	Hydrologic analysis	101
6.2	Hydraulic analysis	103
6.2.1	The resistance	103
6.2.2	The load	104
6.2.3	The reliability and the probability of failure	105
6.3	Loss analysis and risk quantification	107
6.4	Evaluation of uncertainties	108
7	Summary and discussion	109
7.1	Hazard analysis	109
7.2	Loss analysis	111
7.3	Risk quantification	112
7.4	Risk management	113
7.5	Deterministic and stochastic approaches	114
8	Conclusions	115
9	References	117
10	Index of tables	127
11	Index of figures	129
12	Appendix: Inundation maps of case study 1	131
13	Table of abbreviations and variables	139
14	Curriculum vitae	143

1 Introduction

This chapter first comprises the structure of the dissertation and the definition of terms. Second, it reviews the tasks of flood hazard analysis, of loss analysis and of risk quantification. Then, the design procedures for flood protection schemes, and uncertainties related to the analysis of risks are outlined. Based on this background specific problems are stated, the aims and objectives are presented and finally, the scope of this work is defined.

1.1 Structure of the dissertation

The first part of this dissertation introduces the research. It details the methodology by presenting the tasks applied to analyse flood risks. It also describes the implemented deterministic and stochastic approaches.

Chapter 1: Introduction

Chapter 2: Methodology

The second part presents the application of the methodology to two case studies and the specific results.

Chapter 3: Case study 1: Application

Chapter 4: Case study 1: Results

Chapter 5: Case study 2: Application

Chapter 6: Case study 2: Results

The third part summarises and discusses the outcomes of the case studies and draws conclusions from these findings.

Chapter 7: Summary and discussion

Chapter 8: Conclusions

The fourth part contains the references, the indices of figures and tables and the appendix. It also explains the variables and abbreviations used.

1.2 Definition of terms

The following passages present the working definitions of the basic terms in an alphabetical order. Related terms and also partly diverging definitions are summarised in glossaries and publications of BUWAL (1999a), the Bureau of Reclamation (2004), the Society for Risk Analysis (2004), the NOAA Coastal Service Centre (2006) and USEPA (2006), to name a few.

Consequences

Consequences are the result of vulnerable elements being exposed to the materialisation of a specific hazard. As such, it is always a concrete damage, like a number of persons killed or a property destroyed (Ale 2002). The consequences of floods are manifold – mostly negative today, but also positive. This dissertation focused on adverse impacts. The terms consequences, damages and losses are used synonymously.

Exposure

Exposure characterises the number of people and the value of objects and activities that may be adversely impacted by hazards (Darlington and Lambert 2001, Hollenstein 2005). In this dissertation, exposure describes the spatial and temporal relation of the elements at risk to the event occurring, for instance where a building is located in the floodplain.

Hazard

In the context of his work, hazards are defined as possible flood conditions with the potential for adverse consequences. Hazards indicate the appearance of a peril, for instance an inundation described as a flood depth and a flow velocity. Aspects of exposure and vulnerability are not considered in the hazard term, since it focuses on the event or physical condition (Ale 2002, Bureau of Reclamation 2004).

Reliability

Reliability describes the probability that a device will function without failure over a specified time period or amount of usage (Bureau of Reclamation 2004). Consequently, the reliability and the probability of failure add up to one. The probability of failure may directly be used for quantifying risk (Jonkman et al. 2003).

Residual risk

This dissertation follows the definition of BUWAL (1999a), Plate (2002) and Merz (2006), who describe the residual risk as the remaining part of the risk after implementing a protection system. The residual risk covers the accepted risk, the unknown risk and the risk due to false judgement or inadequate countermeasures and decisions.

In contrast, the new Austrian guidelines for the Federal River Administration, named RIWA-T (BMLFUW 2006a), defines residual risk as the probability of a technical or a human-induced failure of a flood protection system that occurs within a specified time horizon (German: Restrisiko). This guideline further introduces the term 'increased risk' (German: Erhöhtes Risiko) as the probability of an event larger than the design magnitude occurring within a time horizon (See risk quantification).

Risk

Risk in the context of this work is defined as a combination of the consequences of a flood event and its occurrence probability (Ale 2002 p.109). The consequences may arise in a social, economic and environmental dimension and may therefore affect individuals or the society. According to BUWAL (1999a), Plate (2002) and Merz and Thieken (2004), risk consists of:

- A possible natural hazard X
- Its probability of occurrence $p(x)$
- The consequences of the event $L(x)$

Following Ale (2002), this dissertation distinguishes between the risk itself and the metrics and indices used for its quantification.

Risk analysis

Risk analysis is the systematic task to characterise and to quantify risks as far as possible (BUWAL 1999a). Vrouwenvelder et al. (2001) further describe:

- Qualitative analysis: definition of the system and the scope, identification and description of the hazards, failure modes and scenarios.
- Quantitative analysis: determination of the probabilities and consequences of the defined events. Quantification of the risk in a risk number or a graph as a function of probabilities and consequences.

The risk analysis may anticipate potential future events (ex-ante) or may focus on historic events (ex-post). The tasks of a quantitative risk analysis in this work are:

- System description
- Hazard identification
- Scenario definition
- Hazard analysis comprising hydrologic and hydraulic analysis
- Loss analysis
- Risk quantification

Risk assessment

Risk assessment in the context of this work is used synonymously with risk valuation (Kienholz et al. 2004) and risk evaluation (Mock 2001). The task of risk assessment is to judge whether risks, as results of the risk analysis, are acceptable from an individual or a societal viewpoint. Risk assessment is based on the perception and awareness of risks. Slovic (2001 p.23) describes this task as “Risk assessment is inherently subjective and represents a blending of science and judgment with important psychological, social, cultural, and political factors”.

Risk management

Risk management is discussed for instance in Plate (2002) as systematic action in operating a system and in the planning-, design and revision stage for a new a system. The steps of

risk management may be summarised as (Plate and Merz 2001, Vrouwenvelder et al. 2001, Ale 2002, Nachtnebel 2003, Habersack et al. 2004, Kienholz et al. 2004):

- Risk analysis, comprising identification and quantification of risks
- Risk assessment: evaluation of risks on grounds of the results of the former analysis.
- Decisions
- Risk reduction, risk transfer or risk acceptance
- Event management and regeneration

Risk quantification

Ale (2002) emphasises the difference between the risk itself and the metrics and indices used for its quantification. The literature provides numerous of these measures and metrics for quantifying risks (Jonkman et al. 2003, Kelman 2003). A widely used risk measure characterises the risk as the product of the probability of an event and its consequences (UNDHA 1992, Helm 1996, Sayers et al. 2002).

In contrast, 'hydrologic risk' (Chow 1988 et al., DIN 1996) specifies the probability of an event larger than the design level occurring within a defined time period. The new Austrian guidelines for the Federal River Engineering Administration (BMLFUW 2006a) follow this interpretation and define 'risk' in the sense of 'hydrologic risk' without considering potential consequences.

Scenario

A scenario is a hypothetical sequence of events. Scenarios represent the basic units for analysing hazards (BUWAL 1999a). For analysing a large number of possible flood events, a representative distinct set of scenarios is investigated in detail (Van Manen and Brinkhuis 2005). In this dissertation, flood scenarios are investigated by hydrologic and hydraulic analysis.

Vulnerability

The term vulnerability characterises the degree of the negative consequences arising from a hazard impact. In the context of this work, vulnerability is used in a quantitative way, whereas Hollenstein (2005) also found Boolean-kind vulnerability interpretations in his review, indicating if a value is hit or not hit.

1.3 Background

As the background for this dissertation, first, the tasks of hazard analysis, loss analysis and the quantification of risks are reviewed. Then, the design procedures for flood protection schemes and how they consider flood risks are discussed. Finally, uncertainties related to the analysis of flood risks are presented.

1.3.1 Hazard analysis

In Austria, flood hazard investigations have mainly focused on events like a 10, 30 or 100-year flood. This implies that the inundation scenario under study would return on a statistical average every 10, 30 or 100 years. The perception of possible inundation risks and the planning of technical protection systems are often directly linked to these flood events. Now, the practice of analysing up to 100-year floods is criticised as incomplete (Merz and Thieken 2004, Merz 2006), and reconsiderations accentuate the need for investigating and managing larger flood scenarios on Austrian rivers (Habersack et al. 2004, BMLFUW 2006a).

The analysis of flood hazards is based on the hydrologic determination of flood discharges and the hydraulic analysis, which determines the flood depths, the flow velocities, the erosion- and sedimentation processes, the interrelations with structures and other parameters. Since methods for the hydrologic and hydraulic analysis are well described in the literature, two current Austrian issues in the field of flood hazard analysis are discussed here: flood hazard zoning and the design rainfall.

1.3.1.1 Flood hazard zones

In order to delineate areas of flood-related perils on a detailed scale, flood hazard zones have been elaborated for Austrian rivers since the early 1970s (Aigner et al. 2002). A red and a yellow zone are used to map flood-related threats. Hazard zones at rivers are determined from a 100-year design event, whereas hazard zones at torrents base on a 150-year event (see Figure 2.1 for the yellow / red criteria).

The current discussion focuses on the introduction of an additional 'residual flood hazard zone'. This zone shall base on *up to 300-year events* or on flood scenarios resulting from failures of technical protection structures (Faber et al. 2004a, BMLFUW 2006b, Hinterleitner 2006). In contrast, the Swiss system defines the residual hazard zone by a *300-year or larger flood* (BWW et al. 1997). Other approaches work with a simulated extreme scenario or add 0.5 to 1.0 metres to the water level of an observed maximum or the computed 100-year event (Rodriguez + Zeisler et al. 2001, Kleeberg 2005).

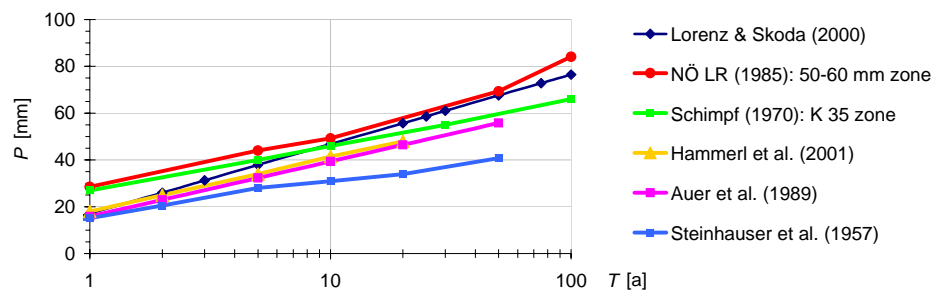
Discussing the most appropriate design return interval for this new zone, it is argued that a 300-year event is backed with a larger likelihood of occurrence and smaller analysis costs (Faber et al. 2004a). Still, there is considerable uncertainty in estimating a 300-year magnitude and larger events may occur, as they were recently observed. At the Lower Austrian Kamp River, the August 2002 peak flow at the Zwettl gauge corresponded to a theoretical 2,000 to 10,000-year recurrence interval (Gutknecht et al. 2002). Another example is the estimated 5,000-year discharge at the western Austrian rivers Sanna and Trisanna in August 2005 (BMLFUW 2005a). This in turn argues for analysing and managing residual risks from larger than 300-year events. On the other hand, high political concerns were experienced by the attempt to map large parts of the former Bavarian floodplains as residual flood hazard zones (Bauer 2004).

This discussion shows that the definition of the analysed scenarios may be a tradeoff between the attempt to cover as many scenarios as possible, the acceptability of the results and the analysis efforts.

1.3.1.2 Design rainfall

Design rainfall data specify the relationship of the precipitation amount, the rainfall duration and the probability. Design rainfall data may be used as an input for flood hazard analysis, and like other hydrologic and hydraulic input data, they are subjected to uncertainties. As an example for these uncertainties, one-hour design rainfall data are presented in Figure 1.1, where the authors used different data and models.

Figure 1.1: One-hour design rainfall data for Wien, Hohe Warte



The last decade's record-breaking rainfall observations and the elaboration of new design rainfall data intensified the discussion on the most accurate estimation procedures for these design values. It appeared that the design data used in the past, such as data from Kreps and Schimpf (1965) and Schimpf (1970), were far exceeded. Pekarek (1997) reported on a two-day rainfall of 248 mm in the Wien River basin, and even higher amounts were gauged in 2002. These observed values were much larger than what could be explained from the extrapolated Kreps and Schimpf design rainfall data. Similarly, the design values derived by Lorenz and Skoda (2000) were locally much higher than other approaches. An analysis with the Lorenz and Skoda data could result in a decreased reliability of existing protection systems.

This discussion shows that there is uncertainty in the design data, the design data may change over time and the design data may as well be exceeded.

1.3.2 Loss analysis

Flood losses cover a social, an economic and an environmental dimension.

Many authors qualitatively compiled these consequences in slightly different ways, for instance Schmidtke (1981, 1982, 2000) or Egli (2002). Egli (1996) in addition suggested a number of quantitative indicators. As part of the European research project FLOODSite, Messner et al. (2006) summarised the types of flood damages, as presented in Table 1.1, and provided further guidance on flood loss analysis.

In Austria, the official procedures for flood loss analysis in the river engineering sector are stated in the 'Preliminary Guideline for Cost-Benefit Analysis for the Federal River Engineering Administration' (BMLF 1980). It draws a distinction to direct and indirect monetary effects as well as intangible effects. Direct effects of protection measures are the prevented losses; effects to those not adversely affected by the prevented floods are named indirect effects. Intangible effects are not quantified in monetary terms, for instance impacts on health and safety or on cultural values. There are methods for an economic valuation of intangibles (Jonkman et al. 2003), but these methods shall not be discussed here.

Table 1.1: Typology of flood damages with examples (Messner et al. 2006, Penning-Rowsell et al. 2003, Smith and Ward 1998)

		Measurement	
		Tangible	Intangible
Form of damage	Direct	Physical damage to assets: - Buildings - Contents - Infrastructure	- Loss of life - Health effects - Loss of ecological goods
	Indirect	- Loss of industrial production - Traffic disruption - Emergency costs	- Inconvenience of post-flood recovery - Increased vulnerability of survivors

A specific issue in flood loss analysis is the limitation of methods and data, such as loss functions and the spatial information on the elements at risk. On one hand Egli (1996), Merz et al. (2004b) and Messner et al. (2006) named a number of flood characteristics that determine the magnitude of losses. These characteristics cover the inundation depth, the flow velocity, the inundation duration, the rise rate, the sedimentation and erosion processes, the water contamination, the time of occurrence and the emergency measures. On the other hand, most analyses use inundation depth-damage functions, and less is known on the quantitative dependency on the other physical flood impact parameters.

In the German-speaking countries, a prominent data source of direct flood losses is the HOWAS database of the Bavarian Water Management Agency in Munich. It contains approximately 4,000 entries of flood damages in Germany, gathered from 1978 to 1994. Buck (1999) and Merz et al. (2004a) analysed this data set in order to obtain loss functions for specific building classes. Those depth-damage curves were applied to many German Flood Management Action Plans (e.g. Hydrotec 2001, Hydrotec circa 2002) and to the analysis of the development of the Traisen River floodplains in Lower Austria (Haidvogel et al. 2004). Niekamp (2001) presented a number of these depth-damage functions, whereas the losses at a flooded building storey L_i were estimated, for instance, by the inundation depth Y in that storey and a factor a_i , specific to that building type.

$$L_i = a_i \sqrt{Y} \quad \text{Eq. 1.1}$$

The HOWAS database is not publicly accessible, and there is a considerable uncertainty introduced by the raw data scatter (Merz et al. 2004a). Much of that uncertainty is based on the large variability of the buildings' vulnerability and on influences as oil, raw sewage and chemicals (Egli 2002, GVL 2004, Kreibich et al. 2005). The HOWAS database covers inundation depths up to two metres.

In Austria, there are no systematically collected and analysed flood loss data. Until 2006, each federal province has used a different method for documenting and processing direct flood damages, and most systems are not suitable for the development of standardised loss functions. As the same institution, namely the Austrian Catastrophe Fund, finances ex-post disaster compensation and flood protection, an optimisation in processing flood damage data would be desirable.

The uncertainties stated for direct flood losses apply even more to indirect damages. Although the vulnerability of several business sectors can be described qualitatively (Egli 1996), much uncertainty is associated with the quantitative and the monetary loss estimation in an ex-ante analysis. The importance of analysing these kind of losses was illustrated for

instance by Petraschek (2004a), who reported of business interruption costs that reached the magnitude of the direct damages.

On a local scale, expert judgement is used for estimating losses from business interruption. On a medium scale, for instance for an area of 4,000 km², the state's economic benchmarks, such as net revenues, may be broken down spatially and temporally. This break-down can be based on land use maps and the ex-post analysis of the interruption duration. The duration of flood-induced business interruptions depends among others on the inundation dept (LFI-RWTH et al. 2001, Rodriguez + Zeisler et al. 2001, Müller et al. 2005). Finally, very little is known on the flood impacts on the long-term competitiveness (Schmidtke 2000).

This discussion shows that only a fraction of possible flood losses can be quantified, an even smaller fraction can be estimated in monetary terms and much uncertainty is associated with these estimates.

1.3.3 Risk quantification

Quantitative expressions of risks provide a basis for risk assessment and risk management. Jonkman et al. (2003) discussed about 25 approaches to quantify risks and classified them by the considered consequences:

- Fatalities:
 - Individual risk: Fatality risk to a single person exposed to a hazard, to a dangerous dose or to a specific activity
 - Societal or collective risk: Fatality risk to groups of persons in a specified area, determined by a function of individual risks or aversion-weighted risks (see p.19)
- Economic damage considering the expected annual losses or aversion-weighted losses
- Environmental damage considering the recovery time of eco-systems
- Considering several types of consequences by integrated risk measures
- Potential damage, which does not account for the probability

In Austria, the legal and administrative regulations (BMLF 1980 & 1994a) require the evaluation of flood losses by a benefit-cost analysis, if a proposed protection scheme costs more than 25 Million Shillings (about 1.8 Mio. €), or, if the scheme has wide economic impacts.

In these regulations, the benefits are determined among others from the reduction of the expected annual flood losses $E(L)$. $E(L)$, as a widely used risk expression is computed by Eq. 1.2 (Kemmerling and Kaupa 1988).

$$E(L) = \int_0^{\infty} L(x)p(x)dx \quad \text{Eq. 1.2}$$

Decisions based on $E(L)$ implicitly presuppose that the losses can be distributed over a long temporal horizon and over a large community, like the activities covered by an insurance company or the taxpayers in a state. It is further assumed that all adverse flood impacts on important values can be reasonably well expressed by the quantity $L(x)$ and that $L(x)$ and $p(x)$ do not change over time.

If a flood protection scheme prevents all kinds of damage up to the design magnitude r , which stands for resistance, Eq. 1.2 can be approximated by:

$$E(L) = \int_r^{\infty} L(x)p(x)dx \quad \text{Eq. 1.3}$$

Uncertainties in Eq. 1.3 are first introduced by the unsteady character of the flood frequencies and the potential damage. Second, uncertainties base on the stochastic nature of the performance of flood protection systems. And third, uncertainties stem from assumptions in the estimation of consequences. The following paragraphs detail these three issues.

First, the frequency of flood losses changes over time. This is due to human interventions in the catchment, to possible climatic alterations and to the accumulation of vulnerable assets in the floodplains. Debene and Nachtnebel (2005) reported for the 30-year flood peak of the Traisen River a 10 % increase, which was induced by river engineering works. Road constructions and land use changes increased the 30-year magnitude by 2 % and 0.5 %, respectively. Haidvogel et al. (2004) stated that the residential, industrial and infrastructural areas within the 100-year floodplains of the Traisen river expanded from 4 % in 1870 to 63 % in 2000. This study also illustrated that the direct economic flood losses had approximately doubled between 1960 and 2000, if a 100- and a 300-year flood scenario was considered.

Second, there is uncertainty in the reliability of levees. The issue of possible levee failures became obvious in the 2002 floods, where about 20 Austrian dikes broke (Habersack and Moser 2003). Merz et al. (2004b) investigated 31 levee breaches in Germany, where overtopping caused almost each second levee failure. As half of the breaches were due to other reasons showed that a number of failure mechanisms have to be considered in the analysis. Thus, the actual resistance r of a protection structure may be described as a random parameter with the probability density function $p(r)$. The expected annual losses therefore amount to:

$$E(L) = \int_{r_{min}}^{r_{max}} p(r) \left(\int_r^{\infty} L(x) p(x|r) dx \right) dr \quad \text{Eq. 1.4}$$

The mathematical procedure for considering the variability in the resistance r in Eq. 1.4 may also be used to account for the variability in the loss function $L(x)$ and the variability in the probability density $p(x)$.

Third, each way to quantify risk in an ex-ante analysis is based on assumptions. After implementing technical flood protection schemes, the residual hazards are assigned with a low probability. The expected annual losses will therefore be rather small, but the maximum losses may be catastrophic. The risk expression by means of $E(L)$ may hence be criticised, as it does not appropriately consider a society's limited ability to recover from disasters (Schmidtke 2000). The risk expression and the risk policy should consequently account for the worst-case scenario, as proposed by Schmidtke already in 1982. He advocated two governance principles that aim to reduce the total expected costs and to minimise the maximum adverse impacts. An approach to the latter principle now appeared in the Austrian guidelines for the Federal River Engineering Administration (BMLFUW 2006a p.16). For new flood protection schemes with a design magnitude below the 300-year event, the guidelines demand for measures to reduce the residual risk.

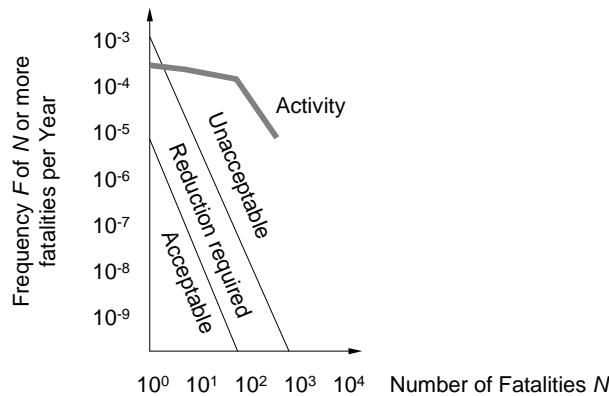
To accentuate low-probability - high consequence events, risks may be expressed by risk-curves (indicating the frequency of losses, e.g. Figure 1.2), by loss matrices or by weighting events with aversion-functions.

Kaplan and Garrick (1981) recommend quantifying risks by a curve of probability and consequences since a single number cannot fully communicate the idea of risk. BUWAL (1999b) and Merz and Thieken (2004) suggest quantifying risks by a matrix of possible hazard-scenarios and their consequences. Such a 'risk-matrix' may cover the economic dimension and the impacts to human life (Table 3.8). Although both references assign probability statements to the consequences, they neither focus on weighting losses within each dimension nor integrate them over different dimensions.

Risk-aversion functions are used for defining safety targets for particular activities or hazards (Ale 2002). Such regulations define an acceptable and an unacceptable range from the

number of fatalities N and the frequency F of N or more fatalities occurring in a year (Figure 1.2). These curves of acceptability reflect a society's aversion to large-consequence events. In Figure 1.2, one fatality, occurring with a probability of 10^{-4} per year, is perceived as negative as 10 fatalities with a probability of 10^{-6} (Faber and Stewart 2003). In this case, the aversion of larger consequences would be expressed by a factor of 10. Empirical or analytical F - N curves are also used for flood risk quantification of existing schemes, such as polders (Vrijling 2001). Relating a flood scenario to the number of victims, however, introduces relative large uncertainties (van Manen and Brinkhuis 2005).

Figure 1.2: Safety targets for societal risks in The Netherlands compared to a specific hazard or activity (Adapted from Faber and Stewart 2003)



Jonkman et al. (2003) discuss a number of societal risk metrics which include continuous aversion-functions. One of those is the perceived collective risk indicator R_p (Bohnenblust 1988) which considers the number of fatalities n , its probability density function $p(n)$ and the aversion function $\varphi(n)$:

$$R_p = \int_0^{\infty} n \varphi(n) p(n) dn \quad \text{Eq. 1.5}$$

This outline shows that there are a number of approaches to combine hazards, probabilities and consequences in a quantitative risk expression. The approaches apply different degrees of generalisation and result in different risk expressions that range from a single number to a multi-dimensional matrix. Further, there are several uncertainties affecting the risk expression and some facets of risk may not be sufficiently considered in the quantification of risk.

1.3.4 Design procedures for flood protection schemes

This chapter reviews six design procedures for flood protection schemes. The first three approaches are less complicated in their application, but they do not reveal the actual system reliability and the consequences of failure scenarios. The next two approaches are more complicated but they reflect the reliability and the consequences in a more realistic way. Finally, a holistic approach is outlined which focuses on flood management than only on flood prevention. However, such a clear distinction of the design procedures may not necessarily be found in the design practice (Merz 2006).

1.3.4.1 Empirical design

Flood dikes may be designed to withstand a historic event, such as the largest flood on record, to which a safety height of 0.5 to 1.0 metres is added (Merz 2006). Another empirical

approach increases the largest observed event by 50 to 100 %. This procedure was used to obtain the design magnitudes for spillways of large barrages (Chow et al. 1988). Empirical design approaches focus on the prevention of flood hazards, but they do not consider the consequences of possible flood scenarios after implementing the protection scheme.

1.3.4.2 Upper bounds of hydrologic loads

Upper bounds of hydrologic loads can be obtained from the regionalisation of observed maximum flow events, from estimating the probable maximum precipitation (PMP) and from calculating the probable maximum flood (PMF). Merz (2006) outlined where and how PMF concepts were used, how such estimates fit into the probability theory and that PMF estimates were also exceeded (p.104). Design approaches against the upper bounds of hydrologic loads do not include an analysis of flood consequences after the implementation of the protection scheme.

1.3.4.3 Return intervals

Design procedures based on return intervals are widely used in Europe (Merz 2006). The Austrian design approach for technical flood protection is named 'normative', where design targets depend on different land uses in the floodplains. This gradation of the design targets reflects different consequences, but a detailed flood loss analysis is not necessarily included in the design approach. Some principles in the recently revised 1994 technical guidelines for the Federal River Engineering Administration (BMLF 1994a) were:

- Areas of first-rate cultural or economic value and major central residential areas should be protected from any possible flood.
- Residential areas, significant economic areas and transport routes should be protected against up to 100-year events.
- For single dwellings, business or commercial objects, a 30-year design magnitude may be used.
- Agricultural land and forests shall not be particularly protected.

These return intervals determine the design water level. The levee crest is then planned by adding a safety height (freeboard) of up to 1 metre to the design water level, in order to account for factors that are not considered in computing the design load (Nachtnebel and Klenkhart 2004). Based on conservative assumptions, the average return period of a failure will be larger than the return period of the design load.

The 100-year design level has been widely used throughout Austria, and along the Danube River only the Cities of Vienna and Linz have larger design levels (Faber et al. 2004b). BWG (2001) described a comparable normative approach implemented in Switzerland, where each canton defines ranges of design flood frequencies for specific land use classes.

1.3.4.4 Probability of failure

This design concept is based on a tolerated probability of failure of the flood protection scheme. In the design process, the load and the resistance are both considered as probability distributed parameters that may change over time. In contrast, the return interval approach regards only the design load as a probability distributed parameter. Stochastic design procedures are used for complex systems such as coastal defence schemes. Typical tools in the design process are event tree- and fault tree analyses (CUR 1990, Vrijling 2001). The design for an accepted probability of failure may be rather complicated (Merz 2006) and it does not include a detailed loss analysis.

1.3.4.5 Risk-based design

Flood protection may be designed by risk-based procedures, which are solved, for instance, by an economic optimisation of the design magnitude (Plate 1993, HEC 1996, Vrijling 2001, Tung 2002, Jonkman et al. 2003, Merz 2006). Economic design principles aim to minimise the total of the expenditures for a safer system and the expected value of the economic damage. By that, risk-based approaches require a detailed loss analysis. Due to the big analysis efforts (Merz 2006), risk-based approaches are mainly applied to large-scale schemes, as coastal flood defence systems. In 1993, the dike design procedures in The Netherlands were changed from an accepted probability of overtopping and failure to risk-based approaches. Now, the product of probability and consequences governs the design (CUR 1990, van Manen and Brinkhuis 2005). Although risk-based approaches are well developed in theory, their practical application faces considerable uncertainties in determining the probability of dike failure scenarios, and in relating flood scenarios to a number of victims (van Manen and Brinkhuis 2005).

1.3.4.6 Integrated approach

All planning procedures described so far determine the design of technical protection systems. But further measures are necessary to minimise the immediate catastrophic flood impacts on the people and the values at risk. This necessity also applies to the risk-based design of technical protection schemes, if the consequences are only considered by the expected annual economic losses and if the preparedness, the disaster response and the risk mitigation are not enhanced. To overcome this shortfall, the state of the art design and management approaches use integrated concepts (Plate and Merz 2001, Plate 2002, Nachtnebel 2003, Habersack et al. 2004, Kienholz et al. 2004). These approaches rely on a collaboration of all actors and make use of technical and non-technical measures for managing risks (Table 1.2).

In Austria, some of these integrated principles are already stated in the new technical guidelines for the Federal River Engineering Administration (BMLFUW 2006a) and in the flood hazard mapping guidelines (BMLFUW 2006b): the call for considering the occurrence of events larger than the design magnitude and of failure scenarios, and the requirement for implementing measures to mitigate such events.

1.3.5 Uncertainties

As it was indicated in the former chapters, there are manifold uncertainties associated with the analysis of flood risks. Fritzsche (1986) and Merz (2006) therefore preferred the term 'risk estimation' instead of 'risk calculation'. Petak and Atkisson (1982) suggested not considering the results of risk analysis models as facts, since much uncertainty is inherent in the modelling results.

First, there is uncertainty in the occurrence and the magnitude of extremes, which is specified by a probability density function $p(x)$. Then, there is uncertainty due to the lack of knowledge and the imperfect system description, which is affecting the quantification of the hazard X , the consequences $L(x)$ and the probability density function $p(x)$.

The former type of uncertainty describes the natural variability. It is also called aleatory or irreducible uncertainty. More accurate data and models may diminish the latter type of uncertainty, which is denoted as epistemic or reducible. Merz (2006 p.58) found in his review that many scientists suggest a separate treatment of these types of uncertainties. He concluded that aleatory uncertainties are properties of the system under analysis, but epistemic uncertainties rather characterise the analysis itself. Merz further distinguished between three partly overlapping fields of uncertainty: the definition of scenarios, the models and the model parameters. Thus, the sources of uncertainty are:

- Not all scenarios can be considered, since humankind is not aware of all potential future consequences (Kaplan and Garrick 1981). This applies to natural hazards as well as to health risks. Therefore, a part of the residual risk will remain unknown today.
- Models simplify processes and base on assumptions. Further, the resulting information refers to a specific spatial and a temporal resolution.
- The selection of appropriate probability distributions and loss functions
- Diverging expertises on rare events that have not been observed (Morgan and Henrion 1990)
- The limited sample size and the sampling period
- Measurement errors of a systematic and a random type. Damage of gauging stations
- Temporal changes in the investigated phenomena
- Omitted correlation of parameters
- Subjective weighting of effects (Haimes 1998) such as integration and trade-offs of social, economic and environmental aspects within the risk analysis

Approaches for quantifying and processing uncertainties may be summarised as stochastic concepts, methods employing a set of different assumptions or scenarios and approaches with interval numbers, for instance fuzzy logic.

Stochastic concepts may be solved analytically, discretely or by Monte Carlo modelling in case of complex systems. Such concepts were described for instance for the engineering sector (Ang and Tang 1975, Plate 1993) or for flood statistics (Kite 1988, Stedinger et al. 1992, DVWK 1999, Haan 2002).

For performing Monte Carlo simulations, time-consuming deterministic models may be substituted by 'reduced form models'. In such a model, the computational loop is repeated with a set of pre-calculated simulation results instead of the computation-intensive simulation process itself (Compton et al. 2004). Reduced form models were also used in flood risk analyses (Apel et al. 2004).

Depending on the selected approach, the results of the uncertainty analysis may be presented by probability curves and confidence intervals, by fuzzy sets, by a number of estimates (such as high / mid / low) or by other qualitative descriptions (Merz 2006).

1.4 Problem statement

Two types of problems appear from the review of Chapter 1.3. Although many discussed issues refer to the Austrian context, the problems in analysing flood risks are not limited to Austria.

Flood risks are unknown

In Austria, flood risks and residual risks are rarely analysed and quantified. This may be based on limitations of methods and data, on missing regulations and on the analysis costs. Even less attention has been paid to residual risks, since such events were not addressed in the mandatory guidelines (BMLF 1994a).

In the aftermath of the 2002 floods, some deliberations on reducing the residual risk became compulsory in the new guidelines (BMLFUW 2006a). Still, there is no official Austrian document with contemporary guidance on analysing flood risks, and the only paper addressing this issue (BMLF 1980) covers only a fraction of risks.

Flood risks are multi-dimensional

The discussion on the quantification of risks shows that appropriate risk expressions have to account for two partly diverging principles: risk expressions should be simple enough for the engineering practice and decision making, and they should be as realistic and detailed as possible.

The first principle advocates risk measures as the product of probability and consequences or the expected losses. But in particular, this product is criticised as an incomplete risk expression, nonetheless, it is suitable for comparing risks and making resource decisions (Helm 1996).

The second principle is more appropriate for considering uncertainties, multiple dimensions of risk and qualitative approaches. Risk expressions in between those principles have to integrate social, economic and environmental aspects and make tradeoffs. In Austria, the Preliminary Guidelines on Cost-Benefit Analysis in Flood Protection (BMLF 1980) consider mostly the expected direct monetary damage and give little guidance on how to consider and integrate the intangible effects.

1.5 Aims and objectives

From the analysis of the catastrophic August 2002 floods in Austria, a number of recommendations were drawn. One of them was to intensify the use of flood risk analyses as part of an integrated flood risk management (Habersack et al. 2004). This dissertation shall provide a methodological and an applied contribution to the field of flood risk analysis, and it shall, in particular, consider the Austrian context. Flood risk analyses may be used for risk comparison, for risk communication, for setting priorities for public funding, for project optimisation, for the elaboration of risk sharing options and for cost-benefit analysis.

The following aims are therefore defined as:

- This dissertation aims to demonstrate how residual flood risks can be analysed.
- An extended framework shall be developed for considering various uncertainties.

Table 1.2 outlines how the aims of this dissertation contribute to the management of flood risks (Plate and Merz 2001, Vrouwenvelder et al. 2001, Ale 2002, Plate 2002, Nachtnebel 2003, Habersack et al. 2004, Kienholz et al. 2004).

Table 1.2: Aims of this dissertation in the context of flood risk management

Flood risk management	Aims of this dissertation
Risk analysis	Main focus of this dissertation (Figure 1.3). Covered by methodology and applications
Risk assessment	Partly covered as part of the applications
Reduction of loads by: Technical measures Non-technical measures	Covered as part of the applications (Table 1.3) Not covered
Reduction of losses by: Technical measures Non-technical measures	Covered as part of the applications (Table 1.3) Not covered
Risk-burden sharing	Not covered
Emergency management	Partly covered as part of the applications (Table 1.3)
Regeneration	Not covered

Based on the aims of this dissertation, the objectives are defined as:

- A generic methodology for flood risk analysis shall be presented, comprising a sequence of hydrologic, hydraulic and loss modelling. The methodology will analyse flood risks by investigating possible flood scenarios, their probability of occurrence and their consequences (Figure 1.3).
- Uncertainties in the analysis of risks will be integrated by deterministic and stochastic approaches (Figure 1.4, Table 1.3).
- The generic methodology shall be presented and discussed by its application to two cases studies, where one case study is dedicated to each approach (Figure 1.4, Table 1.3).

Figure 1.3: Main focus of this dissertation in the context of risk assessment (Adapted from Mock 2001)

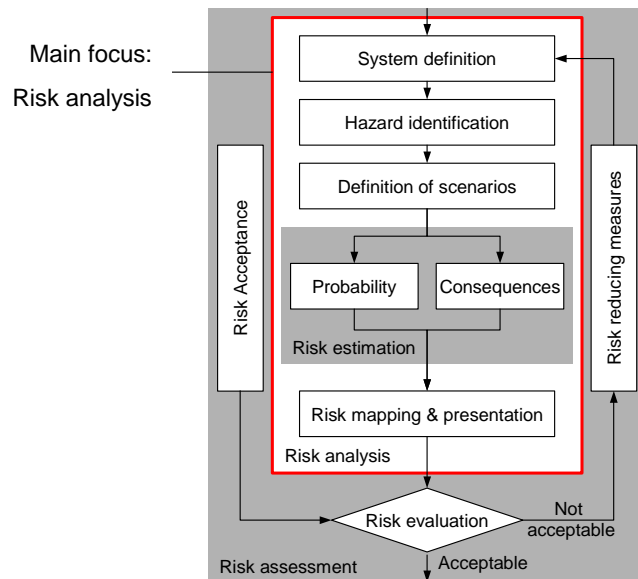
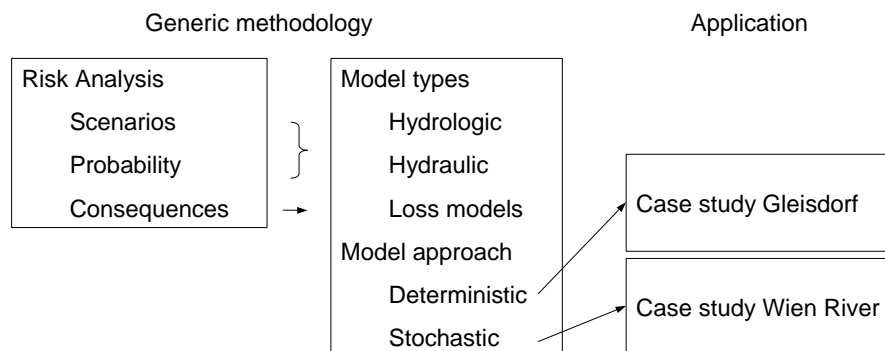


Figure 1.4: Overview of the objectives of this dissertation



The objectives for applying the methodology to the case studies, with respect to the selected model types and the approaches, are detailed in Table 1.3.

Data and materials for both case studies based on research projects of the author of this dissertation. These projects were carried out from 2001 to 2005 at the Institute of Water Management, Hydrology and Hydraulic Engineering at the University of Natural Resources and Applied Life Sciences, Vienna. The Austrian case studies referred to the Raab River in Gleisdorf (Faber et al. 2005), which is located in the province of Styria, and the Wien River in the City of Vienna (Compton et al. 2002 & 2004, Faber et al. 2003).

Table 1.3: Objectives for applying the methodology to the case studies

	Deterministic approach: Case study Gleisdorf	Stochastic approach: Case study Wien River
Hydrologic models	Deterministic rainfall-runoff model: Computation of a set of scenarios. Selection of a sub-set of these scenarios with distinct return periods as the input into the hydraulic model	Stochastic peak flow simulation for several return periods by - Monte Carlo simulations of design rainfall, coupled with rainfall runoff modelling - Monte Carlo modelling of peak flows from extreme value statistics
Hydraulic models	Deterministic analysis of following scenarios: Levee overtopping, bridge jam, blocked weir, levee failure, bank vegetation changes and flood detention basin failure. Using the input of hydrologic model	Monte Carlo simulations with a deterministic hydraulic model and the input of the stochastic hydrologic model: Analysis of floodwall overtopping and structural wall failure scenarios. Computation of system reliability
Loss models	For hydraulic modelling results: Deterministic loss estimation with two standardised loss function approaches, enquiry results and statistical data	Deterministic loss estimation with upper- and lower bound estimates
Analysis of risk management options	Reduction of loads (by alterations in the levee system and increasing the system reliability). Reduction of losses (by reducing the buildings' vulnerability)	Reduction of loads (retention scheme upgrades, flood wall strengthening). Reduction of losses and emergency management (mobile barriers)
Evaluation of uncertainties	Evaluation of uncertainties in the hydrologic model, partly in the hydraulic model and in the loss estimation	Evaluation of uncertainties in the hydrologic and the hydraulic models and in the loss estimation.

1.5.1 Defining the scope

The following paragraphs state issues that are not aims of this dissertation, in order to clarify the scope of this work.

In this dissertation, flood losses are addressed in monetary terms, although this kind of damage covers only a section of the wide range of potential socio-economic flood impacts. A number of issues in quantifying flood losses are therefore left open to future research.

So far, monetary risk estimates have a cumulative character that conceals who or what may suffer losses, who or what benefits from selecting a particular option and how countermeasures could be financed. Traditionally, the general public funds large parts of the hazard prevention, whereas the group of beneficiaries is smaller. The distributions of costs and benefits, as well as risk sharing instruments, are also not covered in this dissertation.

Some management options are analysed in the case studies, but designing new site-specific mitigation measures is not an objective of this dissertation. State of the art approaches use integrated management concepts, which are not addressed in an all-embracing way.

A risk expression refers to a particular date and a system state. There is no doubt that risks change over time, since there are alterations in the vulnerability, in the frequency of hazards and in the protection systems. All these factors are subject to ongoing research, but analysing the unsteady character of risk is not an aim of this dissertation.

2 Methodology

This chapter describes the tasks in the analysis of flood risks and gives an overview on the deterministic and stochastic approaches. The analysis tasks are described below as the identification of hazards, the definition of scenarios and the estimation of flood losses. This generic methodology is then applied to two cases studies, presented in Chapter 3 and Chapter 5.

In principal, the analysis of flood risks may be based on two approaches: an anticipative study of potential future events for existing or for planned system states (ex-ante analysis) and the investigation of events that already occurred (ex-post analysis). Since the catastrophic flood events of interest have not occurred at the rivers under study, ex-ante analyses were the methods of choice.

2.1 Hazard identification

The hazard identification focused on a qualitative but comprehensive compilation of possible influences that govern the formation of flood perils. In general, the approaches of gathering information involved:

- 1 On site inspections
- 2 Study of maps and technical documents
- 3 Analysis of hydrologic records
- 4 Documentation of historic events
- 5 Modelling and plausibility checks

The identified hazards were governed by an interaction of natural phenomena, technical components and human interventions, which included:

- 1 Hydrologic events
 - Flood peaks and flood hydrographs
- 2 Reliability of protection systems
 - Levees and floodwalls
 - Mobile barriers
 - Flood detention reservoirs
 - Bridges and weirs
 - River bank and floodplain vegetation
 - Sediments
- 3 Human intervention as part of the operational flood management

2.2 Scenario definition

From the large range of possible flood events, described by the hazard identification, a set of scenarios was defined, which covered the hydrologic extreme input and aggravating hydraulic impacts. Those scenarios were subsequently analysed by two modelling approaches. In the first approach, the model parameters were treated as precise information. The second approach allowed for a wide-ranging variability of the model parameters in order to cover many possible effects during the flood events.

The scenario definition typically comprised the determination of average return periods for the hydrologic loads. Then, parameters for those elements were defined that could influence the river- and floodplain flow processes and the flood hazards. This led to the definition of scenarios with- and without structural and operational failures occurring.

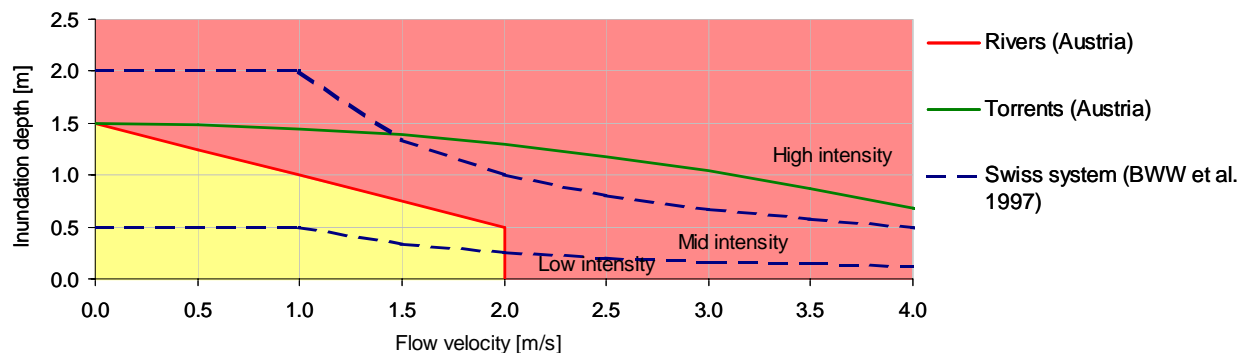
2.3 Loss analysis

The analysis of flood losses was based on a monetary quantification. The relation of the flood intensity and the magnitude of losses was estimated by two concepts, which comprised loss functions and expert judgement.

Loss functions return either absolute values or they specify loss fractions that are to be multiplied by the values of the objects. Within a particular object class, loss functions describe average properties, or they refer to a unit area or a length and allow for varying object sizes.

The loss estimation in this work followed the methods of BUWAL (1999a & b), which suggested loss fractions and absolute losses for the three flood-intensity classes of Figure 2.1. These classes are a central part of the Swiss hazard mapping system (BWW et al. 1997). In Switzerland, similar approaches for damage estimation were developed for torrents, for avalanches and for rock-falls. The corresponding Austrian criteria for the red and the yellow hazard zones at rivers (BMLFUW 2006b) and at torrents (BMLF 1994b) are slightly diverging (Figure 2.1). For non-standard objects, such as industrial sites, expert judgement was suggested by BUWAL (1999a & b) for more accurate loss estimation.

Figure 2.1: Flood intensity classes for loss estimation, and hazard zones defined by the inundation depth and the flow velocity



The case studies presented in this dissertation referred to a local scale of several square kilometres. Studies at scales up to several thousand square kilometres employed different data sources of land uses and combined them with disaggregated macroeconomic capital stocks. This approach was applied to areas like the Rhine River lowlands (Rodriguez + Zeisler et al. 2001) and to the German Province of Nordrhein-Westfalen (LFI-RWTH et al. 2001).

2.4 Modelling approaches

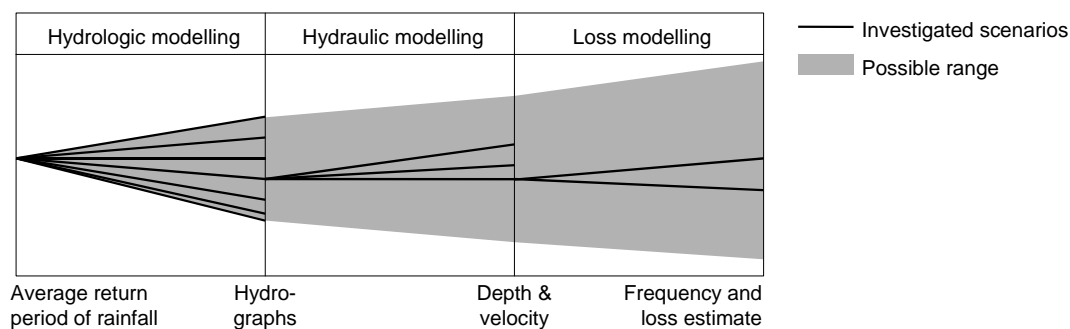
Two kinds of uncertainties were considered in the modelling approaches: the irreducible uncertainty in the occurrence and magnitude of extremes and the uncertainty due to the imperfect system description. To cover the broad range of possible extreme flood events, first, a scenario-type approach was applied, which was based on deterministic models. A Monte Carlo-type was used in the second approach, which accounted for the randomness in the model parameters. Both approaches are presented in the following chapters.

2.4.1 Deterministic approach

The first approach made use of deterministic modelling concepts, where the employed models processed all input parameters as precisely known numbers. For considering the uncertainty due to the natural variability, the deterministic model outputs were assigned to an average return interval of the hydrologic input. The epistemic uncertainty was accounted for by establishing a set of hydrologic and hydraulic scenarios. In these scenarios, different model parameters and partly different model types were implemented.

The deterministic approach is shown in Figure 2.2 for one particular average return interval. The scenarios were defined to cover a wide range of possible inundation situations, each causing a specific loss magnitude. The definition of particular scenarios was based on several data sources, on modelling results and, to some extent, on an inevitably subjective judgement. In Figure 2.2, the black lines indicate the scenario definition and the performed modelling sequence. The computed flood losses were then assembled in a matrix, which quantified the risk as the frequency of flood damages. Finally, expected annual losses were computed from that risk matrix.

Figure 2.2: Definition and modelling of scenarios in the deterministic approach (Adapted from Fuchs 2005)



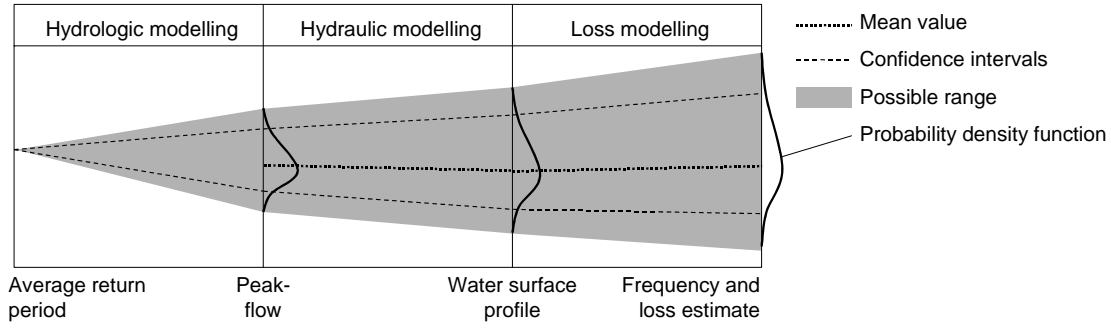
2.4.2 Stochastic approach

The stochastic modelling approach made use of the same model types as the deterministic framework, but it allowed for an input data variability that was specified by probability density functions. By this, the output again acquired a distributed character and was finally integrated into expressions like the probability of failure and the expected annual flood losses. The simulated processes were assumed as steady in the time domain.

The stochastic approach made use of Monte Carlo modelling, where a large number of deterministic simulations with randomly generated input data was performed and analysed with frequency histograms. The framework for the numerical modelling sequence is shown in Figure 2.3. This was similar to the concept proposed by HEC (1998) for uncertainty estimation in flood damage analysis and the stochastic framework of Apel et al. (2004). The latter authors used Monte-Carlo simulations with complex deterministic results for modelling flood risks at the Rhine River.

In contrast to the deterministic approach outlined in Figure 2.2, a justified functional relationship between the computed water surface and the inundation losses could not be developed in the stochastic case study. Therefore, the hydrologic and hydraulic results were linked to the loss modelling procedure by the probability of failure. This approach still allowed the estimation of risk as the frequency of losses and as the expected annual losses, which were both computed for several states of the protection system.

Figure 2.3: Modelling of flood losses in the stochastic approach



2.4.2.1 Reliability and probability of failure

In Monte Carlo modelling, the independently sampled input parameters are addressed as basic random variables. Both, the natural variability and the parametric uncertainties may be expressed by such variables. Applying this concept to river engineering, the basic random variable of the load may be the annual maximum flow or the corresponding water surface elevation, and the level of a floodwall crest may be the resistance (Figure 2.4).

In a technical sense, the reliability R and the probability of failure P_F are closely linked (Eq. 2.4). Although several authors denote the mathematical definition of P_F in slightly different ways, the idea is the same (Ang and Tang 1975, CUR 1990, Plate 1993; Eq. 2.1 - Eq. 2.3). These equations use the design resistance r and expose it to the stress s that is described by its probability density function $p(s)$. The design resistance is also denoted as x^* , the load and its probability density function are also indicated by x and by $p(x)$, respectively. The safety margin is defined as $z = r - s$ (Plate 1993) and has the probability density function $p(z)$.

$$P_F = P(x > x^*) = \int_{x^*}^{\infty} p(x) dx \quad \text{Eq. 2.1}$$

$$P_F = P(s > r) = \int_r^{\infty} p(s) ds \quad \text{Eq. 2.2}$$

$$P_F = P(z < 0) = \int_{-\infty}^0 p(z) dz \quad \text{Eq. 2.3}$$

The reliability is a number between 0 and 1 and indicates the probability of no failure occurring during a specified time horizon. In this work, the investigated time horizon, the probability density functions and the reliability referred to one year.

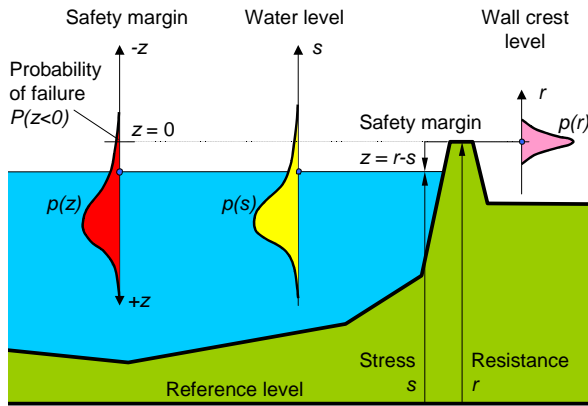
$$R = 1 - P_F = \int_0^{x^*} p(x) dx \quad \text{Eq. 2.4}$$

In these equations, it is implicitly assumed that the protection system will serve its purpose exactly up to the resistance level x^* . More realistically, the resistance is not perfectly known and it may instead be described by a probability density function (Faber and Stewart 2003) or by fuzzy sets. An example for determining P_F by the stochastic variables r and s is presented in Figure 2.4, where the probability density function of the resistance is denoted as $p(r)$. For statistical dependent parameters r and s , the probability of failure is determined by:

$$P_F = \int_0^\infty \left(\int_0^r p(r,s) dr \right) ds \quad \text{Eq. 2.5}$$

In some rather exceptional cases, the probability of failure in Figure 2.4 can be solved analytically (Plate 1993).

Figure 2.4: Example for determining P_F from the basic random variables r and s



In many cases, Monte Carlo simulations are used for obtaining numeric solutions. Such simulations are in particular applied, if there are more than one failure modes to be considered, and if r and s depend on a set of basic random variables. The probability of failure is then approximated from the total number of simulations n and the number of simulations with a failure occurring, n_F :

$$P_F \cong \frac{n_F}{n} \quad \text{Eq. 2.6}$$

In this work, Monte Carlo simulations were used to solve Eq. 2.6, conditional on defined average return intervals. By that, most of the simulations covered very seldom flood events, which were of particular interest. The total probability theorem (Ang and Tang 1975, Plate 1993; Chapter 5.5.3) was finally used to determine P_F from the conditional results.

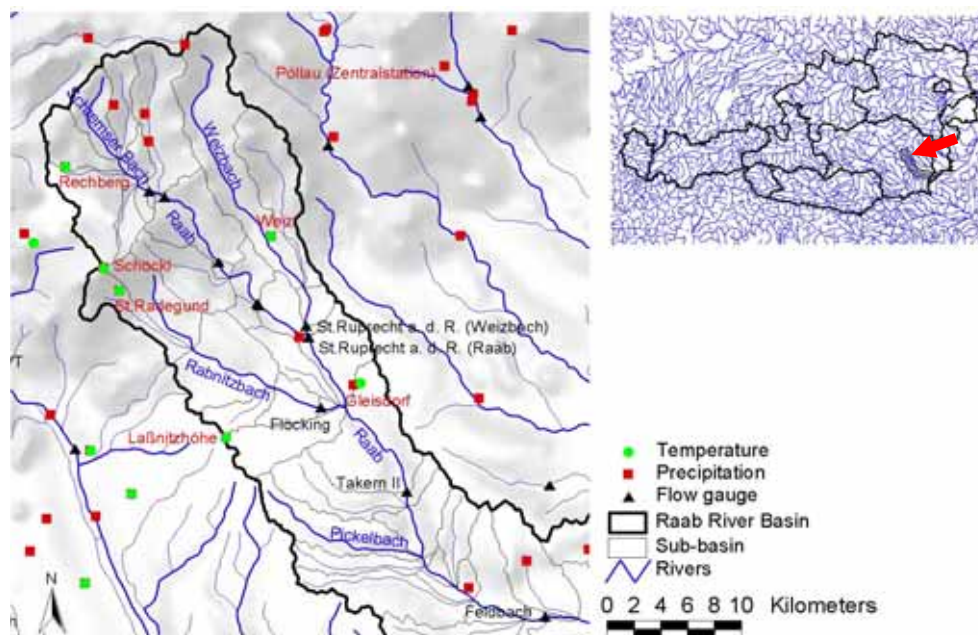
3 Case study 1: Application

3.1 System description

Case study 1 focused on the Styrian township of Gleisdorf and its adjacent communities that are located about 20 km east of Graz. As built areas and projected industrial sites were exposed to inundations of the Raab River, the technical flood protection system was recently upgraded. This system, designed for a 100-year event, was completed in the late 1990s. It employs levees, floodwalls and an offline retention basin. Meanwhile, large parts of the former floodplains were developed as industrial areas of high importance, so the vulnerability of the hinterland has increased.

The Raab River catchment draining to Gleisdorf ranges from altitudes of 360 to 1,800 meters and totals to 453 km². The Raab River drains 323 km², and the Rabnitzbach tributary covers 130 km² at the confluence in Gleisdorf. The average annual precipitation amounts from 785 to 900 mm, whereas the highest values are found in the northern and northwestern ranges (BMLFUW 2005b). Table 3.1 shows the observed maximum daily precipitation in about 100 years, which ranged up to 120 mm. Figure 3.1 introduces the Raab River basin in Austria and marks the gauging stations used in this study. The Raab catchment down to gauge Takern II was considered by the hydrologic analysis.

Figure 3.1: Raab River basin and gauging stations (BMLFUW 2005b)

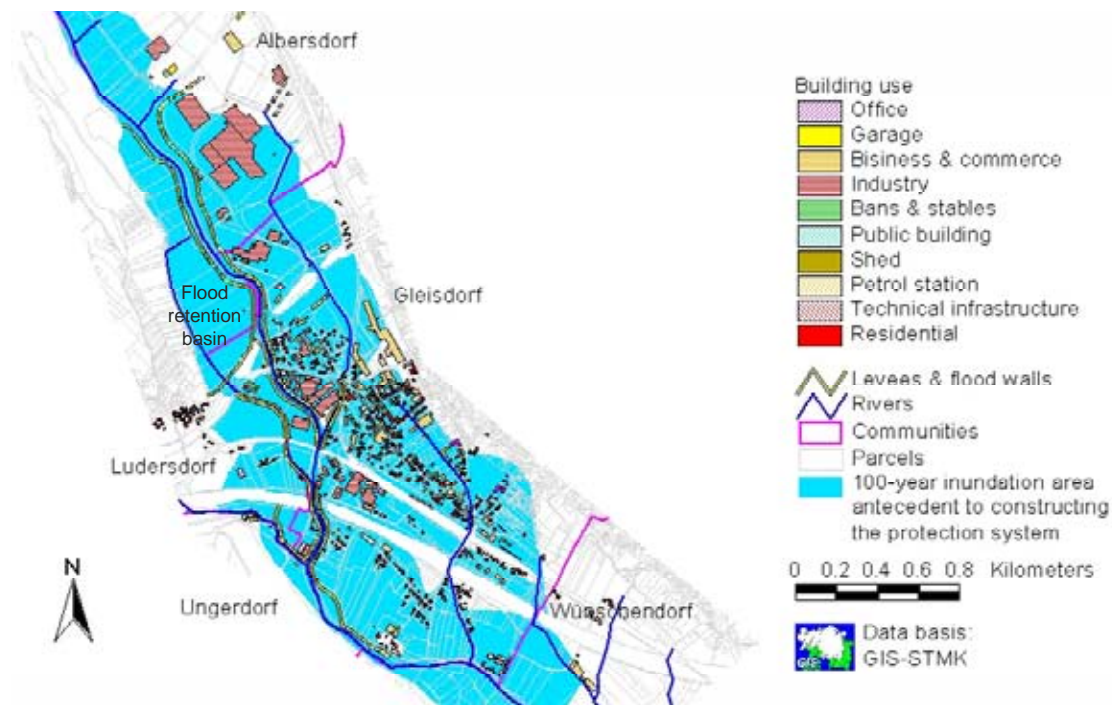


Low-lying parts of the Gleisdorf region are situated on the approximately one kilometre wide alluvial plains of the Rivers Raab and Rabnitzbach. Remarkable for this area is the small floodplain slope and several transport embankments, which cross the Raab valley. Of specific concern is also the demanding land use for commercial and industrial purposes, and for intensive agriculture.

Table 3.1: Maximum observed daily precipitation (BMLFUW 2005b)

Station	Maximum daily precip. [mm]	Year	Beginning & end of rainfall series		Years of observation
Laßnitzhöhe	112.4	1914	1902	1998	97
Rechberg	113.3	1971	1971	1998	38
Schöckl	121.6	1931	1901	1998	98
Weiz	119.7	1900	1900	1998	99
Gleisdorf	96.5	1919	1901	1998	98

Figure 3.2: The Gleisdorf model domain, the former 100-year floodplain and the technical flood protection system



The system for the hydraulic analysis covered the river network with its bridges and weirs, the levees, the bank vegetation, the retention basin and the floodplain topography. The loss analysis considered the buildings (Figure 3.2), the transport infrastructure and economic activities.

3.2 Hazard identification

The focus of the hazard identification was primarily set on site inspections, modelling and studies of planning documents, as historic flood data for the present system was lacking. In the course of the analysis, two floods were observed. The larger event, which occurred in August 2005, was estimated as a 10 to 15-year flood at the Raab River (R. Schatzl, personnel comment, 2005-11-14). Although the protection system was designed to withstand a 100-year event, some issues appeared at the new technical flood protection scheme. Summarizing all sources of information, the relevant hazards were identified as:

- 1 High flow at the Rivers Raab and Rabnitzbach exceeding the design magnitudes
- 2 High flow at the Rivers Raab and Rabnitzbach combined with
 - Jammed bridges
 - Blocked barrage weirs
 - Levee failure
 - Changed bank vegetation and sedimentation
 - Failure of the flood detention basin
- 3 Rainfall and high flow at the hinterland tributaries
- 4 High groundwater levels and inundations from the underground drainage network

3.3 Scenario definition

The definition of flood scenarios was based on a combination of hydrologic and hydraulic aspects. A scope of the probabilities of the hydrologic loads was set in the contract for this analysis. It suggested investigating 100 to 1,000-year events at the Raab River and simulating an event that would correspond to the catastrophic August 2002 storms, which were observed in northern Austria. The hydraulic aspects covered elements that govern the inundation flow process and system components that might fail.

Most of the identified hazards, as combinations of hydrographs and possible hydraulic conditions, would lead to high water levels at Raab River. This was recognised as most critical for the vulnerable hinterland. By using a few representative model set-ups and additional qualitative assessments, a large number of possible events was reduced to a small number of scenarios. These defined scenarios are summarised in Table 3.2 and further detailed in the hydrologic analysis (Chapter 3.4) and in the hydraulic analysis (Chapter 3.5).

Table 3.2: Scenario overview

Scenario	No.	Description, peak flow of River Raab hydrograph	Approximated average return interval T [a]
State antecedent to the construction of protection measures			
Without levees	1	Steady flow, 200 m ³ /s	100
State 2005 with completed protection measures			
Scenarios without technical or operational failure (Chapter 3.5.1)	2a	Steady flow, 200 m ³ /s for 4 hours	100
	2b	Hydrograph with a peak flow 189 m ³ /s	100
	4	Hydrograph with a peak flow of 245 m ³ /s	300
	5	Hydrograph with a peak flow of 310 m ³ /s	1,000
	6	Hydrograph with a peak flow of 400 m ³ /s, comparable to the August 2002 event	5,000
Bridge jam (Chapter 3.5.2)	3	Hydrograph with a peak flow of 189 m ³ /s, while flow areas under bridges are partly jammed	Hydrograph: 100
Levee failure (Chapter 3.5.3)	7	Hydrograph with a peak flow of 400 m ³ /s, comparable to the August 2002 event, with sudden levee breach at the time of peak flow	Hydrograph: 5,000
Closed weir gate (Ch. 3.5.4)	8	Hydrograph with a peak flow of 189 m ³ /s, while one of two barrage weirs remains closed	Hydrograph: 100
Bank vegetation (Chapter 3.5.5)	9	Calculation of present (2005) conditions, and possible extreme plant succession states	Water levels: 10 years and larger
Failure of flood retention basin (Chapter 3.5.6)	10	Technical and operational failure of single system components and structural failure. Qualitative assessment of model results from the scenarios above, flood observations 2005 and literature review	Not specified
Inundation of the hinterland (Chapter 3.5.7)	11	Flooding due to several reasons not specified before. Assessment by model results of the scenarios above and flood observations 2005	Not specified

3.4 Hydrologic analysis

This chapter details the hydrologic aspects of the scenario definition. The hydrologic analysis first aimed on searching possible and likely patterns in the locally observed extreme precipitation. Combined with the extrapolation from rainfall statistics, those features were fed in a rainfall runoff model, to obtain hydrographs of both main rivers at their confluence in Gleisdorf. Then, the peak flow probabilities were re-evaluated in the light of the outcomes of the rainfall runoff model and the flow statistics. The analysis finally resulted in a selection of hydrographs, which were further processed in the hydraulic analysis.

3.4.1 Analysis of extreme rainfall patterns

The analysis of observed extreme events should point out, if floods were more likely caused by rainfall of typical durations, by specific temporal intensity patterns and by particular antecedent soil moisture conditions. The investigated data covered hyetographs from the 21 largest events between 1987 and 2004. The rain gauges Rechberg, Schöckl, Laßnitzhöhe, Gleisdorf and Weiz, and the flow gauge Takern II were used in this analysis.

The following parameters were investigated:

- Season and month of the peak flow
- Total precipitation of the event
- Storm duration
- Maximum precipitation aggregates in 3, 6, 12 and 24 hours
- 7 day-precipitation totals antecedent to the flow peak
- Temporal rain intensity pattern
- Lag time from the precipitation centre to the peak flow

3.4.2 Design rainfall

Design rainfall data were obtained from the analysis of local records and checked for their consistency with published design values. Alternative extreme rainfall scenarios covered the Probable Maximum Precipitation (PMP) and a situation corresponding to the catastrophic rainfall of August 2002. In the latter scenario, the main precipitation was assumed to be dropped in the river basin under study.

The following chapters describe the data and methods used for establishing design rainfall events.

3.4.2.1 Extreme value statistics

As local rainfall records of sufficient length were available (Table 3.3), statistical methods were used for processing annual maxima series. Aggregates from one hour to two days were extrapolated by Gumbel distributions to 100 and 1,000-year events. The parameters of the Gumbel distributions were estimated by the method of moments.

3.4.2.2 Design rainfall by Lorenz and Skoda

The design data according to Lorenz and Skoda (2000) represented the most recently developed design storm concept. These design rainfall data covered average return intervals up to 100 years and rainfall durations from five minutes to twelve hours. The underlying concept described convective storms by using a meteorological model with stationary storm

cells, and extreme boundary conditions were assumed. The model theory presupposed, that the relative coarse gauging network would not sufficiently detect the largest rain depths within a convective event. Further, an assumed 5 % measurement bias in the observation data was corrected.

Convective storms are usually events of shorter durations, so the authors recommended the usage of their design data for up to six-hour rain events. Design rainfall data by Lorenz and Skoda are considerably higher than what is obtained by other methods. So, a former 100-year event might be regarded as a five to ten year event according to Lorenz and Skoda.

The Federal Hydrologic Service delivered these design data for several rain gauges in the river basin.

Table 3.3: Rain gauges used for extreme value statistics

Rain gauge	Length in years	Resolution in hours
Rechberg	36	12
Schöckl	45	
Gleisdorf	40	
Weiz	40	
Laßnitzhöhe	30	1 and 12

3.4.2.3 Design rainfall by Kreps and Schimpf

The design rainfall data by Kreps and Schimpf (1965) and Schimpf (1970) were, for a longer time period, the only available design rainfall values, that covered the entire Austrian territory. These design data were tabulated for durations from one hour to two days and for average return intervals up to 100 years. The design data were derived from 713 rain gauges with more than 20 years of observation. The spatial information was obtained by defining four zones from the annual maxima of daily rainfall. The criteria for these zones based on a value that was exceeded by 90 % of the observed annual 24 hour-maxima. In the Raab River basin, the so-called K 35 criterion applied, as the 90 % value was between 30 and 40 mm. Discussions on the accuracy of these design values were already presented in Chapter 1.3.1.2.

3.4.2.4 Probable Maximum Precipitation

The estimation of the Probable Maximum Precipitation (PMP) was based on the procedure described by Hershfield (1961 & 1965). He suggested an approach similar to extreme value statistics, where the K -fold standard deviation of an annual maximum series was added to its mean. For this extreme K -value, Hershfield developed nomograms for durations of five minutes, one hour, six hours and one day.

Lorenz and Skoda (2000) suggested another estimation method for the PMP, which was based on fitting a curve to several published record amounts of precipitation.

$$P_{Record} = 50.54D^{0.5} \quad \text{Eq. 3.1}$$

Here, the maximum rainfall P_{Record} is expressed in mm, and the corresponding duration D is introduced in minutes.

3.4.2.5 Areal rainfall reduction

Design storms ideally refer to a point or to the funnel area of a rain gauge. As precipitation intensities reduce with the increasing spatial extension of the rainfall event, areal reduction factors (*ARF*) are widely used for the determination of the basin-wide precipitation.

It appeared, that applying diverse areal reduction methods to different point design rainfall data reduced the big deviation of the design values. This procedure seemed justified by the assumptions in the design concepts. However, the areal reduction method can significantly change the design rainfall depths, and a subjective selection of a reduction method represents a source of uncertainty (Figure 3.3, Figure 4.6).

The large areal reduction by Eq. 3.2 (Skoda et al. 2003) was applied to the relatively large design rainfall data by Lorenz and Skoda (2000).

$$ARF = \text{EXP}(-k A^{0.59})$$

$$k = (0.0447 h_i) + 0.0026$$
Eq. 3.2

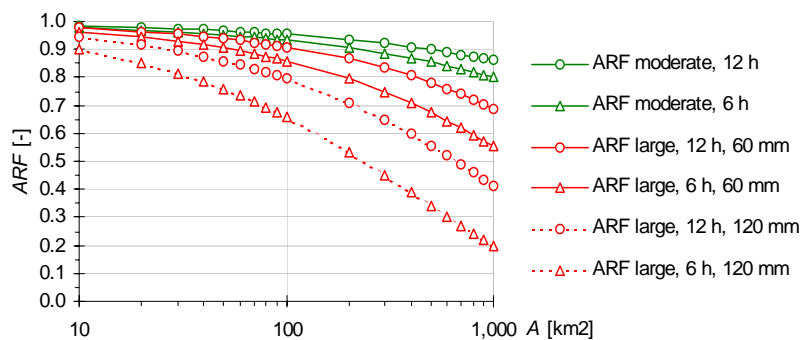
The areal reduction equations employ the catchment area A in km², the rainfall duration D in minutes and the precipitation intensity h_i in mm/min, for D larger than 15 minutes.

The moderate areal reduction by Eq. 3.3 (Lorenz and Skoda 2000) was applied to the design rainfall data from the extreme value statistics, from Kreps and Schimpf and from the PMP.

$$ARF = \text{EXP}(-k A^{0.50})$$

$$k = 0.19 D^{-0.56}$$
Eq. 3.3

Figure 3.3: Areal reduction factors *ARF* for a large and a moderate rainfall reduction



3.4.2.6 August 2002 storms

As an alternative design approach, a semi-empirical worst-case scenario was constructed from the catastrophic storms of August 2002. This event hit northern parts of Austria and caused rainfall magnitudes not observed before. It was assumed that this rainfall field moved to the Raab catchment and remained stationary over some days, as it did in some Upper- and Lower Austrian regions. This scenario might have been materializing if the Genoa depression system of August 2002 took a slightly different track.

Therefore, rainfall records from four stations in northern Austria were transformed to hyetographs in the Raab basin, covering the period from August 5 to August 14. First, an average hyetograph of the rain gauge data from Freistadt, Gars am Kamp, Litschau and Allensteig was produced in a one-hour resolution. Subsequently, the division through the four station's average of the long-term August totals returned a normalised hyetograph. Finally, the normalised hydrograph was multiplied with the long-term August precipitation of the Raab

basin rain gauges. A further areal reduction was not applied, as the original rainfall records were obtained from an area of several thousand km².

ZAMG (2002) provided the August 2002 records and BMLFUW (2005b) and Hammerl et al. (2001) published long-term means.

3.4.3 Rainfall runoff modelling

Rainfall runoff modelling aimed to compute flood hydrographs of the Rivers Raab and Rabnitzbach at their confluence in Gleisdorf.

The catchment model COSERO (COntinuous SEmidistributed RunOff model), a development of IWHW-BOKU with due respect to the HBV model of Bergström (1992) was used. Within COSERO, Hydrologic Response Units (HRUs) of flexible shapes are conceptualised by soil columns. Each column represents a surface soil layer on top of three linear storages. These storages characterise the surface runoff, the interflow and the base flow, and also flood routing modules base on linear storages. Just to name a few, Fuchs (1998), Nachtnebel et al. (1999) and Kling (2002) described the model and its applications to various spatial and temporal scales. The model setup, the edits and the computations are handled by the user interface of the Modular Modelling System (Leavesley et al. 1996).

The model catchment comprised four sub-basins that were defined by the flow gauges with appropriate data. The HRUs were derived from these sub-basins and the intersection of three land use classes, three soil types and two classes of altitudes. Precipitation and temperature data were regionalised by means of Thiessen polygons. The model parameters were determined by an a-priori parameter estimation, based on regional data, and by calibration. After a validation phase, the sub-basin at the outlet was further subdivided, as the calibration gauge Takern II was located somewhat downstream the Gleisdorf study area. Finally, hydrographs of the Rivers Raab and Rabnitzbach in Gleisdorf were computed for the following characteristics:

- The average return interval of the precipitation was 100 and 1,000 years
- The design rainfall events had a duration of 1, 3, 6, 12, 24 and 48 hours
- The temporal rainfall patterns comprised pronounced precipitation intensities in the first and in the last third of the model rainfall. Further, a rainfall intensity pattern with two slightly pronounced peaks and a few block rainfall events were modelled.
- The antecedent moisture conditions were wet or dry, respectively
- The scenario corresponding to the August 2002 event

3.4.4 Probability estimation of peak flows

Basically, probabilities were assigned to the design storm depths, but the design storms produced a large variability in the peak flows. This variability was based on different antecedent soil moisture conditions, on different temporal rainfall intensities and partly on different rainfall durations.

The estimation of the flow probabilities used the peak discharges from the modelled 6 to 48-hour rainfall events, as they produced the largest floods. The 100-year peak flow was estimated as the average of the peak discharges from these 100-year rainfall events. The 1,000-year event was determined correspondingly. These magnitudes were confirmed by the expertise of the Styrian Hydrographic Service (Stubenvoll 1994) and by the hydrologic investigations, which were carried out for the retention basin design (Sackl 1995).

3.4.5 Selection of hydrographs

The selection of hydrographs aimed to pick out a few typical flow curves from the 54 modelled rainfall runoff scenarios in order to use them in the hydraulic analysis. The Rabnitzbach River did not play an important role in this selection process, as it had a minor influence on the most critical Raab River reaches. The criteria used in the selection process were:

- 1 The ratio of the modelled peak flows at Raab River (up- and downstream the retention basin) and the design discharge capacities. The selected scenarios should cover events where the system is loaded close to capacity and when it is overloaded by various degrees.
- 2 The maximum water levels in the retention basin. These levels were computed by the standing retention method and the relations of water levels, outflows and volumes that were used in the planning documents (Sackl 1995). The maximum computed water levels in the retention basin were related to the levels of the
 - Spillway weir, indicating overflows and inundation downstream the reservoir,
 - Lowest reservoir impoundment levee crest, leading to backflow from the reservoir into the river,
 - Lateral inflow weir level, indicating reduced inflow into a fully filled reservoir.
- 3 An optical assessment of the hydrographs and of the peak flows, which were plotted against the storm duration (Figure 4.7).

Table 3.4 exhibits the outcome of the selection of hydrologic scenarios. In order to compare possible inundations before and after the construction of the protection scheme, the 100-year inundation area without the scheme was included as scenario 1. Scenario 3, which is not specified in Table 3.4, was one of the failure scenarios, and it is described in Chapter 3.5.2.

Table 3.4: Selected hydrologic scenarios

Type	Scenario No.	Description, peak flow of Raab River hydrograph	Approximated average return interval T [a]	Hydraulic analysis method
Hydrologic scenarios	1	Without the protection scheme. Steady flow of 200 m ³ /s	100	1D steady flow model (Turk 1997)
	2	Hydrograph, peak flow of 189 m ³ /s, steady flow of 4 hours at 200 m ³ /s	100	Hydrodynamic 1D – 2D simulation of the current (2005) state with completed protection measures.
	4	Hydrograph, peak flow of 245 m ³ /s	300	
	5	Hydrograph, peak flow of 310 m ³ /s	1,000	
	6	Hydrograph, peak flow of 400 m ³ /s, comparable to Aug. 2002 event	5,000	

3.5 Hydraulic analysis

This chapter details the hydraulic aspects of the scenario definition (Table 3.2). It informs how the system states with and without technical or operational failure were analysed, and it presents the computation methods.

3.5.1 Scenarios without technical or operational failure

Scenarios of this type covered events, where no structural, technical or operational failure occurred during the simulated floods. In these scenarios, which may be regarded as optimistic assumptions, the inundations resulted from exceeding bankfull discharge, from overtopping and from backwaters. The relevant hydrographs were already presented in Table 3.4.

The analysis of the scenarios specified from Chapter 3.5.1 to Chapter 3.5.4 made use of the 1D-2D hydrodynamic model, which will subsequently be presented

3.5.1.1 1D-2D hydrodynamic model

The selection of an unsteady two-dimensional inundation flow model was based on two requirements: computing flows of primarily unknown hinterland paths and accounting for the controlled offline detention basin. DHI's Mike Flood 2004 package was purchased due to its user-friendly GIS interfaces, its computation module for real time controlled structures and its capability to base simulations directly on an elevation raster and on cross sections. Finally, DHI made a special offer.

The hydraulic simulation package comprises routines for simultaneously computing discharge in the main rivers, using the 1D model Mike 11, and floodplain flow, with the 2D model Mike 21. This is achieved by allowing an exchange of mass and momentum between these two models in each computational time step.

Besides flow computations in the river network, the 1D routines were used for the computation of bridges, weirs and gates and for the definition of boundary conditions (DHI 2004a). In Mike 11, the depth-averaged flow computations base on the conservation of mass and momentum, whereas the balancing equations are solved with the implicit finite difference algorithm (Abbott and Ionescu 1967). This algorithm alternately calculates points of flow and water depth. The frictional losses were computed by the formula of Manning-Strickler.

For bridge computations, the FHWA WASPRO (Federal Highway Administration, Water Surface PROgram) method was used, as it accounts for various discharge conditions, ranging from a free water surface to the overflowing of submerged decks. Lateral and inline weirs were computed by means of Poleni's formula ($v \propto h_0^{3/2}$) with an adaptation to consider free flow and submerged overflow conditions. Here, h_0 indicates the difference of the not-influenced upstream water level and the weir crest level, and v is the flow velocity.

The flow computation at the controlled vertical gate in the retention basin's ground outlet comprised routines for free surface flow, pressurised outflow by means of Toricelli's formula ($v^2 \propto 2gh$) and submerged flow. Further, there were routines for damping numerical instabilities. Here, h corresponds to the water depth.

The depth-averaged 2D model Mike 21 FM (Flow Model) computes flow depths and velocities on a rectangular grid. A finite difference algorithm solves the flow equations by the balances of mass and momentum. Extra routines allowed for wetting and drying of the grid cells.

Similar to the boundary conditions, the 1D functions handled all exchange processes between Mike 11 and Mike 21. Both models were established and tested as stand-alone set-

ups, and they were finally coupled by the definition of three types of exchange links (DHI 2004b).

3.5.1.2 Model setup

The basic geometry data described the 1D river network by the cross sections and by the bank coordinates, which were surveyed from April to June 2005 (Figure 3.4). They were checked for consistency, converted to fit format requirements and imported into the graphical user interface of the DHI modelling package. There, some preprocessing tasks were undertaken such as editing inline structures, assigning Manning-Strickler frictional coefficients and completing the cross sections with information from the planning documents and the 1-meter digital terrain model. The hydraulic radius definitions considered a single flow segment in relative narrow river cross sections, whereas wider cross sections were subdivided into a main channel and a left and a right overbank.

As calibration data was not available, literature values were used for the Manning-Strickler frictional loss coefficients, ranging from $k_{St} = 25$ to $27 \text{ m}^{1/3}/\text{s}$ in the main channels of Raab and Rabnitzbach. $12.5 \text{ m}^{1/3}/\text{s}$ was estimated for the overbanks, $20 \text{ m}^{1/3}/\text{s}$ for the smaller creeks and tributaries and $35 \text{ m}^{1/3}/\text{s}$ for the stone-lined channels.

Model boundary conditions were defined by the inflow hydrographs of the Rivers Raab and Rabnitzbach, and zero inflow was assumed for the small tributaries in the Gleisdorf region. To reduce the computational time, hotstart-files were used which specified the initial conditions at a flow of $50 \text{ m}^3/\text{s}$ in the Raab River.

For computing overland flows, a 10-metre elevation grid was derived from the 1-metre digital terrain model (Figure 3.4). In the largest parts of the 10 m grid, the cell elevations were represented by arithmetic means. Manual adaptations were necessary for underpasses and where the raw data did not provide plausible numbers.

The levee crests instead were described by the mean value of those 1-metre raster elevations that were located within a 0.5-metre buffer either side of the levee axes. The levee axes were manually derived from AutoCAD plan views, from iso-lines, from topographic edges and from cells of zero flow accumulation. The latter were relative high-points into which none of the adjacent grid cells drain. They were identified by the ArcView extension 'Hydrologic modelling'.

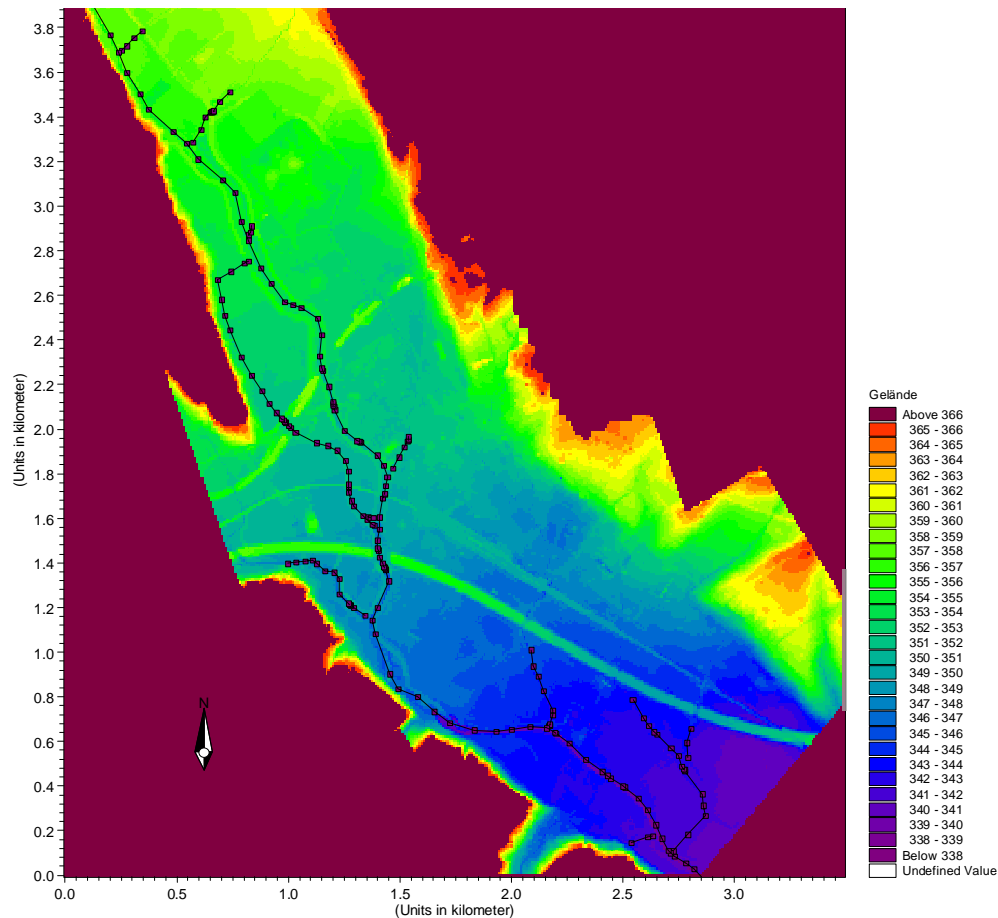
The floodplain's surface roughness values, in terms of Manning-Strickler coefficients, were estimated and assigned to the polygon-shapes of the land register, that were finally converted into a 10-metre grid. Although the land register is rather a legal document than a real land use inventory, it specifies buildings, roads, fields, meadows, forests and others reasonably well. Both, the elevation model and the roughness data were imported into the hydraulic model as ArcView ASCII grids.

The 1D and 2D simulations were at last connected by three kinds of links:

- 'Standard links' were applied at the beginning or the end of a 1D branch. They connected the 1D branch to one or more 2D cells via an internal water level boundary condition.
- 'Lateral links' represent a lateral weir along a defined river stretch. Here, the weir crest levels were defined in the cross section as the levee crests or as the level of the bankfull discharge. Other lateral links were defined at the elevation of specified grid cells.
- 'Zero flow links' disables the discharge into the right or upper adjacent grid cell. These links were implemented in those 2D cells where the 1D model already covered the flow process.

For minimising numerical instabilities, a computation time step of one second was used, and some parameters were adjusted as it was suggested in the manuals (DHI 2004a & b).

Figure 3.4: 10-metre elevation grid and river cross sections from the 2005 survey and from planning documents



3.5.2 Bridge jam scenario

Bridges often reduce the active flow area of a cross section, and floating debris such as logs, washed off timber and large bales of compressed straw may further jam this area. Within the study reach, ten bridges cross the Rivers Raab and Rabnitzbach. One of them is in particular exposed to jams, since it has been built with one mid-pier and a relative low bridge deck.

Scenario 3 investigated the inundation hazards due to bridge jams. Like in other failure scenarios, the employed parameters were rather coarse estimates, as little is known about the most likely jam formation and its relation to a particular discharge.

Scenario 3 used the 100-year flow hydrographs of scenario 2, but assumed that the bridge geometries were altered as a consequence of jammed debris. This hydrograph was selected, as it would allow drawing a clear distinction between a failure state and the proper state, which was already modelled. The following assumptions were made for the bridge geometries:

- 1 Bridges with one pier (B 65 Bridge and Urscha Bridge):
 - The lower deck was defined 0.75 m below the surveyed level
 - The flow area, obstructed by the jammed pier, was increased from 3 % to 10 %
- 2 All others bridges without piers:
 - The lower deck was defined 0.3 m below the surveyed level

3.5.3 Levee failure scenario

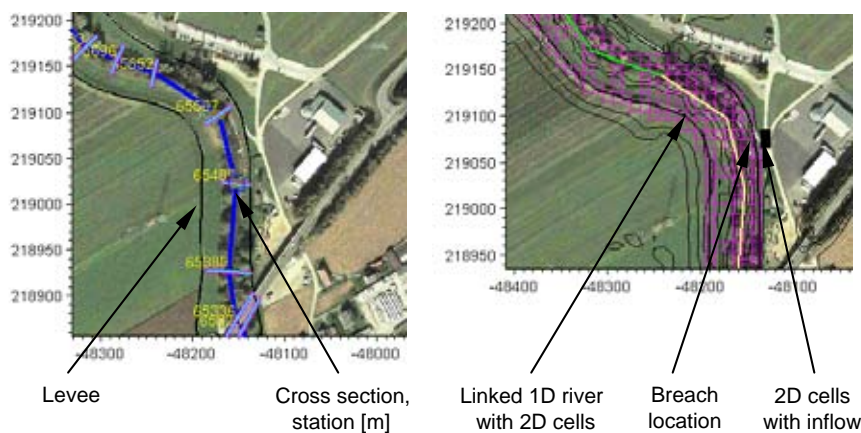
A levee breach may be the consequence of several mechanisms, such as overtopping, the formation of sliding faces, internal erosion or saturated dam bodies.

The levees constructed in the study area have been built mainly as earth-fill dams, and they were generally not designed to withstand overtopping. Erosion and breaching may therefore be a consequence of uncontrolled overflowing, as it was modelled in scenario 7. Rough assumptions covered the failure location, the hydrograph and the breaching process, since a detailed dam break analysis would have gone beyond the scope.

River stretches of smaller bankfull capacity, relative slender protection structures and areas of large potential damages were therefore considered as possible breach locations. The modelled levee failure was finally defined at the outer dike in a right hand bend of River Raab, where the inflow into the hinterland would affect wide parts of industrial and residential areas (Figure 3.5). This location represents the downstream end of the narrowing levees and a site where the lateral stopbank has been constructed relatively slender.

As inflow boundary conditions served the hydrographs of scenario 6, and it was presumed, that a sudden failure would occur at the time of the maximum flow. The simulation started with an intact protection system, and it was interrupted immediately before the breach would occur. That flow situation was described in new hot-start files, which provided the initial conditions for continuing the simulation with an additional direct flow connection from the 1D river into two cells of the 2D hinterland model (Figure 3.5). This corresponded to lowering the levee crest by 1.75 meters.

Figure 3.5: 1D river (l.), links with 2D cells and breach location



3.5.4 Failure scenario of weirs

The study reach comprised two in-stream weirs for hydropower generation and powering sawmills (Figure 3.6). Both are equipped with two movable gates that have to be opened under rising discharges. Besides jamming of the mid-piers, as it was observed in the August 2005 flood, and bed load depositions downstream the barrage, the most critical issue is the timely opening of the gates.

The opening of both weirs requires an operator intervention. The downstream weir is equipped with flap gates, and floods are conveyed over the turned-down gate sections. The upstream weir instead has been built as a segment underflow gate, which is opened by lifting the gate sections. Therefore, the opening mechanism of the downstream weir is relatively robust to increasing flows, whereas the upstream weir is more exposed to failure, which was analysed in scenario 8. The upstream gates must be opened before any floating debris jams the movable gates, as this additional weight might inhibit any lifting. Opening the gate too

early would reduce the energy production and might cause a deposition of floating debris immediately upstream the weir, which was also observed in 2005.

Scenario 8 examined a possible inundation caused by failing to open one of the two gate sections of the upstream weir. Therefore, a slight change was made to the model setup of scenario 2 which acted as a reference for a 100-year event. The modifications referred to the crest level of one gate which was assumed as closed. It was raised from the fixed concrete weir level to an elevation slightly larger than the surveyed upstream water level.

Figure 3.6: Weirs in Gleisdorf. The downstream Gliederwehr (l.) and the upstream Felberwehr during low flow in January 2005



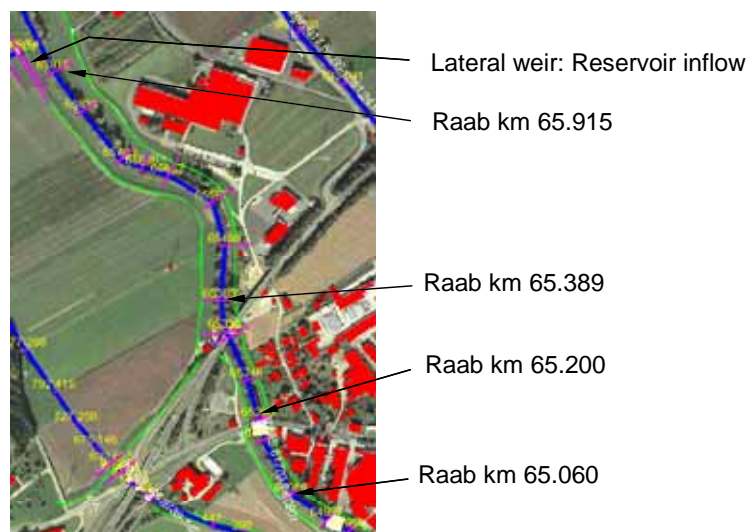
3.5.5 Bank vegetation scenarios

The dependency of the bank- and floodplain vegetation on one side, the flood flows on the second side, and the erosion and sedimentation on the third side was analysed in scenario 9, with respect to a possible decrease in the protection level. This was of particular interest, since considerable parts of the study area's river cross sections were overgrown, and bushes and trees were successively populating the overbanks. Vegetative growth again can be amplified by fertile sediment depositions in the wake of receding floods.

The investigated sub-scenarios comprised a current state (Summer 2005) and several potential future developments. For the current state, the location, the spacing and the diameters of the higher vegetation were mapped on cross section plots. In the assumed future scenarios, bushes and trees had larger diameters and less spacing, or the vegetation strips had spread over larger parts of the cross section. The flow calculations were made for water levels of particular interest: when inflow into the retention basin begins, when water spills into the overbanks and when the bankfull discharge is reached. Investigations focussed on the increasingly constricted river reach, where the vegetation influence was analysed in four cross sections (Figure 3.7).

For analysing the bank vegetation scenarios, the flow computation method differed from the hydrodynamic simulations. It explicitly considered different spacings and diameters of partly submerged perennial plants, and it accounted for exchange processes of mass and momentum in the interfaces of homogenous cross section segments. Flow calculations according to Manning-Stickler instead would regard vegetation in a too general way and neglect the resistance coefficient's dependency on the flow depth. The employed computation basics combined the flow formula of Darcy – Weissbach, the friction approach according to Colebrook and White and ways to consider vegetation parameters as presented by Mertens and Pasche (DVWK 1991). Lehmann (2005) developed the necessary iteration algorithms for the frictional coefficient λ and provided a user-friendly visual basic implementation.

Figure 3.7: Cross sections for analysing vegetation scenarios



3.5.6 Flood retention basin failure scenarios

One of the flood protection system's main features is the off-line flood retention basin, located at the right overbank. It has been designed to reduce a 100-year flood event with a peak flow of $200 \text{ m}^3/\text{s}$ to $165 \text{ m}^3/\text{s}$, corresponding to a 30-year event. The storage area is normally used for agricultural purposes, but from a 10-year flow on, a fixed lateral weir feeds the basin. The storage is equipped with a controlled ground outlet that is placed directly under the spillway. As the reliability of the protection system along the most sensitive Raab River reaches depends on the flow retention, possible scenarios associated with the retention basin were investigated.

Saurer and Baumann (1992) and Krainer (2003) suggest three principal scenarios for flood retention basins, which provided the basis for this investigation: a proper state of all structural and operational components, partial failure situations of particular elements, and finally, a total failure corresponding to a dambreak. These general states were adapted to the Gleisdorf retention basin, and they were qualitatively evaluated. This evaluation based on information from the planning documents (Turk 1996 & 1997), the digital elevation model, observations of the August 2005 flood as well as model results from several other scenarios.

Possible failures of the inflow structure could stem from a prematurely filled reservoir and a bias in designing or constructing the lateral inflow weir. Other failure mechanisms, such as a jammed inflow structure were not addressed as likely at the Gleisdorf scheme.

Another failure mechanism was identified as uncontrolled flow over the reservoir impoundment dam. A rough investigation of the crest levels revealed that one particular stretch might be exposed to uncontrolled overflowing. There, the crest level was built only 0.4 metres above the spillway's weir level. Hydrodynamic computations were used to examine if this uncontrolled overflow was possible.

The last two main elements of the retention basin are the base outlet and the spillway. The retention basin's base outlet is a rectangular concrete culvert with a vertical underflow sluice gate. It is controlled by the downstream water level to limit the basin outflow to the drainage channel's discharge capacity (Turk 1996). Jamming or falsely closing the outlet, for instance due to a power breakdown, would increase the likelihood of an overspill, yet these spills might partly flow back into the drainage channel. Similar consequences to the developed downstream areas would arise if the filled retention basin would be released by falsely opening the base outlet gate. However, as overspilling was part of other already analysed scenarios, a separate investigation of possible base outlet failures was not performed.

Potential scenarios of the spillway were distinguished into spillway activation and structural failures. The former was already modelled, whereas the latter seemed very unlikely, due to its design to withstand a 5.000-year event. It was therefore not further investigated.

3.5.7 Hinterland inundation scenarios

Flood hazards have been discussed as far as they emanate from the water of the main rivers flowing *over* the protection system. Yet, two more somewhat different situations were considered.

First, flows *through* the protection system were identified. In the study area, a number of below-grade pipes drain into the main rivers. Most of them are equipped with gravity driven flap gates and manual closing organs. Experience from other rivers shows that automatic flap gates were often jammed with debris. By this, water from the river flows into the drainage system and subsequently into the buildings.

The second situation was defined as high water levels in the smaller Gleisdorf tributaries, which concurrently appear with high flows in the receiving Raab River. A rough qualitative assessment based on the observations of the 2005 event and on the critical review of the hydraulic model results.

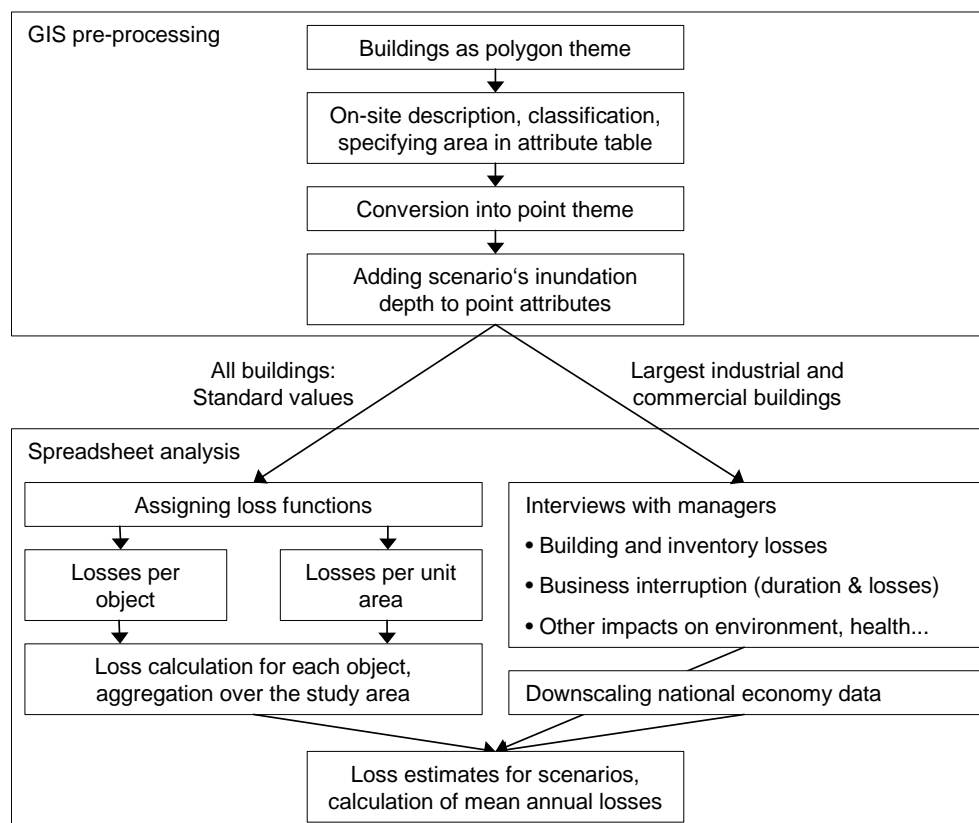
3.6 Loss analysis

This chapter details, how losses were estimated for the computed flood scenarios. The loss analysis used two approaches for monetary flood damage estimation. In the first approach, the loss functions of BUWAL (1999a) and BWG (2002) were adapted to the local situation (Chapter 3.6.1). The second approach intended to refine the loss estimates in the industrial and the commercial sector (Chapter 3.6.2).

Figure 3.8 exhibits the loss estimation procedure, where the basic data on the objects at risk were pre-processed by means of a geographical information system (GIS). The polygon themes of buildings and roads were taken from the land register, whereas line themes of railroads were digitised. Buildings, as a basic unit for direct flood loss estimation, were defined as immobile objects with a permanent roof. Onsite inspections provided information on the building class and gave the basis for adding new-built objects to the GIS dataset.

The building polygons were then converted into a point theme with a specification of the building area in the attribute table. The final GIS procedures were to transfer the inundation scenario's maximum flow depths from grid data into the building's attribute table and to conduct manual adaptations for some objects. Losses were finally calculated with the attribute table's information on the inundation depth, the building area, the building class and the loss function (Chapter 3.6.1).

Figure 3.8: Loss estimation procedure



3.6.1 Direct loss analysis

Direct losses were estimated by an adaptation of the approach described by BUWAL (1999b) and BWG (2002). In this approach, magnitudes of losses were estimated for the three

classes of flood intensities. For each flooded object in the study area, the relevant information on the intensity was derived from the 2D hydraulic analysis.

The hydraulic model results showed that, according to criterion 2 in Table 3.5, the flood intensities in the developed areas were low. So the governing criterion for the estimation of losses was the inundation depth, which kept below two metres.

Table 3.5: Flood intensity classes for loss estimation (BWW et al. 1997)

Intensity class	Criterion 1: Inundation depth h	Criterion 2: Flux vh = depth * velocity
Low	$h < 0.5$ m	$vh < 0.5$ m ² /s
Mid	0.5 m $> h > 2$ m	0.5 m ² /s $< vh < 2$ m ² /s
High	$h > 2$ m	$vh > 2$ m ² /s

For the three classes of flood intensities (Figure 2.1, Table 3.5), BUWAL (1999b) and BWG (2002) specified loss estimates for the building structure and the inventory. These estimates were tabulated as absolute losses in Swiss Franks and as loss ratios. These absolute estimates per unit of building area and per object were converted to the Austrian price level of 2004 by three steps, resulting in the loss functions of Table 3.6.

- 1 Conversion into an equivalent '1999 Euro' by the exchange rates of the Swiss National Bank (2005)
- 2 Adaptation to the Austrian 1999 price level by the ratios of the Comparative Price Level Indicators for the Gross National Product (GNP) (Stapel et al. 2004, table 5)
- 3 Accumulating the 1999 data to 2004 by the ratio of the nominal Austrian GNPs per capita (Statistik Austria 2005a). Similar benchmarks for accumulating are the GNP (Petraschek 2004b), the Building Price Index (Kranewitter 2002, Merz et al. 2004a) and the Consumer Price Index (Kraus 2004).

Table 3.6: Loss functions for the flood intensity classes (in €)

Class according to BUWAL (1999b), BWG (2002)	Low flood intensity		Mid flood intensity	
	a) Per building	b) per m ²	a) Per building	b) per m ²
One and two-family residential houses	8,402	90	44,810	532
Multi-family residential houses	11,202	106	50,411	588
Business & commercial buildings	28,006	308	140,031	1,400
Industrial buildings	33,607	375	196,043	1,960
Barns & stables	2,801	62	22,405	294
Sheds & garages	1,120	11	8,402	115

These loss functions in Table 3.6 and the underlying values of residential buildings were then checked for accuracy by using several value estimates and data from ex-post and ex-ante analyses (Table 3.7).

For residential buildings, the conversion described before resulted in a local value of 3,360 € per m² area or approximately 300,000 € per object. This was found in satisfactory accuracy with data obtained from insurance companies, market prices and guidance for valuating buildings in the province of Styria.

First, the average new insured values of a residential building and of the inventory of a household were stated as 300,000 € and 70,000 €, respectively (T. Hlatky, personal comment, 2005-02-28). Second, insured values in the range of 1,900 € to 3,700 € per m² were estimated from data of the Wiener Städtische Insurance Company (Haidvogl et al. 2004). Then, values of approximately 3,000 € per m² were approximated from local market prices of two residential buildings. And finally, by assuming an average house had two storeys of residential use, the regional replacement cost estimate of Kranewitter (2002) would result in about 3,000 € per m² building area.

Table 3.7: Ex-ante (a) and ex-post (p) building losses for accuracy evaluation of the applied loss functions

Average loss in 1,000 €	Price level	Event	Comment	Source
21.3	2000	100-yr. event & failure of protection system	Computed for the Flood Action Plan Sieg, Germany (a)	Hydrotec (circa 2002)
22.5 – 32.5			Literature survey on 5 studies (a, p)	Haidvogl et al. (2004)
25.6 & 28.5	2004	100-yr. event in Pottenbrunn & Lilienfeld, Lower Austria	Average depth of 0.5 m (a)	Haidvogl et al. (2004)
20	2003	Several floods in Austria	Analysis of 383 flood damages (p)	Kraus (2004)
9.8 / 22.5	2004	HOWAS database analysis: Flooded residential cellar / cellar & storey (p)		Merz et al. (2004a)
9.0 / 22.6	2004	Flooded residential cellar / cellar & storey (water) (p)		GVL (2004)
25.1 / 54.6	2004	Flooded residential cellar / cellar & storey (water & oil) (p)		GVL (2004)
11.9 / 38.7	2004	Flooded residential cellar / cellar & storey (p)		BWG (2004)

Loss functions for the transport infrastructure were approximated by BUWAL (1999a & b) and BWG (2002) by clean-up costs and by estimated amounts of sediment depositions. They assumed, that flow depths of less than 0.5 metres would cause no mayor depositions, and inundation depths up to two meters would leave a sediment layer of 0.25 metres.

The above described conversion led to an estimated clean-up cost of 17 € per cubic metre sediment which corresponded to 4.25 € per square metre flooded road and to 21 € per metre of flooded railway track. These loss magnitudes matched up to approximately 5 percent of the road building costs, summarised by Kraus (2004), with a range of 2.5 to 10 percent.

3.6.2 Loss analysis for the industrial and the commercial sector

The focus of the loss analysis for these two sectors was set on the damage to buildings and the inventory as well as on the losses associated with flood induced business interruptions.

The largest industrial and commercial objects in the study area were therefore identified, and managers were asked to give a questionnaire-based interview on possible physical flood impacts and their economic consequences. In order to improve the response quantity and quality, a face-to-face interview guidance was offered.

Another loss approximation method was applied, as the success of the interview campaign was highly depending on the voluntary cooperation of the managers and on the representative's capability to quantify possible flood damages.

Following the suggestions of BUWAL (1999b) and Booyesen et al. (1999), the losses were estimated by the product of the disruption duration and the average revenues of the affected businesses. Flood induced business interruptions were by that conceptualised as binary events. This was a rather rough assumption, as there will be a recovery phase between a complete standstill and the normal operation (Müller et al. 2005).

For the affected region, the business interruption losses were approximated by the interruption duration D in days, the number of affected workplaces n and the per-capita revenues of an average day r . For a particular flood scenario, those figures were added over s economic sectors.

$$L \cong \sum_s D_s n_s r_s \quad \text{Eq. 3.4}$$

This approach first required a functional relationship of the interruption duration and the flood intensity. In some ex-ante studies, relations between the business interruption duration and the inundation depth were used (LFI RWTH et al. 2005, Sönnichsen 2003). These relations presumably stem from ex-post analyses.

Müller et al. (2005) presented in their ex-post analysis how the disruption duration increases with the inundation depth. These data were obtained from a survey on German businesses hit by the August 2002 flood. The mean standstill time for inundation depths up to 0.5 m was 18 days, but it took approximately 55 days until a normal business state could be achieved. Inundation depths from 0.5 to 2 metres caused on the average 43 standstill days and about 85 days of recovery. However, there was a remarkable variability and skewness in the results, and the mean values were at least twice as large as the medians.

As the average inundation depths in the largest flood scenario was around half a metre, losses of a hypothetical standstill of one and tree weeks were computed.

Second, this approach required assumptions on the number of the affected workplaces in different economic sectors. The assumptions on the affected workplaces were based on the most recent employment statistics of the Austrian communities, dating back to May 2001 (Statistik Austria 2005b). As this communal data also referred to businesses located on higher grounds, further assumptions on the affected portion of workplaces were necessary.

And third, gross revenues (turnover) and the net revenues were recognised as the most suitable economic indicators. For these indicators, Statistik Austria (2005c) provided national per-capita averages for several sectors for the year 2003. The gross revenue was regarded as an absolute upper bound, since it also covers costs that may not arise during a standstill. Further, the gross revenues may account for particular goods more than once, if they were produced and purchased in the inundated area. The net revenue was used as a lower bound. It was defined as the turnover minus production costs under the consideration of taxes and subsidies (Statistik Austria 2005c).

3.7 Risk quantification

This chapter presents, how the analysis of hazards (Chapter 3.2 to 3.5) and the analysis of losses (Chapter 3.6) were combined for quantifying risks. These results were therefore summarised in the Risk Matrix (Table 3.8), indicating the loss estimate $L_{i,j}$ for each of the i considered objects and the j analysed scenarios. The risk matrix further provided the basis for computing the expected annual losses.

Table 3.8: Risk Matrix (Adapted from BUWAL 1999b)

		Scenarios S_j with $j = 1 \dots m$				
		S_1	...	S_j	...	S_m
Objects O_i with $i = 1 \dots n$	O_1					
	...					
	O_i			$L_{i,j}$		
	...					
	O_n					
Aggregated losses from scenario j				ΣL_j		
Return period of scenario j				T_j		
Expected annual losses		$E(L) = f(\Sigma L_j, T_j)$ with $j = 1 \dots m$				

Being aware of the limitations of the expected annual losses $E(L)$, as discussed in Chapter 1.3.3, this single metric was used to summarise the figures in the risk matrix. Its computation required a numerical approximation to Eq. 1.2, which was based on:

$$E(L) \cong \sum_{k=1}^k P_k L_k \quad \text{Eq. 3.5}$$

In Eq. 3.5, P_k indicates the occurrence probability of k possible losses, and for simplicity reasons, L_k stands for ΣL_k .

To solve Eq. 3.5, the j data pairs obtained by modelling were first complemented by assumptions on the return period of no loss occurring and on the losses for events exceeding the largest modelled scenario. Second, the interpolation of a large number of k data points (L_k, T_k) between the (L_j, T_j) pairs allowed the following approximation:

$$P_k \cong \frac{1}{T_k} - \frac{1}{T_{k+1}} \quad \text{Eq. 3.6}$$

By interpolating the k data points at each single year on the return period axis, Eq. 3.6 was re-written as:

$$P_k \cong \frac{1}{T} - \frac{1}{T+1} = \frac{1}{T(T+1)} \quad \text{Eq. 3.7}$$

Third, the losses L_j were interpolated correspondingly. This gave a stepwise-continuous expression $L_k = L(T)$, which was finally combined with Eq. 3.7 to:

$$E(L) \cong \sum_{T=1}^{\infty} L(T) \frac{1}{T(T+1)} \quad \text{Eq. 3.8}$$

The interpolation of $L(T)$ was performed by assuming L would increase stepwise linearly with T or with $\log T$, respectively.

An alternative approach to solve Eq. 3.8 was also tested, where the probability-weighted losses $L(T)/(T(T+1))$ of the j scenarios were interpolated at each single year on the return period axis to k data pairs. Again, a stepwise linear behaviour of L was assumed over T or over $\log T$, respectively.

The expected annual losses were first computed for the scenarios without structural or operational failure. Then, estimated probabilities were assigned to specific failure events, and the resulting changes in the expected losses were calculated. Finally, a hypothetical damage expectation was computed by assuming the protection system has not been built and the vulnerability of the floodplains corresponded to the 2005 land use.

4 Case study 1: Results

The results of case study 1 are presented as the outcomes of the hazard analysis, the loss analysis and the risk quantification, whereas the hazard analysis is split into the hydrologic and hydraulic analysis.

4.1 Hydrologic analysis

The hydrologic results first detail the analysis of extreme rainfall patterns, the design rainfall and the areal rainfall reduction. Then, the outcomes of the rainfall runoff modelling are presented and finally, the probabilities of peak flows are estimated.

4.1.1 Analysis of extreme rainfall patterns

The research on 21 local extreme rainfall events showed rather a wide possible range of hyetographs than one typical rainfall characteristic. On one hand, the variability in the rainfall duration, the temporal intensity pattern and the antecedent precipitation was very large, and on the other hand, the sample was rather small. This however, allowed a parameter estimation suitable for rainfall runoff modelling but no stochastic analysis of the extreme rainfall attributes.

Most of the analysed events occurred in July, August and October, but also a few winter floods were on record. The most critical general weather situations in the summer season were Mediterranean depression systems of the Vb type, like the extreme events in August 2002 and 2005.

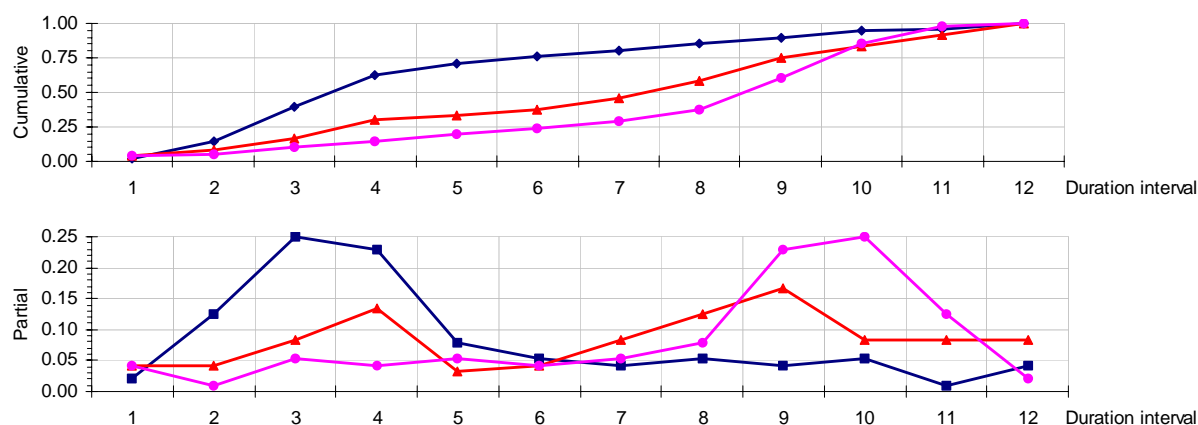
Most of the temporal rainfall intensity distributions could be described by one of the patterns presented in Table 4.1. Higher rain intensities at the end of the main precipitation event appeared slightly more frequently. In contrast, three out of the seven largest runoff situations were driven by rainfall with the highest intensities in the beginning, combined with large pre-event precipitation. The analysis further showed wide ranges of event durations and of average intensities, so a set of various possible rainfall scenarios was defined.

Table 4.1: Rainfall intensity patterns of the 21 analysed events

Rainfall intensity pattern	Number of events
Highest intensities in the beginning	4
Little intensity variation and weakly pronounced ends	6
Highest intensities in the end	7
No data available with appropriate temporal resolution	4

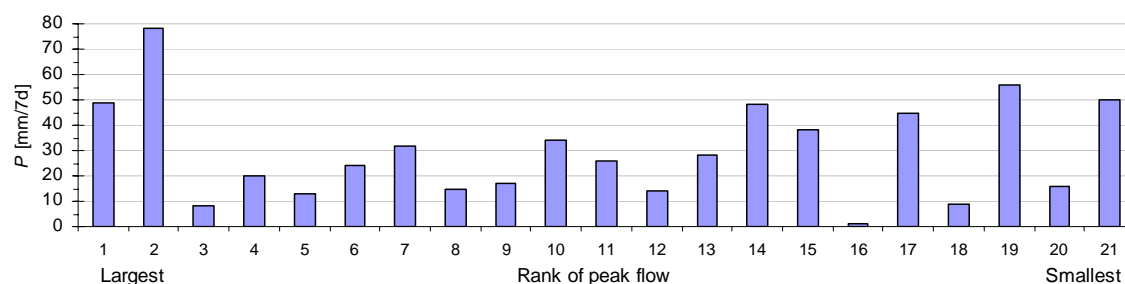
The three possible temporal rainfall intensity patterns were then conceptualised by the curves shown in Figure 4.1. For rainfall runoff modelling, they were applied to the extrapolated 12-hour rainfall depths and analogously to the 24 and 48-hour events. They characterised storms with one peak at the beginning, one peak at end and two weakly pronounced peaks, respectively.

Figure 4.1: Cumulative and partial distribution of rainfall intensities over the rainfall duration



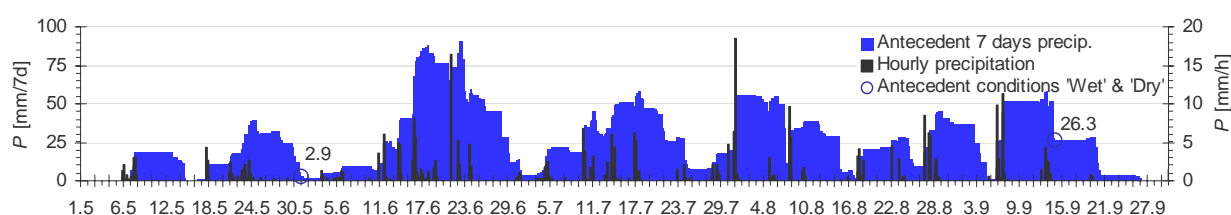
The seven-days antecedent rainfall (Figure 4.2) ranged from 1 to 78 mm, with a mean of 30 mm, and a standard deviation of 19 mm. In some cases, the distinction between event rainfall and antecedent rainfall was based on a rather subjective judgement. However, the variability of antecedent conditions was accounted in the modelling process by defining two initial soil moisture conditions that represented a wet state and a dry state.

Figure 4.2: Seven-day antecedent rainfall of 21 analysed events



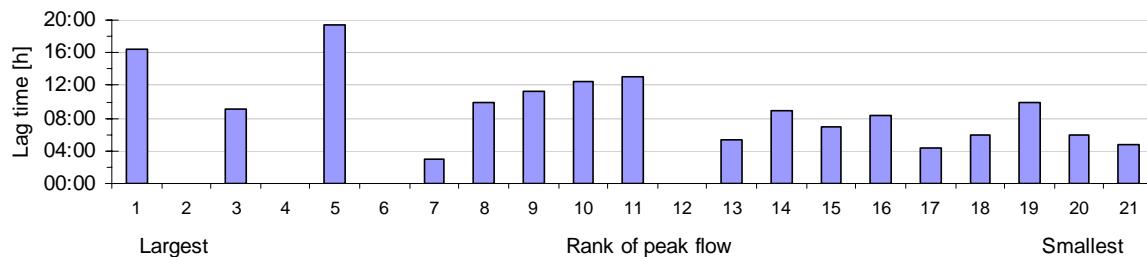
The initial soil moisture conditions in the rainfall runoff modelling were computed from continuous hyetographs, where a part of the observed May to September 1997 series was substituted by the design rainfall events (Figure 4.3). For the dry state, the beginning of the design events was set to June 1, with 2.9 mm of seven-day antecedent rainfall. For the wet state, the beginning of the design events was set to September 15, corresponding to 26.3 mm of seven-day antecedent precipitation. In comparison with the antecedent rainfall in the SCS-CN method (Soil Conservation Service, Curve Number) and the observed average, the used values seemed relatively low. The SCS-CN method comprised three classes of five-day pre-event rainfall and defined 30 to 50 mm for the intermediate soil moisture class. This class was recommended for rainfall runoff modelling (DVWK 1984).

Figure 4.3: Observed hourly rainfall, seven-days antecedent rain and the definition of the antecedent soil moisture conditions 'Wet' and 'Dry'



The average lag time was twelve hours, but it showed a large variability (Figure 4.4). The lag times of the largest events on record were substantially higher, or not reproducible from the temporal data resolution. As the lag time and the observed storm durations showed a large variability, it seemed reasonable to model a range of rainfall durations, from a few hours up to two days.

Figure 4.4: Lag time of 21 analysed flood events



4.1.2 Design rainfall

The extrapolated design rainfall depths are summarised in Table 4.2. The average rain depths of the extrapolated gauges are plotted versus the rainfall duration in Figure 4.5. On the average, the 1,000-year rainfall events exceeded the 100-year rain depths by 35 %. This ratio amounted to 67 % for the one-hour rainfall, and it ranged around 30 % for all other rainfall durations. This divergence of the one-hour data had no influence on further computations, since the one-hour rainfall was recognised as not critical.

At the Rechberg rain gauge, the average of 1,000-year rainfall events was 59 % larger than the 100-year events, and at the Weiz gauge, this figure was 15 percent. At all other stations, this figure was somewhere in between those two levels.

Table 4.2: Extrapolated 100 and 1,000-year point design rainfall depths in mm

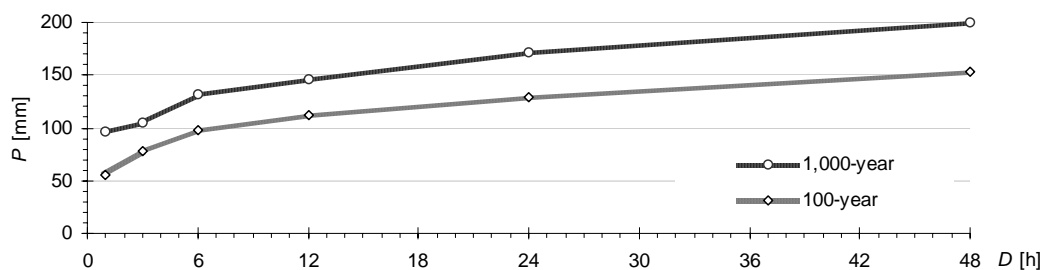
<i>T</i> = 100 a						
Duration [h]	1	3	6	12	24	48
Rechberg	94.8	135.4	168.5	195.6	242.2	267.8
Schöckl	48.5	69.2	86.7	99.1	111.5	146.6
Laßnitzhöhe	45.0	62.9	78.6	91.1	114.2	129.9
Gleisdorf	40.9	56.7	71.4	82.9	87.1	111.3
Weiz	46.3	64.2	81.0	93.7	92.6	112.6
Average	55.1	77.7	97.2	112.5	129.5	153.6
<i>T</i> = 1,000 a						
Duration [h]	1	3	6	12	24	48
Rechberg	200.1	209.1	263.3	291.8	347.5	371.6
Schöckl	85.8	89.9	113.4	125.6	138.9	183.8
Laßnitzhöhe	59.0	81.7	103.4	113.8	148.9	177.9
Gleisdorf	70.9	74.0	93.8	103.2	108.4	139.7
Weiz	65.4	68.5	86.2	95.5	113.2	127.7
Average	96.2	104.6	132.0	146.0	171.4	200.1

Remarkable were the larger design rainfall depths for the Rechberg gauge. One outlying event in the underlying data might explain these values, since extraordinary large data for Rechberg were not found in other precipitation characteristics, such as the largest observed daily precipitation (Table 3.1), the average annual totals and the convective design rainfall depths (BMLFUW 2005b).

The extrapolated design rainfall depths (Table 4.2) were not further adjusted to meet the demand for a monotonous increasing rain depth with the increasing rain duration. This demand was fulfilled by the averages (Figure 4.5) but not by the extrapolated data of all rain gauges. In particular, the 24-hour figures of Weiz seemed rather uncertain. In a more detailed analysis, the extrapolated design rainfall data should be adjusted to a monotonous behaviour. However, as only a few stations and rainfall durations were affected by this uncertainty, this issue was not further resolved.

For obtaining longer data series and for a better description of the temporal rainfall behaviour, it might be reasonable to have a look at adjacent stations with a high temporal resolution and to use analogue data. This might provide series of up to 100 years.

Figure 4.5: Average extrapolated 100 and 1,000-year point design rainfall depths



A comparison of these extrapolated rainfall data with the design values of Kreps and Schimpf (1965) showed that for some stations, Kreps and Schimpf estimated rather smaller data for shorter durations and larger data for 24 and 48 hours.

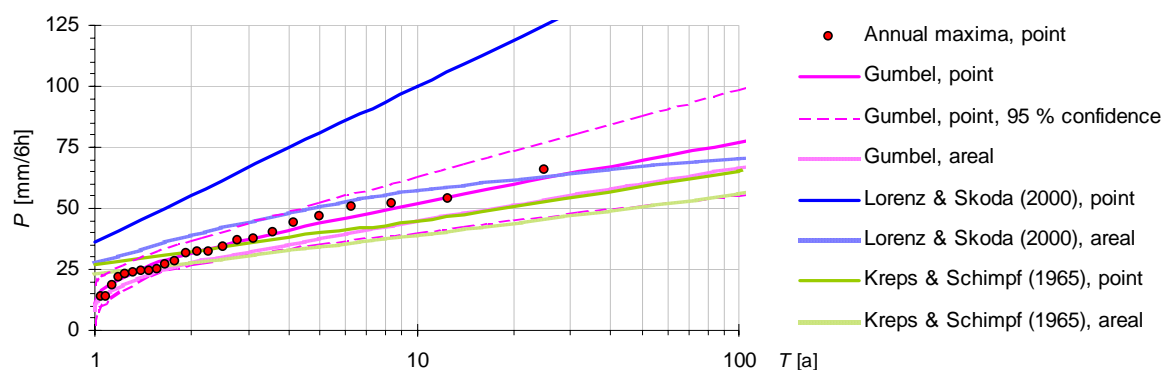
Assigning probabilities to the transformed August 2002 rainfall event revealed two issues. The largest August 2002 aggregates of up to twelve hours corresponded to ten to hundred-year events, but the 24 and 48-hour totals exceeded the extrapolated 1,000-year magnitudes partly far. Still, the Probable Maximum Precipitation estimates were much larger than the transformed 2002 event.

4.1.2.1 Areal rainfall reduction

Applying different areal reduction methods to the available design point rainfall data diminished the large deviation of the Lorenz and Skoda (2000) data from other design values and resulted in reasonable design data (Figure 4.6).

The deviation of the design rainfall data also showed the importance of selecting an appropriate areal rainfall reduction method. The current discussion on the most suitable point design rainfall data should therefore be accompanied by the discussion on adequate areal rainfall reduction methods. Attempts were made for instance by Sivapalan and Blöschl (1998), who included the correlation length of observed local extremes in the areal design rainfall computation.

Figure 4.6: Six-hour point- and areal design rainfall depths at gauge Laßnitzhöhe



4.1.3 Rainfall runoff modelling

Rainfall runoff modelling produced hydrographs of the rivers Raab and Rabnitzbach in a one-hour resolution. Most influential on inundation hazards was the discharge at Raab River, which is characterised in Table 4.3. Comparative magnitudes for evaluating the simulated peak flows were the protection system's 100-year design magnitude of 200 m³/s (Stubenvoll 1994), and the 5,000-year design value for the spillway of the flood retention basin with 400 m³/s (Sackl 1995). The simulated peak flows therefore ranged from amounts that should be handled safely by the protection system up to the two-fold of the design magnitude, where wide areas of the hinterland were expected to be flooded.

At rain durations of six hours and more, the 1,000-year rainfall events produced on the average 77 % larger peak flows than the 100-year events, if the antecedent soil moisture conditions were dry. Wet antecedent conditions caused an average increase of 40 percent.

Table 4.3: Overview of the modelled hydrographs of River Raab

Model rainfall event: Duration [h], temporal pattern		Average return period T of rainfall [a]	Peak flow Q_{max} [m ³ /s]		$\frac{Q_{max}(T = 1,000)}{Q_{max}(T = 100)}$		$\frac{Q_{max}(Wet)}{Q_{max}(Dry)}$
			Antecedent conditions		Antecedent conditions		
			Dry	Wet	Dry	Wet	
1	Constant intensity	100	13	134	7.2	2.3	10.3
		1,000	94	304			3.2
3	Constant intensity	100	57	232	2.3	1.5	4.1
		1,000	132	341			2.6
6	Constant intensity	100	111	290	1.9	1.4	2.6
		1,000	216	420			1.9
12	Peak at beginning	100	117	272	1.7	1.4	2.3
		1,000	199	370			1.9
	Peak at end	100	155	341	1.7	1.4	2.2
		1,000	260	461			1.8
	Two moderate peaks	100	136	278	1.7	1.4	2.0
		1,000	225	376			1.7

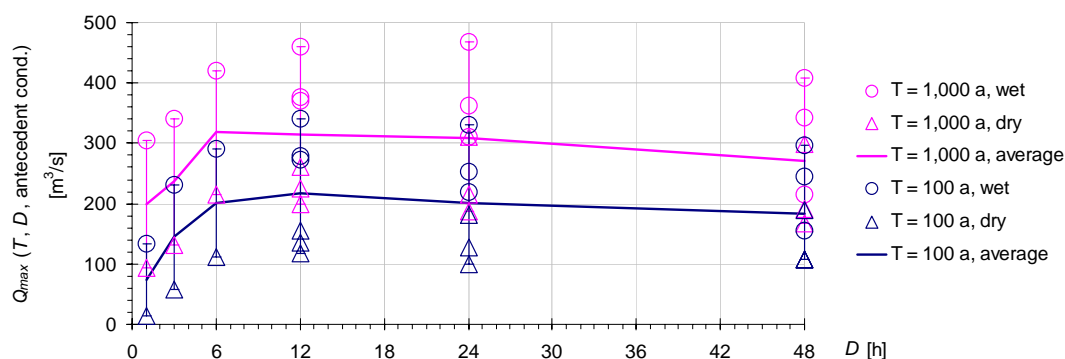
Model rainfall event: Duration [h], temporal pattern		Average return period T of rainfall [a]	Peak flow Q_{max} [m ³ /s]		$\frac{Q_{max}(T = 1,000)}{Q_{max}(T = 100)}$		$\frac{Q_{max}(Wet)}{Q_{max}(Dry)}$
			Antecedent conditions		Antecedent conditions		
			Dry	Wet	Dry	Wet	
24	Peak at beginning	100	99	252	1.9	1.4	2.5
		1,000	187	362			1.9
	Peak at end	100	181	331	1.7	1.4	1.8
		1,000	310	468			1.5
	Two moderate peaks	100	128	219	1.7	1.4	1.7
		1,000	216	311			1.4
48	Peak at beginning	100	108	245	1.8	1.4	2.3
		1,000	191	342			1.8
	Peak at end	100	189	296	1.6	1.4	1.6
		1,000	299	409			1.4
	Two moderate peaks	100	107	155	1.6	1.4	1.4
		1,000	168	215			1.3
Transformed Aug. 2002 event			400	509			1.3

Wet antecedent soil moisture conditions led to flood peaks, which were on the average twice as large as under dry conditions. The biggest floods were further computed from events with rain intensity peaks at the end. Averaging all modelled events, these peak discharges were 41 % larger than those from rain intensity maxima at the beginning, and they were 50 % larger than the peak flows caused by two moderate rainfall intensity peaks.

The peak discharges were then analysed with respect to the rainfall duration (Figure 4.7). It appeared that durations below six hours were not crucial, and that the average peak flows from 100 and 1,000-year storms grouped around 200 and 300 m³/s, respectively. Influences of the rainfall duration on the peak flows were therefore only weakly pronounced, when the average curves were considered for durations larger than six hours.

The transformed August 2002 event was modelled with both antecedent moisture conditions. As wet antecedent conditions would twice account for the soil saturation, wet conditions were regarded as not plausible. Further discussions of the transformed August 2002 scenario therefore refer to dry antecedent conditions, where the peak flow corresponded to the reservoir spillway's 5,000-year design value.

Figure 4.7: Peak flows at Raab River for different rainfall durations



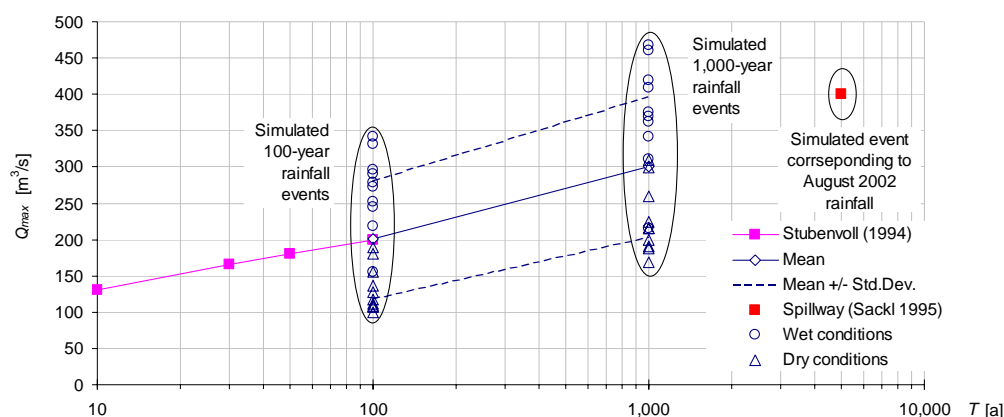
4.1.4 Probability estimation of peak flows

This chapter informs on the probability estimates that were assigned to the simulated flood scenarios. The estimation was based on the average peak discharges of the simulated 100- and 1,000-year rainfall runoff events from 6 to 48 hours rain duration and on external hydrologic expertises. The averaged model results and the design values for the protection system (Stubenvoll 1994, Sackl 1995) were found in a good compliance (Figure 4.8). By that, the 100- and 5,000-year peak discharges of 200 and 400 m³/s were confirmed, and in addition, a 300-year peak flow was estimated with 250 m³/s and a 1,000-year peak flow with 300 m³/s.

Primarily, the data variability in the modelled 100- and 1,000-year peak flows in Figure 4.8 seemed rather large. This variability was quantified by coefficients of variation of 41 and 32 percent, respectively. In comparison, the standard errors in the Gumbel peak flow statistics at gauge Takern II amounted to 13 and 14 percent.

Yet, the variability in the rainfall runoff results shall not be understood in a stochastic sense, since only the rainfall depths, but neither the antecedent soil moisture nor the temporal rainfall patterns, were assigned to a probability. Theoretically, this stochastic estimation could be obtained from a correlation analysis of the antecedent soil moisture conditions, the temporal variation of rainfall intensities and the rain depths. Practically, the small sample of recorded extremes did not reveal this information.

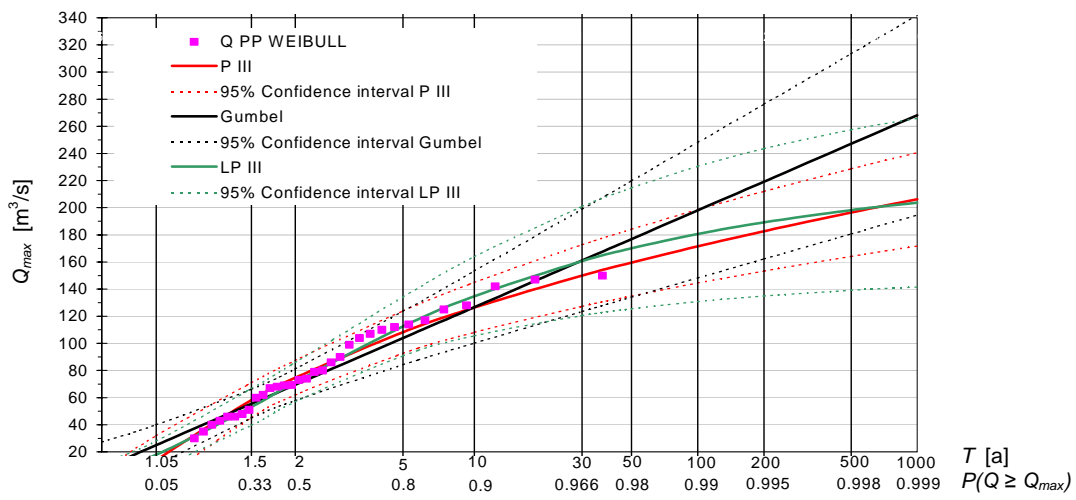
Figure 4.8: Data for probability estimation of Raab River peak flows



The annual peak flow statistic for gauge Takern II showed comparative magnitudes of a 100-year event (Figure 4.9). The Gumbel extrapolation revealed a 100-year event of 200 m³/s and a 30-year event of 160 m³/s. For larger return intervals, the rainfall runoff modelling provided higher peak flows than the flow statistics. The Pearson (P III) and Log-Pearson distribution (LP III) returned smaller values and were understood as less plausible.

The good compliance of 100-year flows seemed rather surprising, since the flow gauge's catchment amounts to 498 km², and the modelled Raab basin area upstream Gleisdorf covered 352 km². These results could partly be explained by the natural retention in the relative wide floodplains and the application of different analysis methods and data. Deviations were further presumed to originate in implicitly conservative assumptions in estimating the design rainfall events, in the parameter estimation of the rainfall runoff model and in the uncertainties, associated with the measurement of extremes.

Figure 4.9: Annual peak flow statistics for gauge Takern II



4.2 Hydraulic analysis

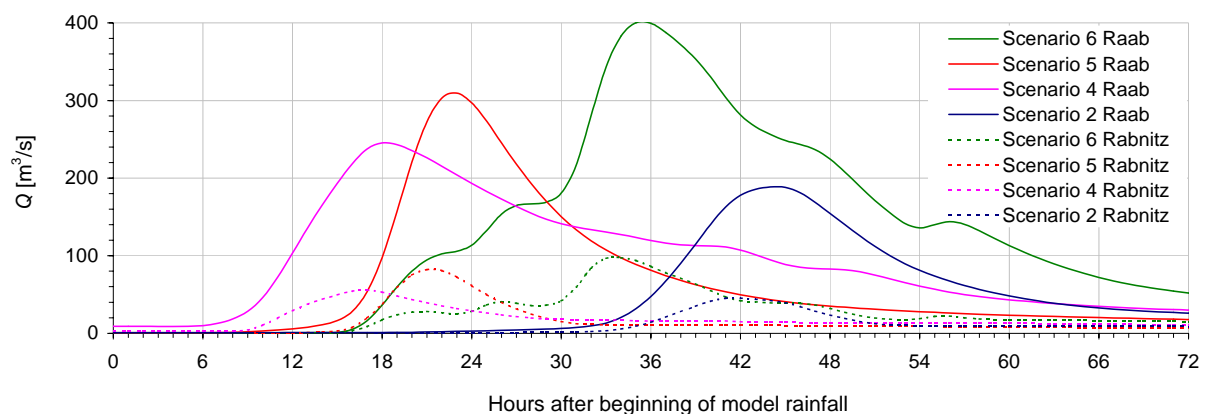
This chapter presents the results of the analysed flood scenarios. It first covers the findings from the hydrodynamic modelling of the rainfall runoff events in Table 4.4 (Chapters 4.2.1 to 4.2.4), and then, it illustrates the outcomes from further quantitative and qualitative analyses (Chapter 4.2.5 to 4.2.7).

Table 4.4: Selected rainfall runoff events for hydrodynamic modelling

Scenario	Antecedent soil moisture conditions	Areal design rainfall, 5 station average [mm]	Temporal design rainfall intensity	Rainfall duration
2, 3 & 8	Dry	131	Peak at end	48 h
4	Wet	110	Peak at beginning	24 h
5	Dry	145	Peak at end	24 h
6 & 7	According to transformed Aug. 2002 hyetographs	230	According to transformed Aug. 2002 hyetographs	54 h

For hydrodynamic modelling, the hydrographs of the rivers Raab and Rabnitzbach were defined as inflow boundary conditions to the hydraulic model domain (Figure 4.10). Although calibration data for the hydraulic model were not available, observations of the August 2005 flood were used to complete and discuss the model results.

Figure 4.10: Raab and Rabnitzbach hydrographs of selected rainfall runoff events



4.2.1 Scenarios without technical and operational failure

The results of the hydrodynamic modelling are mapped as the maximum flow depths and the inundation extents (Appendix: Inundation maps of case study 1). In nearly all of the modelled scenarios, the animation of the hydraulic computation results showed similar temporal inundation processes. Therefore, the most important results are outlined in Table 4.5 with increasing flow magnitudes. The indicated discharges describe the Raab River inflow into the model domain at km 67 and the local flow magnitudes, wherever they are more relevant.

Table 4.5: Inundation process with increasing flow at Raab River

Flow [m ³ /s]		Description of overflowing and inundated areas
km 67	Local	
60		Restructured reaches in between the levees are inundated.
70		Inundation of the left Raab bank upstream the protection system, reaching inland to the railway embankment and flooding a non-permanent greenhouse
< 140		In case of a bridge jam, right bank overflowing upstream the B 65 Bridge, affecting one residential building
140		Starting inflow into the flood retention basin
	150	In case of a bridge jam, left bank overflowing upstream the B 65 Bridge, affecting several residential, commercial and industrial buildings
		Left and right bank overflowing downstream the levee system: inundation of areas close to the mouth of the left tributary Gleisbach and wide ranges of the floodplains that are mainly used for agriculture
		Right bank overflowing up the upstream weir and inundation of extensively used areas
	150 - 160	Right bank overflowing upstream the B 65 Bridge, affecting one residential building
		Flood detention in the retention basin begins
	170	Inundation of the main road B 65 and a farm at the right bank
220 - 250	180	Overflowing of the left bank concrete floodwall upstream the main road B 65 into built areas. Overflowing of the left bank directly downstream the bridge
		Inundations along the reservoir outflow trench due to exceeding its bankfull discharge capacity and the activation of the spillway. Overspilling water is retained at the railway embankment
250 - 280		Overflowing of the left bank levee close to the industrial areas, starting at km 66.5. Inundation of industrial and commercial buildings
		Inundations of large parts of the low-lying Gleisdorf areas on both banks. Railway and highway embankments govern hinterland inundation flows
290 - 360		Uncontrolled flows over the retention basin impoundment dam: inflow from River Raab at km 66.5 and backflow from the basin at km 65.5

In general, that the protection system worked well in the simulations, as it prevented the largest built areas from being flooded by a 100-year flow at Raab River. Nevertheless, the protected areas were still exposed to residual flood hazards. Although the scenario definition and the assessment methods in this analysis and in the design of the flood protection system (Turk 1996 & 1997) diverged, the similarity of the affected areas was remarkable.

4.2.1.1 Flow velocities

The hydrodynamic simulations pointed out, that the largest flow velocities in the developed areas did generally not coincide with larger inundation depths. Local velocities up to 2 m/s were found where water flows over low road embankments and where the flow was constricted by road- and railway dams. Higher velocities combined with larger depths occurred in flooded underpasses and in the main rivers.

The product of depth and velocity represented the flow velocity's influence on the flood intensity and the flood losses (Figure 2.1, Table 3.5). These maximum products were in the

range of $0.3 \text{ m}^2/\text{s}$, corresponding to the low flood intensity in the classification of BWV et al. (1997). So the governing criterion for the loss estimation was the maximum inundation depth.

4.2.2 Bridge jam scenario

Jammed bridges turned out as a significant increase to flood hazards. According to local observations, the occurrence of floating debris from various sources was likely to occur during extreme events. In the simulation with jammed bridges, overtopping incurred at lower discharges, inundation depths were larger and built areas at the left bank were more likely affected (Figure 4.11). The inundated areas due to a 100-year flow with jammed bridges were only slightly smaller than the affected areas at a 300-year event without any jams. Although the applied assumptions were rough, the impacts are clearly to see.

Figure 4.11: Inundations without (l.) and with jammed bridges. The exposed B 65 Bridge is marked (r.)



4.2.3 Levee failure scenario

In the investigated levee breach scenario, large parts of the left bank floodplains were already inundated antecedent to the failure. Within several minutes after the assumed collapse, high flow velocities, at least 2.5 m/s , occurred close to the breach location. The scenarios without and with a levee failure (Scenario 6 & 7) showed a relative good compliance of the inundated areas, although slightly higher flow depths followed the simulated breach. It seemed as if the region exposed to residual flood hazards was mainly determined by the topography, since higher discharges in the left bank floodplain did not significantly expand the inundated area.

4.2.4 Failure scenario of weirs

Flow simulation with one closed weir gate at the upstream barrage showed a strong re-distribution of the discharges. The maximum flows were $135 \text{ m}^3/\text{s}$ through the opened weir gate and $30 \text{ m}^3/\text{s}$ over the closed weir gate. The upstream water levels were up to one meter higher than under proper conditions and reached exactly the bankfull level. Nevertheless, the model did not show any additional inundation in the protected areas. The closed weir gate reduced the bankfull discharge by about $1/3$, from 220 to $140 \text{ m}^3/\text{s}$. Although modelling did not show a dramatic inundation in this scenario, the dependency of the protection system's reliability on the opening of the weir gates was clearly revealed.

The August 2005 Raab flood showed two additional issues at the upstream weir that were not revealed by the simulations.

First, the observed immediate up- and downstream water levels were higher than what would be expected from the simulations. These deviations might be caused by model generalizations and parameterisations and by the sedimentation of fresh bed load downstream the weir. Bed load was deposited during the flood event, so the actual cross section geometries differed from those surveyed in Spring 2005.

Second, the inundation damages adjacent to the weir were not caused by water flowing over protection structures but by the flow through openings below the river water surface, that were not designed or executed thoroughly. This in turn is hardly ever considered in modelling, since it would require large efforts in data gathering and analysis. However, it illustrated the importance of incorporating the local observations and the lessons learned from failure events in the definition of flood hazard scenarios.

4.2.5 Bank vegetation scenarios

The flow computation presented in Chapter 3.5.5 allowed a quantitative assessment of discharge situations under changed bank- and floodplain vegetation scenarios. These computations were further used for an appraisal of the frictional coefficients implemented in the hydrodynamic model.

The computations for four cross sections confirmed the selected Manning-Strickler frictional coefficients, although these figures based on estimates and not on calibration data. The flows computed by the method of Lehmann (2005) for the cross section at km 65.389 were 3 % to 15 % smaller than what was obtained by the Manning-Strickler equation. This interval corresponded to the plausible range of the equivalent absolute surface roughness of the riverbed. At the cross section at km 65.915, the flow derived with Manning-Strickler was also found within this plausible range.

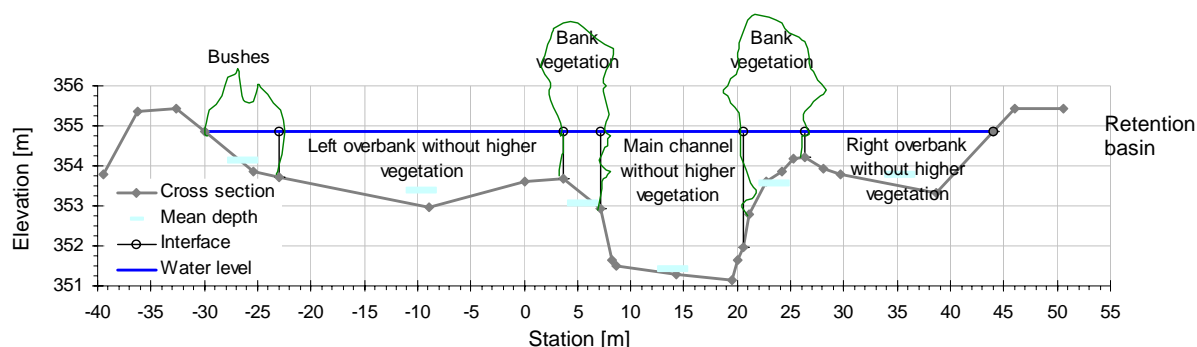
The variation of the average plant spacing and the diameter of the current bank vegetation revealed the impacts of possible plant succession on the flood discharge. A particular focus was set on the expansion of higher rigid plants to the open flow areas and on the development of a dense perennial vegetation cover.

The reduction of the spacing of the higher bank vegetation elements lead to a slight to moderate flow increase at the cross sections at km 65.200 and at km 65.060. A larger spacing again caused lower flows, whereas increasing the diameters and reducing the spacing surprisingly produced a slight flow increase. These unexpected results could be physically explained by a decreasing mass- and momentum exchange between the main channel and the vegetated banks and by the formation of a compact active flow subdivision at the main channel with a smaller wetted perimeter. However, it was not clear if Lehmann's method considered this phenomenon. Increasing only the vegetation diameters caused the expected flow reduction up to 25 %, which corresponded to the discharge limitations after the simulated bridge jam.

The investigations of all cross section showed that the 2005 vegetation state imposed no considerable reduction to the designed flow capacities. Vegetation development on the shoulders of the riverbanks can therefore be tolerated as long as the current open flow subdivisions are maintained. In general, the vegetation influence on the flood discharges was about as large as the influence of the estimated equivalent absolute main channel roughness.

The cross section at the downstream end of the lateral weir, which feeds the retention basin, is shown in Figure 4.12. It comprises a main channel and wide overbanks covered with grassland and strips of perennial vegetation. The flow velocities in these strips reached up to 0.1 m/s, so these corresponding discharge amounts were negligibly small. Also possible sediment depositions were not crucial.

Figure 4.12: Cross section at km 65.915: Homogenous flow subdivisions with higher plants and areas without higher vegetation



Uncertainty estimates for these computations were derived from increasing the equivalent absolute roughness of the main channel bed from 0.15 to 0.3 m and of the overbanks from 0.3 to 0.4 m. The first change reduced the flow in the main channel by 10 percent and the total flow by 6 percent. The second change at both overbanks caused a 20 % and a 8 % flow reduction in the left and right overbank, respectively. This corresponded to a 6 % total discharge decrease.

Table 4.6 summarises the discharges for the 2005 state and the flow reductions due to scenarios of different plant spacings and diameters. It appeared that solitaire trees, placed in a rather large distance, and plant rows in the main flow direction did not change the flow capacity substantially. A closed vegetation cover in the overbanks instead caused a considerable discharge reduction.

Table 4.6: Cross section at km 65.915: Flows under the current conditions (2005, row 1) and flow changes due to different vegetation scenarios

Vegetation			Flow					
Plant spacing		Mean plant diameter	Left overbank		Right overbank		Total	
in flow direction	transverse to flow		flow	reduction	flow	reduction	flow	reduction
a_x [m]	a_y [m]	d_m [m]	Q_l [m ³ /s]	ΔQ_l [m ³ /s]	Q_r [m ³ /s]	ΔQ_r [m ³ /s]	Q_{tot} [m ³ /s]	ΔQ_{tot} [m ³ /s]
-	-	-	41	-	12	-	141	-
10	10	0.1	40	- 2 %	12	0 %	140	- 1 %
3	3	0.1	34	- 17 %	11	- 8 %	133	- 6 %
1	1	0.1	17	- 59 %	7	- 42 %	112	- 21 %
1	1	0.3	7	- 83 %	3	- 75 %	98	- 30 %
1	10	0.1	37	- 10 %	11	- 8 %	136	- 4 %
1	10	0.3	31	- 24 %	10	- 17 %	129	- 9 %

The relative results in Table 4.6 are more significant than the absolute flow figures, as the obtained numbers were subjected to some parametric uncertainties, and assumptions were made for the ground slope. These assumptions were necessary since the survey's invert slopes were considerably larger at the adjacent cross sections, which would produce flows magnitudes beyond the plausible range.

Although the results of Table 4.6 complied reasonably well with the hydrodynamic model results, the underlying surface roughness estimates might be too large. The observed

discharges of the August 2005 event were in the range of 131 to 148 m³/s, but the observed water levels were about half a metre lower than what appeared from all calculations. These flow data referred to the closest up- and downstream gauges (R. Schatzl, personnel comment, 2005-11-14).

4.2.6 Flood retention basin failure scenarios

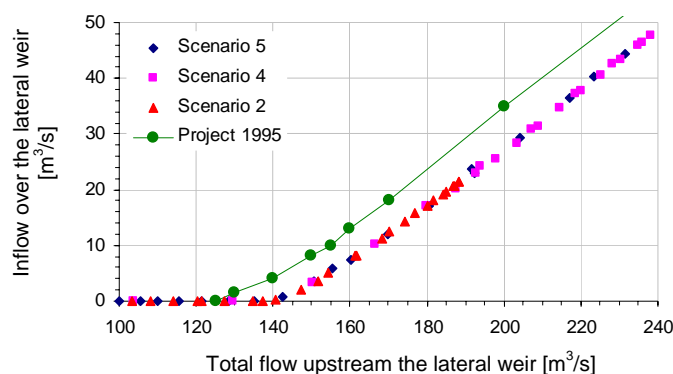
The analysis of the flood retention basin revealed an issue at the lateral inflow weir. The weir was designed for being activated at 125 m³/s, corresponding to a ten-year event, but the actual magnitude might be larger. The hydrodynamic computations suggested 140 m³/s for this activation flow. From the August 2005 observations, it may be gathered that this magnitude might be even higher.

This issue was not based on diverging geometry data since the weir crest levels, as planned and as derived from the digital elevation model, diverged by less than five centimetres. These data sources corresponded surprisingly well.

Furthermore, the only major difference between modelling steady conditions at 200 m³/s, and an unsteady flow with a 189 m³/s peak was the maximum filling of the retention basin. The hygrograph's peak presented as Scenario 2 in Figure 4.10 was rather flat, and corresponded to a large volume, but nevertheless the reservoir was not significantly filled.

These findings implied that the weir crest might have been too high and that the detention would be activated too late and perhaps by an insufficient amount (Figure 4.13). Conservative assumptions in the design phase, such as using relative large frictional loss coefficients, could account for these findings. But there is doubt if this issue would have been exhibited so clearly from the results of not calibrated models. These findings demonstrated that an accurate design of a lateral weir is highly dependent on an appropriate water surface modelling. Performing a sensitivity analysis with varying roughness coefficients could lead to a more robust design, if calibration data is not available.

Figure 4.13: Discharge at the Raab River and the inflow into the retention basin over the lateral weir according to the 1995 project (Sackl 1995, Turk 1996) and to the scenario results



In the early phase of this analysis, the controlled opening of the retention basin's base outlet appeared as a possible option for managing residual flood risks, since there were less sensitive land-uses at the right bank, downstream the reservoir. The simulations showed, that this would not have the intended effect, as the lateral weir limited the inflow into the retention basin. And the retention basin water level, which might be controlled, had little influence on the inflow. Still, adapting the existing weir and constructing an additional overflow structure could reduce the flow at the critical Raab River reaches. Conveying a larger fraction of the total Raab discharges into the retention basin would reduce the residual flood hazard, which is arising from an uncontrolled overflowing of the left bank levees that protect the industrial and the residential areas.

Finally, the reservoir's spillway and the base outlet appeared as rather robust structures compared to the alternative construction types discussed in Krainer (2003). An unintended closing or a jamming of the outlet's underflow sluice gate would increase the likelihood of activating the spillway. This scenario was not in particular modelled, since overflows were already considered as part of the scenarios without technical and operational failure (Chapter 4.2.1).

4.2.7 Hinterland inundation scenarios

Another phenomenon was observed during the August 2005 flood, which lay beyond the modelled processes. Local inundations occurred from precipitation with high intensities in the immediate Gleisdorf region. 149 mm of rain were measured in Gleisdorf from August 20, 12:00 a.m. to August 22, 7:00 a.m. (Tibet and Paar 2005). This occurred simultaneously with high flows at Raab River. Smaller and partly culverted tributaries spilled over, and they could not drain into the main rivers. Other local inundations were caused by small changes in the draining trenches as part of road construction works. These observations pointed out, that the defined and analysed flood scenarios should as well cover small, local storms in conjunction with human interventions in the floodplain.

4.2.8 Conclusions on the hydraulic analysis

Generally speaking, the applied hydraulic modelling tools proved suitable for simulating hydrologic extremes as well as failure events, and they mostly provided credible results. In many areas, the simulated inundations were confirmed by the August 2005 observations. Nevertheless, a few issues deserve further attention.

First, the cross section survey did not cover all the details that turned out as substantially influencing the inundation flows, such as culverts in the hinterland and underpasses. This required some inevitably subjective definitions and assumptions that were associated with some uncertainties. Further assumptions were necessary for the hydraulic effects of railway embankment dams that were built from coarse gravel. However, the model accuracy could be refined to some extent for instance by conducting a second survey session after the first results were available.

Second, most hydraulic simulations considered discharges over dams and walls, but possible flow paths through structures remained concealed. This issue appeared at the upstream weir, as discussed before, and also in areas that were flooded in August 2005, where the model did not produce any flow. These areas were located in the floodplain of Rabnitzbach River, and it can be assumed that these inundations originated from openings in an elder levee.

And third, the absence of calibration data caused surprisingly small deviations from the water levels that were observed in August 2005.

4.3 Loss analysis

This chapter presents the outcomes from the direct loss analysis and from the loss analysis for the industrial and the commercial sector. Flood losses were estimated for the scenarios with particular average return periods. In general, the loss estimation procedure produced credible results and outcomes subjected to large uncertainties.

4.3.1 Direct loss analysis

Direct losses were estimated for five building classes, for roads and for railway lines. The number of the affected buildings was low for the 100-year event, but it rapidly increased, as the mixed-use areas and industrial areas were inundated (Table 4.7).

Table 4.7: Number of affected buildings

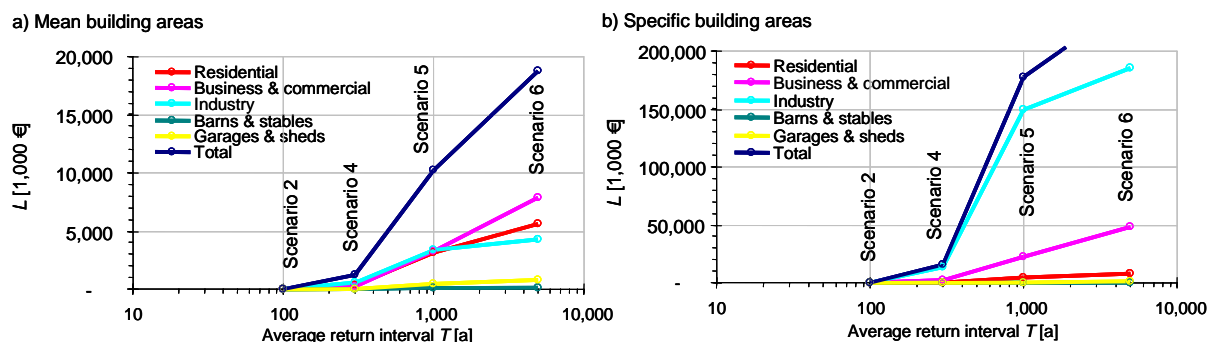
Scenario, average return interval, building class	Scenario 2 $T = 100$ a	Scenario 4 $T = 300$ a	Scenario 5 $T = 1,000$ a	Scenario 6 $T = 5,000$ a
Residential	1	26	134	198
Business & commercial	-	8	63	93
Industrial	-	11	24	31
Barns & stables	-	4	7	8
Garages & sheds	-	17	109	170
Total	1	66	337	500

Cumulative and average monetary loss estimates were derived by

- using an average building area suggested in BUWAL (1999a) and BWG (2002)
- accounting for the specific building area.

The totals of the computed losses to all affected buildings are plotted in risk curves (Figure 4.14), and they are summarised in the risk matrix (Table 4.8).

Figure 4.14: Frequency of cumulated direct losses, estimated by two methods



In both methods, barns and garages provided the smallest amounts of damage. Within the average building area approach a), the major fractions of the total losses were spread

similarly over the residential, the commercial and the industrial building classes. Considering the specific building areas b), the industrial and the business sector's losses prevailed by far.

Table 4.8: Risk matrix: Cumulated direct losses to buildings, estimated by two methods

Cumulated losses in 1,000 €, building class, estimation method		Scenario 2: T = 100 a	Scenario 4: T = 300 a	Scenario 5: T = 1,000 a	Scenario 6: T = 5,000 a
Residential	a)	45	364	3,103	5,598
	b)	25	540	4,624	7,868
Business & commercial	a)	-	224	3,221	7,870
	b)	-	1,766	21,984	48,024
Industrial	a)	-	532	3,406	4,291
	b)	-	13,103	149,609	185,039
Barns & stables	a)	-	50	98	140
	b)	-	348	418	483
Garages & sheds	a)	-	19	428	817
	b)	-	11	361	860
Total	a)	45	1,190	10,255	18,715
	b)	25	15,768	176,995	242,274

The plausibility of these results was evaluated by means of the average losses per affected building (Table 4.9). The figures for residential buildings, garages and sheds appeared most credible, no matter which estimation method was used. Beside the results for one small and relative deeply flooded residential building in scenario 2, the approach b) provided larger losses. Estimation method b) appeared as more accurate for residential buildings, but it seemed problematic for the large commercial buildings, for agricultural barns and for stables (Table 3.6).

Table 4.9: Average direct losses to buildings, estimated by two methods

Average loss in 1,000 €, building use, estimation method		Scenario 2 T = 100 a	Scenario 4 T = 300 a	Scenario 5 T = 1,000 a	Scenario 6 T = 5,000 a
Residential	a)	45	14	23	28
	b)	25	21	35	40
Business & commercial	a)	-	28	51	85
	b)	-	221	349	516
Industrial	a)	-	48	142	138
	b)	-	1,191	6,234	5,969
Barns & stables	a)	-	13	14	18
	b)	-	87	60	60
Garages & sheds	a)	-	1.1	3.9	4.8
	b)	-	0.6	3.3	5.1

In particular those building classes were least suitable for standardisation, where the largest average losses were computed. So the loss estimates for the business, the commercial and the industrial buildings were highly uncertain. However, method a) seemed more accurate for business and commercial buildings, but it might as well underestimate the industrial losses.

The estimated direct losses to roads and railway lines are compiled in Table 4.10. Most of the affected roads and railway tracks were inundated by less than half a metre depth, and, according to the methodology (Chapter 3.6.1), they would not cause any monetary damage. This also applied to the affected railway lines which where to a large extend built on embankments. By strictly obeying the method, there would be no direct damage to the railway tracks. The numbers in Table 4.10 are therefore written in parenthesis. However, the direct loss magnitude to the transport infrastructure corresponded to less than 2.5 % of the direct losses to buildings, so these damages were omitted in the computation of the expected annual losses.

Table 4.10: Flood impacts and direct losses to roads and railway lines

		Scenario 2 $T = 100$ a	Scenario 4 $T = 300$ a	Scenario 5 $T = 1,000$ a	Scenario 6 $T = 5,000$ a
Roads	Total inundated area, in 1,000 m ²	16	37	130	190
	Inundated area of > 0.5 m depth, in 1,000 m ²	5	7	40	88
	Losses as clearing costs, in 1,000 €	21	30	170	374
Railway lines	Flooded length, in km	-	-	2.9	3.4
	Losses as clearing costs, assuming > 0.5 m depth, in 1,000 €	-	-	(60)	(71)

4.3.2 Loss analysis for the industrial and the commercial sector

In order to overcome the large uncertainties, inherent in applying standard data to the business, the commercial and the industrial sectors, and in order to the acquire estimates on business interruption costs, interviews with managers were conducted first. Second, national economic data were broken down to the level of the affected area.

Most of the interviewed managers were concerned about their business being exposed to residual flood risks. A number of larger firms have therefore either installed intern protection measures, or they located sensitive installations in higher storeys. Some companies were insured against elementary damage and business interruption.

During the interviews, the inundation maps proved helpful for discussing possible flood impacts to the buildings and the inventory, but the expected educated guesses of direct and indirect monetary losses were not supplied sufficiently. Only one representative, who's business was recently flooded by about 5 cm, provided the requested information: the direct physical damage costs and the decreased turnover within a four-months period were both estimated at 60.000 to 70.000 €.

A critical issue in this approach was the dependency on the respondent's willingness and capability to estimate potential losses. As this problematic had been anticipated, a brief consultation on possible risk management strategies was offered to the interview partners. Although this incentive was not very helpful in gathering more and better monetary loss

estimates, the campaign at least increased the awareness of flood risks, and finally, it helped disseminating the results of this risk analysis.

The difficulties in the interview session could be explained by three reasons: First, transferring the inundation scenarios into qualitative damage descriptions and further into monetary units was a difficult task. In particular if floods have not been experienced. Second, the representatives were worried on their organisations' reputation as a reliable business partner. There were corporate secrets and concerns that the submitted data and the information of being at risk might be published, even if the publication had used aggregated data. The largest company might still be detected from such aggregated results due to its outstanding size and vulnerability. And third, since the loss estimation was not directly linked to well-elaborated risk management options, the advantage in providing the requested information was not obvious.

The results from the second approach, which was based on national economic data, confirmed that flood induced business interruption costs could range up to the magnitude of the total damage to buildings. The reduction of the flooded area's gross revenue was estimated as 5 million €, and the reduction of the net revenues amounted to 1.5 million € per week of interruption. A three-week standstill, as it was assumed as more likely for the largest inundation scenario, caused a decrease in the gross revenues of 15 million € and in the net revenues of 4.5 million Euros, respectively.

But the methodology and the underlying data allowed only crude loss approximations. Uncertainties were first induced by the assumption of the number and kind of the affected workplaces, and the interruption duration. Second, employing national averages of economic indicators disregarded the variation of the productivity within one economic sector. Then, the basic data did not cover all kinds of trades and services, and the number of jobs has changed significantly since the workplace data was established. So the largest factory with more than 900 employees was not considered in this data. This factory would correspond to a significant increase in the loss figures of the production sector. And finally, it was the gross revenue and the net revenue that were identified as most suitable among the available economic benchmarks, but the most appropriate metric to be used for quantifying flood induced business outage costs, would be somewhere in between these figures.

4.4 Risk quantification

This chapter focuses on the expected annual flood losses, since the risk matrix (Table 4.8) and the frequency of losses (Figure 4.14) have already been presented. The expected annual flood losses based on the damage to buildings, as the estimated losses from business interruptions were highly uncertain and the damage to the transport infrastructure was negligibly small. The outcomes of scenarios without structural and operational failure are first presented. Results from considering the occurrence of particular failure mechanisms conclude this chapter.

4.4.1 Risk quantification for scenarios without technical and operational failure

The computation of the expected annual losses was based on the scenario losses (Table 4.11). Here, the more credible results of the two loss-function approaches were selected. The specific area approach b) was assumed more appropriate for residential buildings and the characteristic areas a) for all other building classes.

Table 4.11: Input data for expected annual loss calculation

Average return period T [a]	Direct building losses in 1,000 €
≤ 30	-
100	25
300	1,365
1,000	11,777
$\geq 5,000$	20,986

The average return period of a flood event without damage occurring was estimated to 30 years, and it was assumed, that the losses would not increase for scenarios larger than the 5,000-year flood.

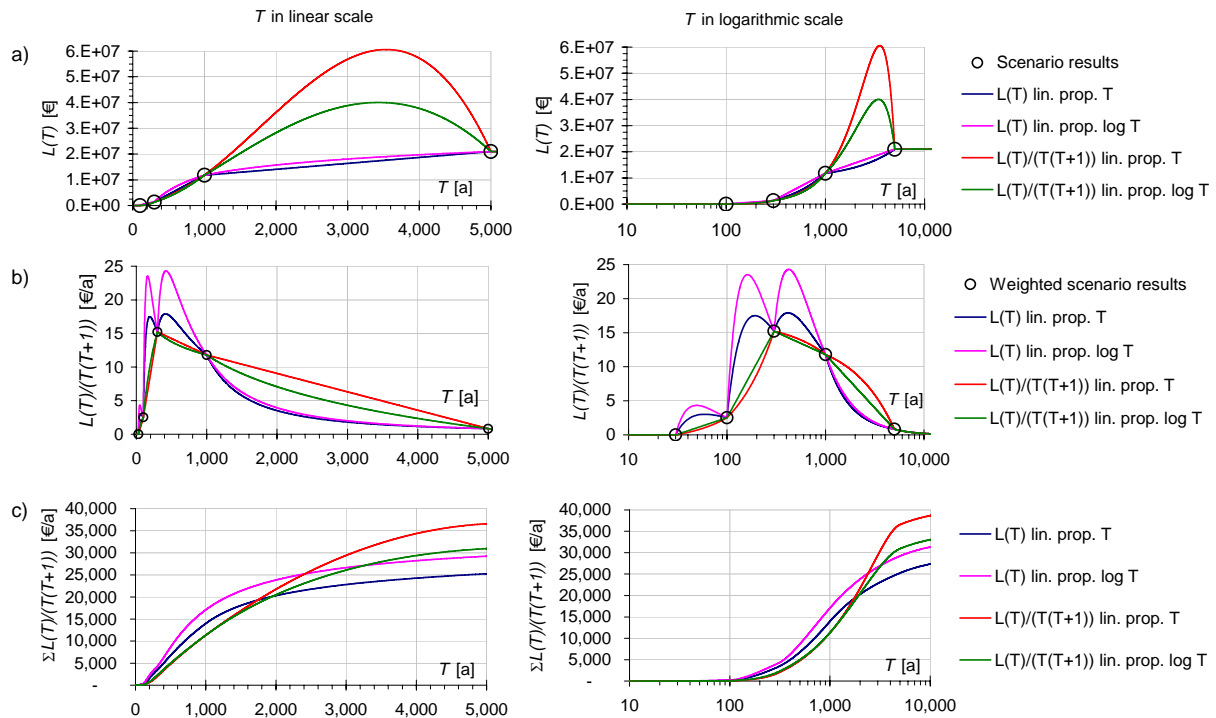
The expected annual losses presented in Table 4.12 were computed by the interpolation methods discussed in Chapter 3.7. Figure 4.15 exhibits the underlying functions, which are plotted on linear and logarithmic return period axes.

Table 4.12: Expected annual losses derived by different interpolation methods

Interpolation method	Expected annual losses in 1,000 €
$L(T)$ lin. prop. T	29.5
$L(T)$ lin. prop. $\log T$	33.4
$L(T)/(T(T+1))$ lin. prop. T	40.8
$L(T)/(T(T+1))$ lin. prop. $\log T$	35.1

The interpolation of $L(T)$ provided plausible curves, but both ways of interpolating $L(T)/(T(T+1))$ corresponded to too large losses between the 1,000 and the 5,000-year scenario (Figure 4.15 a). The different results in Table 4.12 may be regarded as the uncertainty associated with the selection of an interpolation method.

Figure 4.15 Interpolation and numeric integration of expected annual losses: the frequency of losses a), the losses weighted by the probability b) and the cumulated weighted losses c)



The expected annual losses of 29.5 to 33.4 thousand € were addressed as most appropriate for today's system.

From these figures and approximations for a system without protection measures the economic efficiency of the existing flood protection scheme was re-evaluated. Therefore, the scenario losses (Table 4.11) were assigned with modified average return periods, that were approximated from similarities in the inundation areas before and after constructing the protection system: no damage occurred up to a ten-year event and the losses that were estimated for a 1,000 and 5,000-year scenario incurred with an average 30- and 100-year frequency, respectively.

These computations showed that the expected annual losses to today's land-use were 28 times larger if the existing protection system would not have been implemented. Expected annual losses of 827 thousand Euros were derived from a linear loss increase with T , whereas a linear loss increase with $\log T$ came up with 919 thousand €.

A simplified benefit-cost analysis (Table 4.13) used this decreased flood loss expectation as benefits and a reported project cost estimate of 57 million Shillings (Thaller 2002), which corresponded to 4.142 million €.

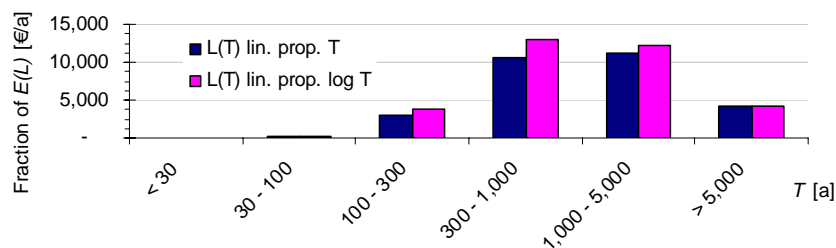
Table 4.13: Simplified benefit-cost analysis for the flood protection system

	Expected values [1,000 €/a]			Discounted present values [1,000 €]		Ratio: Benefits / Costs
	$E(L)_{Without}$	$E(L)_{With}$	Benefits	Benefits	Costs	
$L(T)$ lin. prop. T	827	29.5	797.5	14,559	4,142	3.5
$L(T)$ lin. prop. $\log T$	919	33.4	885.6	16,167	4,142	3.9

According to BMLF (1980) the calculation period for Table 4.13 was 50 years and the interest rate 5 % per year. This resulted in a discounting factor of 18.25593 for the expected annual benefits. The simplified analysis showed that the benefits were about 3 to 4 times larger than the project costs.

For discussing the economic efficiency of possible residual risk mitigation strategies, the expected annual losses were subdivided according the scenario's average return periods (Figure 4.16). The major fractions of the expected annual losses appeared from return periods over 300 years, which corresponded to scenarios where large parts of the floodplains were inundated.

Figure 4.16: Expected annual losses split up according to average return intervals



If an additional technical flood protection measure could prevent all damages up to a 300-year event, it would reduce the expected annual losses barely by 11 to 12 % or by 3.2 to 4.1 thousand Euros per year, depending on the applied interpolation method. But again, a fraction of nearly 90 percent would express the residual risk in terms of the average monetary damage to the buildings. If decisions on managing residual risks were based on these expected values, the prevented expected annual losses would perhaps not justify a larger public investment into a river engineering option.

The expected annual losses so far represented a number that was derived by cumulating losses over all building classes. In the residential sector, an expected annual loss per building was estimated as 59 to 66 Euros, again by the two interpolation methods. This number represents a lower bound solution, since the total expected annual residential losses were divided by the number of affected residential buildings inundated at the largest scenario. This amount, however, might as well be invested by the house-owners for decreasing the building's vulnerability or for expanding the insurance coverage.

4.4.2 Risk quantification considering structural and operational failure

The following results considered the occurrence of structural and operational failures in the estimation of the expected annual losses. Like above, no damage was assumed for up to 30-year events and constant losses were estimated for inundations larger than 5,000-year floods. Table 4.14 further specifies the assumptions and the resulting alterations of the expected annual losses. A key issue in the expected loss estimation was the definition of failure probabilities conditional on particular load situations. In Table 4.14, these conditional probabilities were simplified and set to one.

Considering structural and operational failures caused a significant increase in the expected annual losses. Efforts preventing these failures could therefore reduce the scenario damage to a large extent and the residual expected annual losses by a range of one-third to two thirds.

Table 4.14: Failure scenarios and expected annual losses

Assumptions and description	<i>E(L)</i> , interpolation method			
	<i>L(T)</i> lin. prop. <i>T</i>		<i>L(T)</i> lin. prop. log <i>T</i>	
	1,000 €/a	%	1,000 €/a	%
No structural and operational failure (Table 4.12)	29.5	100 %	33.4	100 %
1) Bridges jam under a 100-year event (scenario 3) and cause damages comparative to those of a 300-year scenario without any structural and operational failure (scenario 4)	45	154 %	52	154 %
2) Levees suffer structural damage at a 300-year event, causing inundations and losses that were computed for a 1,000-year scenario without structural and operational failure (scenario 5)	69	234 %	77	229 %
1) and 2) occur	85	287 %	95	284 %
3) At a 1,000-year event, the inflow into the hinterland is larger due to several reasons, causing losses computed for a 5,000-year event (scenario 6)	42	141 %	47	140 %

5 Case study 2: Application

5.1 System description

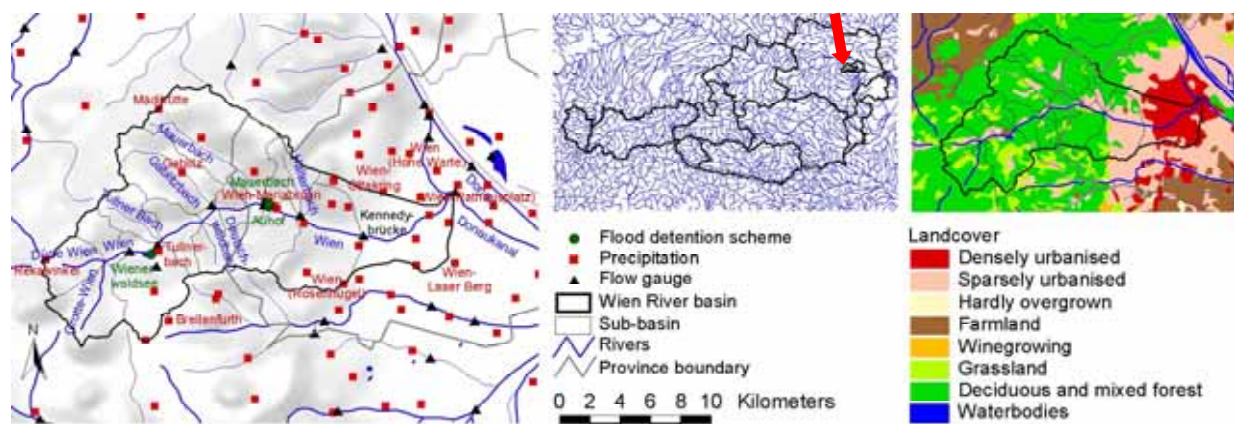
Case study 2 focussed on the flood risk analysis for a particular subway stretch at the Wien River bank in the city of Vienna. The transport route was built in an open section at the right bank of the second largest river in Vienna.

Until the late 19th century, Wien River kept much of its braided character, and anthropogenic uses stayed in a respectful distance to the water. Major changes were made from the late 19th century to 1915 as a consequence of urbanisation, hygienic demands and flood hazards. The riverbed was straightened and deepened, put into open rock- and concrete-lined profiles and in two tunnels of 0.4 and 2.2 km length. The heaped up banks were used for housing, for installing a combined sewer system, for road constructions and for a railway line that was later converted into the U4 subway under study. Yet floods were of major concern, so the railway was protected by a floodwall, and a series of flood retention schemes was constructed upstream the urban river reaches. Both, the hard-regulated 12 km urban river and the retention schemes are still in place, mostly as the architect Otto Wagner designed them. The largest historical flood with an estimated flow of 600 m³/s at the mouth occurred on May 18, 1851 (Bauer et al. 1993).

Large parts of the combined storm sewers in both riverbanks were built from the 1830ies on. Due to intense urbanisation, the channel system is nowadays loaded close to its capacity, even during dry weather, and overflows into the Wien River occur up to 200 times a year. Vienna's combined storm water drainage in the Wien River basin covers approximately 630.000 inhabitants and 35 % of the city's wastewater (Bauer et al. 1993). In addition, many smaller streams drain into the urban storm water network.

Figure 5.1 introduces the Wien River basin and marks the gauging stations relevant for this analysis. The Wien River catchment drains 230 km², whereas the densely urbanised areas cover 57 km². The altitudes range from 650 meter in the western hills to 170 m at the mouth. The average annual precipitation is determined by the topography, so the highest values of approximately 790 mm are found in the western hills, and an average of 530 mm falls in the central urban areas at the mouth (BMLFUW 2005b).

Figure 5.1: Wien River basin, gauging stations and land cover (BMLFUW 2005b)



Recently, the flood retention schemes were upgraded to provide flood protection up to a 1.000-year event and nature-like habitat conditions in the retention basins. Ongoing projects at the Wien River aim to enhance the river's recreational value and to manage the combined storm water discharges by means of large bypass channels. Furthermore, a flood forecasting

system, based on online-rainfall data, was installed in order to issue warnings, to operate the flood retention schemes and to provide sufficient lead-time for installing mobile flood barriers (Bauer et al. 1993, Lazowski and Zuckerstätter circa 2001).

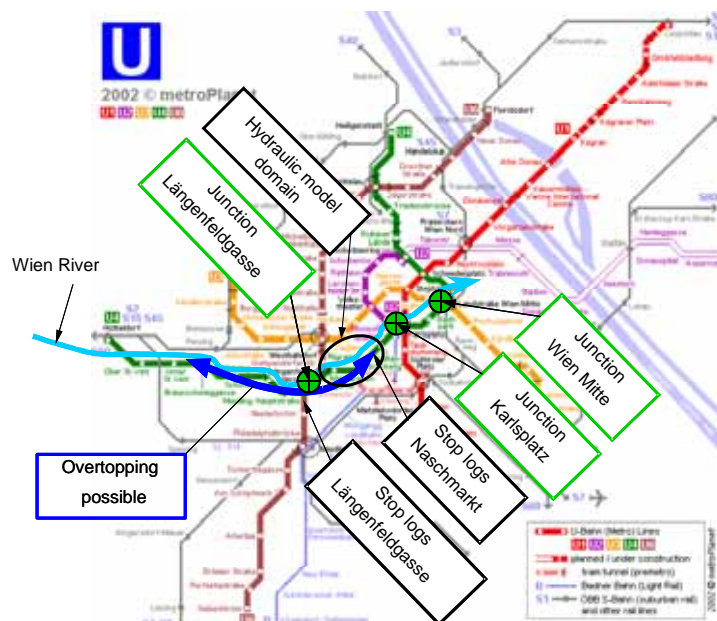
Table 5.1 shows the observed maximum daily precipitation in 50 to 100 years of observation, ranging from 100 mm in the eastern plains of the central City to 175 mm in the western hills.

Table 5.1: Maximum observed daily precipitation from west to east (BMLFUW 2005b)

Station	Maximum daily precip. [mm] Date		Beginning & end of rainfall series		Years of observation
Rekawinkel	135.0	19.05.1911	1901	1960	57
Tullnerbach	155.0	07.07.1997	1901	1998	91
Gablitz	141.5	10.05.1951	1901	1960	55
Mädhütte	175.0	10.05.1951	1901	1998	95
Breitenfurth	102.0	19.05.1911	1902	1960	53
Wien- Mariabrunn	116.5	23.07.1957	1901	1993	91
Wien- Ottakring	102.0	19.05.1972	1949	1998	50
Wien (Rosenhügel)	101.9	10.05.1951	1901	1998	97
Wien (Hohe Warte)	93.1	10.05.1951	1901	1998	88
Wien (Rathausplatz)	95.6	23.07.1925	1901	1998	93
Wien- Laaer Berg	105.2	10.05.1951	1901	1998	88

The subway line exposed to a residual flood risk is mapped in Figure 5.2. It also shows the major transport junctions and the locations of the mobile stop log barriers. Once overtopping at the indicated U4 track happens, the stop logs are designed to prevent inundations of the connected low-lying lines.

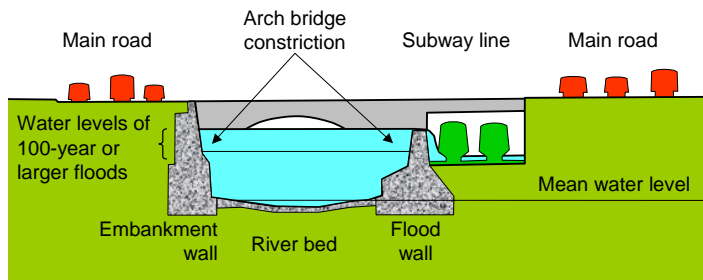
Figure 5.2: Vienna subway system, the model domain at the Wien River and the mobile stop log barriers (Map: MetroPlanet 2002)



Major components of the system under study were the flood retention schemes, the right bank floodwall and the mobile stop log barriers.

The hydraulic model domain was located about 4 km upstream the mouth and covered a 1.6 km long reach in between the two tunnelled sections of the urban river. A schematic cross section is presented in Figure 5.3.

Figure 5.3: Schematic Wien River cross section in the model domain (Adapted from Neukirchen 1993)



5.2 Hazard identification

Flood hazards at Wien River, in particular the threat to the subway line, have been investigated since the 1980s (Neukirchen et al. 1985, IWHW and Gruppe Wasser 1988, Neukirchen 1993 & 1995). These technical documents provided the basis for this case study. Until November 2006, no inundation of the subway line at the Wien River bank happened, although some events raised concerns (Figure 5.4).

Figure 5.4: Wien River upstream gauge Kennedybrücke during dry conditions and the 1975 flood (Photos: MA 45 – Wasserbau & BMLFUW)



High flow events at the Wien River have a flash flood character, since the discharge rises quickly and high velocities occur. Typical for the rural river basin are the steep hills with a small geological infiltration capacity and a small potential for natural retention. Until now, the floods of the rural river basin are overlaid with flood discharges from the urban brooks and from storm water overflows. At the mouth, the runoff contribution from the urban areas can amount to 200 m³/s, which corresponds to one third of an extreme flood (Bauer et al. 1993, Lazowski and Zuckerstätter circa 2001). According to hydraulic estimates and laboratory tests, velocities up to 8 m/s and supercritical flow conditions are possible during extreme events. Further, there are backwater effects upstream the constrictions of historical arch bridges and tunnelled sections (Figure 5.3, Figure 5.11). IWHW and Gruppe Wasser (1988) talk about flow velocities of 5.5 to 6.5 m/s, a wave run-up of up to 0.75 meters and considerably transverse water surface inclinations in bends.

Beside the hydrologic load, the flood hazards are determined from interactions with the technical protection system. The main protection system elements at the urban river reach have been outlined before as the right bank floodwall and the mobile stop log barriers.

The right bank floodwall was built approximately 100 years ago as a brick and masonry structure without any reinforcement (Neukirchen 1993). Today, its condition is determined by aging and maintenance works. The hazards related to the floodwall are overtopping and structural wall failure.

Once the floodwall fails under high flow conditions, water flows into the open subway section, and the slope of the transport route conveys the flood towards mayor subway junctions. In order to prevent subsequent inundations of other U4 stretches and the connected lines, mobile stop log barriers are held available at two locations (Figure 5.2). Their implementation requires a lead-time of approximately six hours, decision-making and labour work. And since the subway operation has to be interrupted for a considerable time, the decision for implementing the mobile barriers will base on a trade-off.

This trade-off and other human factors played a major role in a number of international subway inundations (Compton et al. 2004). Crucial issues, among others, were the decision maker's perception of an emerging catastrophic situation, the timely termination and evacuation of the exposed public transport route and the availability and structural reliability of mobile barriers.

Summarizing that, the relevant flood hazards stem from:

- 1 High flow at the Wien River exceeding bankfull capacity
- 2 High flow at the Wien River combined with structural failure of the
 - Right bank floodwall
 - Riverbed's invert concrete shell
 - Left bank wall
- 3 Reliability of mobile barriers

5.3 Definition of scenarios

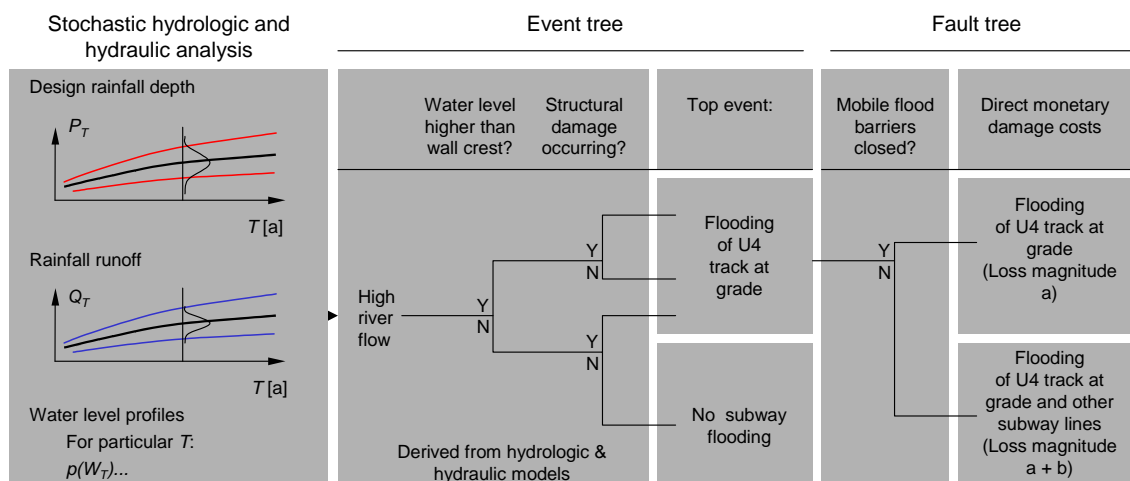
The definition of scenarios was based on hydrologic and hydraulic deliberations on the identified hazards. Table 5.2 summarises the scenarios to be analysed by hydrologic modelling (Chapter 5.4) and by hydraulic modelling (Chapter 5.5).

Table 5.2: Scenario overview

Scenario, description	Analysis method
1) Overtopping of the right bank flood wall	Hydraulic analysis with peak flows derived by:
1a) System state before retention schemes upgrading (pre 1998)	Sampling design rainfall and rainfall runoff modelling (Chapter 5.4.2)
1b) System state after retention schemes upgrading (after 2005)	
1c) System state before retention schemes upgrading (pre 1998)	Sampling from Pearson annual peak flow statistics (Ch. 5.4.3)
1d) System state before retention schemes upgrading (pre 1998)	Sampling from Log-Pearson annual peak flow statistics (Chapter 5.4.3)
2) Right bank flood wall: Performance during flood conditions	Failure evaluation (Page 87):
2a) No structural failure	Assuming perfect structural reliability
2b) Structural failure when exceeding equilibrium conditions	Tipping moment balance
3) Mobile flood barriers: Performance during flood conditions	Failure evaluation (Page 87):
3a) No failure	Assuming perfect structural and operational reliability
3b) Failure	Assuming barriers are not available

The analysis of the identified scenarios was based on the system model (Figure 5.5), which comprised the subsequently presented hydrologic, hydraulic and a loss analysis modules.

Figure 5.5: System model of subway flooding at Wien River



In the hydrologic analysis, design discharges Q_T of seven average return intervals from 10 to 10,000 years were computed for the state before the retention schemes were upgraded and after these works were completed. These computations based on a reduced form of a rainfall runoff model and on flow statistics (Chapter 5.4).

The hydraulic analysis then simulated the water levels W along the river and other load parameters as probability distribution functions p , conditional on particular return periods T (Chapter 5.5.3). The results of each hydraulic model run were analysed for the occurrence of floodwall failures. In the event tree of Figure 5.5, these failures are indicated as Y.

The floodwall reliability was conceptualised by the event tree, which was computed from the hydraulic results (Figure 5.5). The scenario overview in Table 5.2 defined a state of the floodwall without structural failure, following for instance large maintenance efforts, and a state where the stability was purely determined by mechanical equilibrium conditions. This revealed two possible failure scenarios: overtopping of the wall crest without any structural damage and structural damage with a subsequent inundation of the subway track. The first floodwall failure mode was defined as events where the channel's water level exceeded the wall crest level.

The second floodwall failure mode was analysed by a torque equilibrium criterion. This criterion accounted for the load due to the hydrostatic water forces on one side and the resistance due to the self-weight of the floodwall on the other side. The loads were determined from the horizontal component of the water pressure against the floodwall and a vertical water pressure in the floodwall fissures at the wall's base. The latter pressure was assumed as linearly decreasing from the hydrostatic magnitude on the riverside to zero on the subway side. In case the load exceeded the resistance, the floodwall was assumed as breached and the analysed subway stretch at the Wien River bank was understood as inundated. The torque equilibrium criterion was adapted from Neukirchen (1993) who used it with partial safety factors in a deterministic analysis.

The reliability of the mobile flood barriers was conceptualised by the fault tree in Figure 5.5. Instead of estimating probabilities of the possible outcomes, two scenarios were computed for evaluating the difference that a successful intervention could make. These scenarios assumed perfect structural and operational reliability on one side and that the barriers were not available on the other side.

The loss estimation for the subway network was finally combined with the results of the event tree- and the fault tree analysis for the quantification of risk.

5.3.1 Stochastic modelling algorithm

In contrast to case study 1, where a small number of scenarios was manually assembled, a stochastic modelling algorithm automated the analysis of the scenarios that were defined in Table 5.2. The hydrologic and hydraulic models and the event tree (Figure 5.5) were therefore implemented in a number of Fortran codes.

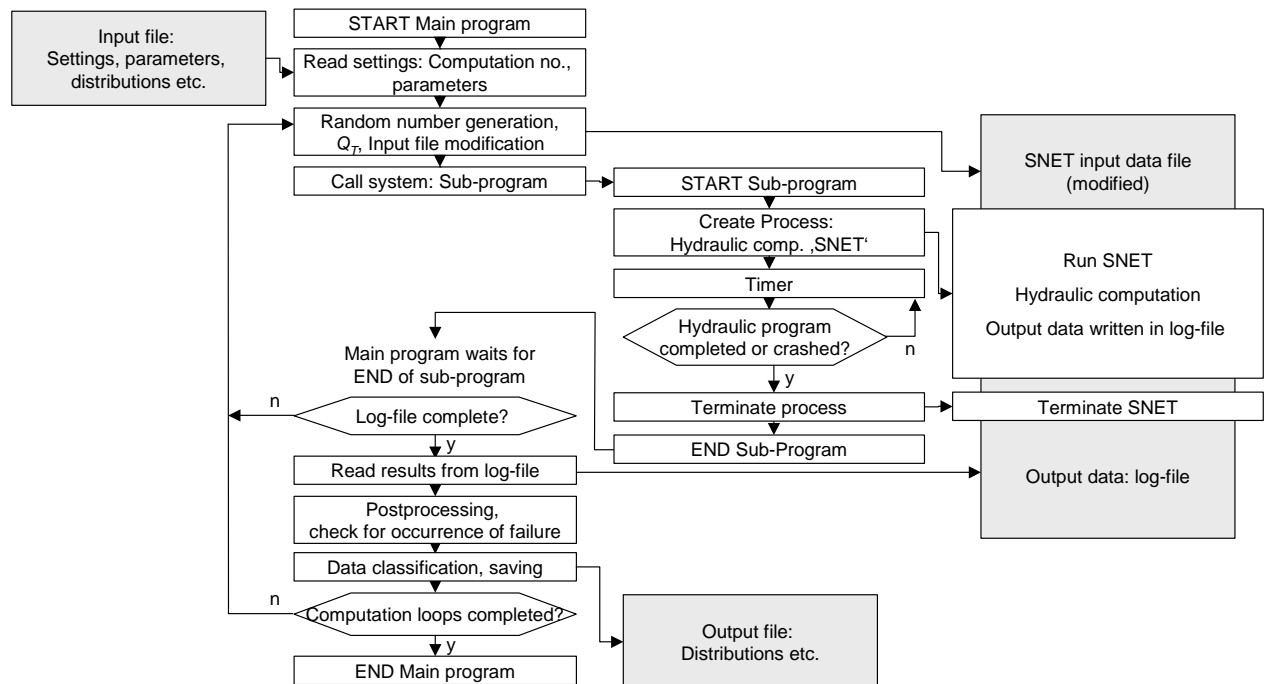
The algorithm of Figure 5.6 handled the following main tasks:

- 1 Generate the basic random variables
- 2 Generate the hydrologic input
- 3 Modify the input file for water surface computations according to task 1 and 2
- 4 Launch the hydraulic model with the modified input file
- 5 Read the hydraulic model's log-file
- 6 Calculate and store the relevant information
- 7 Restart the modelling sequence with task 1

Having saved and classified the output data, the main program completed 3,000 simulations for each of the seven specified average return periods.

The stochastic algorithm comprised a main- and a sub-program, since the hydraulic model of choice was HEC RAS 3.0.1 (HEC 2001) and the source-code of HEC RAS was not available, The genuine hydraulic input file was edited in the graphical user interface of HEC RAS, but the Monte-Carlo simulations employed barely the steady flow kernel 'SNET' of HEC RAS. Controlling SNET was the only task of the sub-program.

Figure 5.6: Flowchart of the stochastic algorithm



5.4 Hydrologic analysis

This chapter describes the procedures for estimating the frequency of peak flows and the associated uncertainty. This in particular included the specification of probability density functions of discharges, conditional on particular average return intervals. For that, two approaches were employed: combining design rainfall with rainfall runoff modelling and using flow statistics.

The first procedure (Chapter 5.4.1 and Chapter 5.4.2) accounted for uncertainties inherent in the design storm depths by defining the areal design rainfall as a basic random variable. This approach allowed an analysis of two different operational states of the flood retention schemes: the pre-1998 state with an uncontrolled retention and the state after the schemes were upgraded and equipped with controllable gates. Sampling a storm depth and transferring it into a peak flow by means of pre-calculated results generated the runoff for hydraulic modelling.

In the second approach, the input for the hydraulic model was sampled from the flow statistics of gauge Kennedybrücke (Chapter 5.4.3).

5.4.1 Design rainfall

The design rainfall data covered the data of Kreps and Schimpf (1965) and the data of Lorenz and Skoda (2000 & 2006) that were already introduced in Chapter 3.4.2. In the systematic of Kreps and Schimpf (1965), the same design data were suggested for the Wien River basin and the Raab River catchment, since both basins were assigned to the K 35 zone. Another set of design rainfall data was based on the 1901 to 1980 rainfall records in Lower Austria (NÖ. LR. 1985). It comprised rain durations up to 48 hours and average return intervals up to 100 years. This design concept also defined zones from the mean extreme daily precipitation, whereas the Wien River catchment was located in the 50 to 60 mm zone. The design rainfall data of NÖ. LR. (1985) have been discussed as too small, and an increase by 20 to 40 percent would lead to more appropriate design values (F. Salzer, personal comment, 2002).

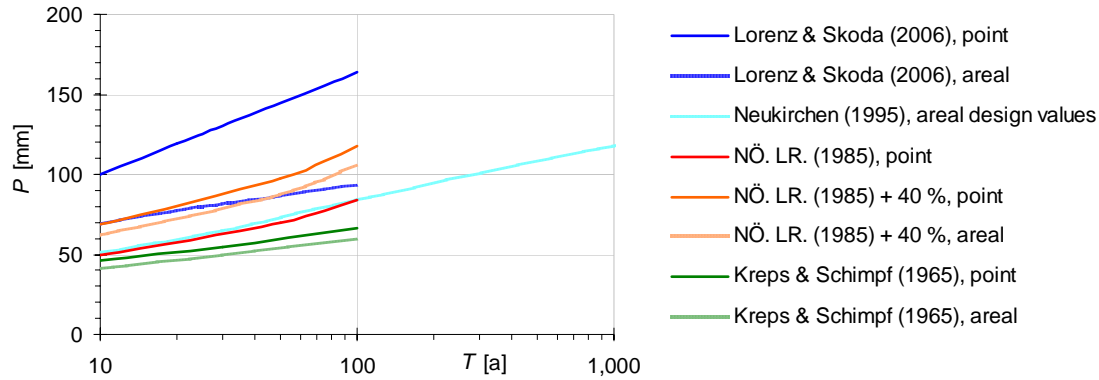
The PMP (probable maximum precipitation) and the transformation of the August 2002 storm provided two additional design events. The methodologies for estimating the PMP and transferring the August 2002 event to other river basins were already presented in Chapter 3.4.2.6. In this case study, the maximum six-hour aggregate of the August 2002 event was used.

As all these design data referred to point rainfall, an areal reduction was performed using the approaches presented in Chapter 3.4.2.5). The results of applying a large areal reduction to the Lorenz and Skoda data and a moderate reduction to all other figures are shown in Figure 5.7, including the point- and the areal rainfall.

The rainfall data of Lorenz and Skoda (2006) based on the methodology published by Lorenz and Skoda (2000). The rainfall data were submitted by Schenekl (personnel comment, 2006-02-27). The areal design rainfall data by Neukirchen (1995), which were used for planning the retention schemes upgrades, were based on the figures of NÖ. LR. (1985).

The deviation of the rain curves in Figure 5.7 gives an idea of the uncertainty in the design rainfall data. A comparative quantitative uncertainty estimation was made by Nobilis (1990) who talked about a 15 % coefficient of variation in the expected extreme rainfall in Austria. Similar ranges were described by Skoda et al. (2003) who discuss the 24-hour rainfall depths in Lower Austria and by the German Weather service DWD (1997).

Figure 5.7: Six-hour point- and areal design rainfall in the Wien River basin



For sampling the design rainfall depth, the expected areal rainfall $E[P(D, T)]$ of the rainfall duration D and the average return interval T was described by a logarithmic function:

$$E[P(D, T)] = u(D) + w(D) \ln T \quad \text{Eq. 5.1}$$

The six-hour aggregate was used for rainfall sampling, as it provided the largest peak flows (Neukirchen 1995). The parameters $u(D = 6 \text{ h})$ and $w(D = 6 \text{ h})$ were manually fitted to the curves in Figure 5.7 as 25 and 13 mm, respectively. The data variability around $E[P(D, T)]$ was assumed as normally distributed with a coefficient of variation of 15 %. Figure 5.8 shows both, the expected areal design rainfall $E[P(D, T)]$ and the data variability in terms of one and two standard deviations either side. This concept described the basic random variable from which 3,000 areal design storm depths were sampled for each return interval (Figure 5.9).

Figure 5.8: Six-hour point- and areal design rainfall data in the Wien River basin and the definitions for rainfall sampling

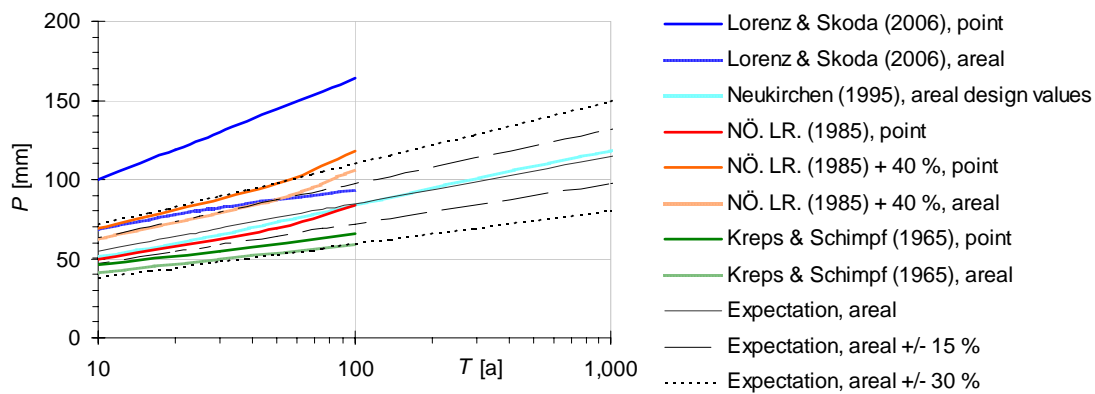
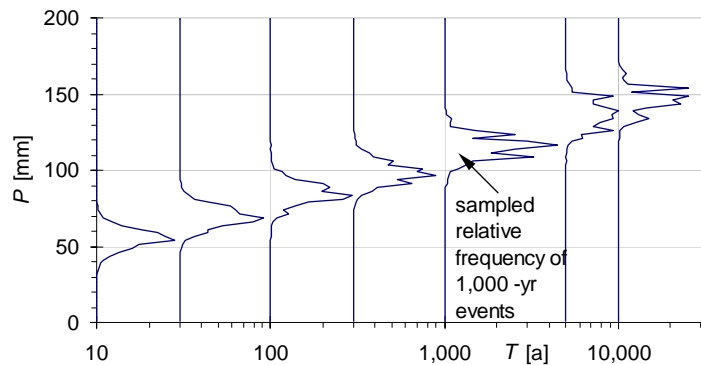


Figure 5.9: Sampled relative frequency of six-hour areal rainfall for several average return intervals (Frequency curves not in scale)



5.4.2 Rainfall runoff modelling

The sampled rainfall was converted into peak discharges by means of pre-calculated results of rainfall runoff modelling. These results were available for the rural Wien River catchment and for the urban catchment that is drained by the combined stormwater system (Neukirchen 1995 & 2000, Table 5.3). Discharges from both drainage areas were added and linearly interpolated. The underlying model for the rural catchment was the semi-distributed, event-based rainfall runoff model IHW (Institut für Hydrologie und Wasserwirtschaft, Karlsruhe) that was calibrated by two flood events in 1991. For the urban areas, the rainfall runoff model of ITWH (Institut für technisch-wissenschaftliche Hydrologie, Hannover) was used that considered hydrodynamic transport and storage processes.

Table 5.3 presents the implemented rainfall runoff relations. The data points obtained from model simulations covered rainfall events up to 134 mm. Data for the largest event were approximated by means of the rational runoff formula and runoff coefficients which were reconstructed from the largest model results.

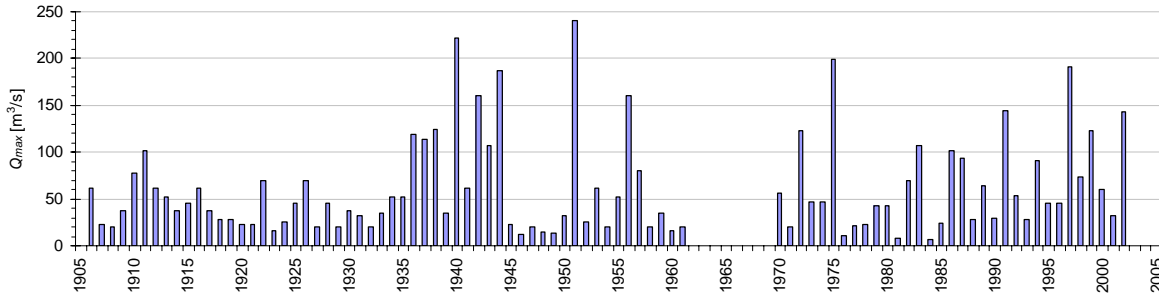
Table 5.3: Rainfall runoff data for the rural and the urban Wien River catchment obtained by modelling and approximations*

Areal rainfall P [mm/6h]	Peak flow Q [m ³ /s]		
	Rural catchment (Neukirchen 1995)		Urban catchment (adapted from Neukirchen 2000)
	Before retention schemes upgrade	Upgrading retention schemes completed	
28	43	43	40
51	120	119	89
65	180	180	96
84	197	226	101
118	434	340	124
134	518	478	132
300*	1,160*	1,070*	296*

5.4.3 Flow statistics

At the gauge Kennedybrücke, observations and manual documentations of water levels began in 1904. Discharges were directly recorded from 1981. As the data from 1962 to 1969 was missing, the annual peak flow series comprised 89 events (Figure 5.10).

Figure 5.10: Annual peak flow series at gauge Kennedybrücke (Data Source: G. Schenekl, personnel comment, 2006-02-27)



Since the flow regime after 1998 has been influenced by the controlled retentions schemes, the flow statistics used the 1906 to 1997 series for analysing the system state before the retention schemes were upgraded. Specific uncertainties in the flood records based on undocumented changes in gauge zero before 1958, varying flow conditions and hydraulic jumps (Pekarek, personnel comment, 2001).

The annual peak flows from the gauge Kennedybrücke were extrapolated by means of Gumbel, Pearson and Log-Pearson distributions whereas parameters were estimated by the method of moments. In addition, the GEV distribution with the L-moment parameter estimation was applied (Stedinger et al. 1992).

It appeared, that the Pearson and the Log-Pearson distributions were most suitable, so the uncertainty estimates for Q_T were derived for both functions. Eq. 5.2 to Eq. 5.5 describe this uncertainty estimation which gave the sampling basis for Monte Carlo modelling: the realisations of Q_T had a mean of the extrapolated magnitude and a standard deviation corresponding to the standard error s_E .

The standard error depends on the distribution type, the sample size n , the frequency factor K and the parameters of the distribution in terms of the sample's standard deviation s_x and the skewness c_s . Approaches for estimating the standard error were presented, for instance, by Kite (1988), DVWK (1999) and Haan (2002). For computing confidence intervals, Kite (1988) described s_E for a Pearson distribution as:

$$s_E(T) \cong \sqrt{1 + Kc_s + 0.5K^2(1 + 0.75c_s^2) + f(K, c_s)} \frac{s_x}{\sqrt{n}} \quad \text{Eq. 5.2}$$

$$f(K, c_s) = 3K \frac{\partial K}{\partial c_s} \left(c_s + \frac{c_s^3}{4} \right) + 3 \left(\frac{\partial K}{\partial c_s} \right)^2 \left(2 + 3c_s^2 + 5 \frac{c_s^4}{8} \right) \quad \text{Eq. 5.3}$$

$$\frac{\partial K}{\partial c_s} \approx \frac{t^2 - 1}{6} + \frac{4(t^3 - 6t)}{6^3} c_s - \frac{3(t^2 - 1)}{6^3} c_s^2 + \frac{4t}{6^4} c_s^3 - \frac{10}{6^6} c_s^4 \quad \text{Eq. 5.4}$$

Here, t is the standard normal deviate of the frequency factor K .

For the Log-Pearson distribution, Eq. 5.2 to Eq. 5.4 refer to the logarithms of the annual flow maxima. Kite (1988) described the standard error of the quantile Q_T by Eq. 5.5, where the flow data is indicated with x and its logarithm with y .

$$s_{E,x}(T) \cong \frac{1}{2} Q_T (e^{e_{E,y}} - e^{-e_{E,y}}) \quad \text{Eq. 5.5}$$

5.5 Hydraulic analysis

This chapter presents the deterministic hydraulic computation core and the basic random input parameters. Both were used in the stochastic model algorithm (Chapter 5.3.1).

5.5.1 Deterministic 1D water surface model

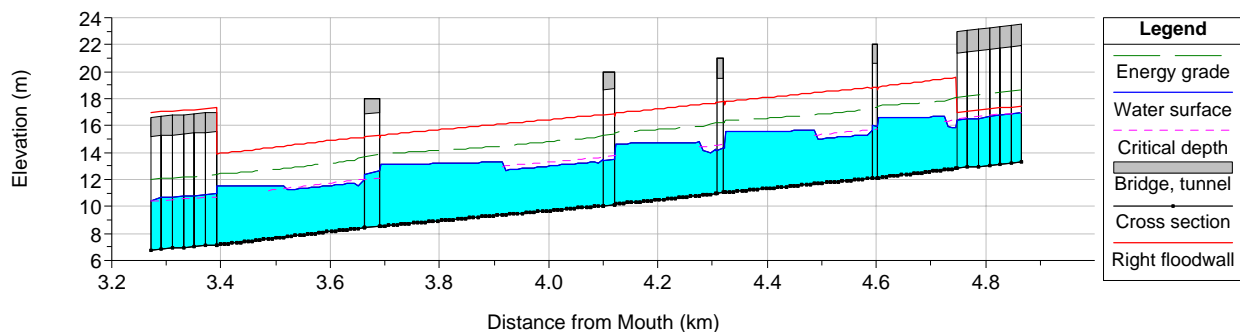
Flood discharge in the urban Wien River may well be modelled by a one-dimensional steady flow, since the cross-section geometries are relatively compact and significant retention processes do not occur in the investigated river reach.

The model setup in HEC RAS 3.0.1 (HEC 2001) comprised 208 nodes over a distance of 1.6 km, including open cross sections and four arch bridges (Figure 5.11). The cross section geometry was adapted from IWHW and Gruppe Wasser (1988). The computations of the hydraulic radius were based on a single flow subdivision, so there were no frictionless interfaces in the active flow areas of the cross sections (Chapters 3.5.5 and 4.2.5). For frictional losses in the riverbed the flow equation of Manning-Strickler was used.

Both, the upper and the lower model edge were tunnelled sections, where the boundary conditions were set to critical depth. This kind of boundary condition was most suitable for computations of varying discharges. Figure 5.11 further shows that water levels were either close to critical depth or the tunnel entrance and the arch bridge constrictions backed them.

The hydraulic model was run in a mixed flow mode that allowed subcritical and supercritical flows in one model run. The momentum balance was used for calculating the water surface through the arch bridges, as the flow conditions may change there. This approach, named 'special bride method', was selected since it is applicable to compute various flow conditions either side of the arch bridge.

Figure 5.11: Deterministic hydraulic model with a water surface profile¹ at 300 m³/s



In HEC RAS, the basic equations for computing water levels in a sequence of cross sections use the energy balance and the conservation of mass. As the basic random parameters were processed in the energy balance and in the momentum balance, both equations are presented in the subsequent chapters.

5.5.1.1 Energy balance

Gradually varying water surface profiles between the cross sections, including the tunnelled reaches, are calculated in HEC RAS by solving the energy equation with the iterative

¹ In Austria, longitudinal profiles are commonly plotted from the left to the right. However, the feature for swapping the orientation has been implemented in later versions of HEC RAS.

'standard-step method'. In subcritical flows, the computation proceeds upstream. Therefore the downstream cross section is indicated as 1, the upstream section as 2 and vice versa in supercritical flow conditions. The iteration for the adjacent cross section starts with an assumed water surface at cross section 2 and calculates the corresponding conveyance K , the kinetic energy head $\alpha V^2/2g$ and the representative frictional slope S_f . With this information, Eq. 5.6 also provides a water surface at cross section 2 that is usually converging towards the assumed value.

Here, Y denotes the water depth, Z the channel invert elevation, V the mean velocity, α the velocity-weighting coefficient, g the gravity acceleration and h_e the energy head loss.

$$Y_2 + Z_2 + \frac{\alpha_2 V_2^2}{2g} = Y_1 + Z_1 + \frac{\alpha_1 V_1^2}{2g} + h_e \quad \text{Eq. 5.6}$$

The energy head loss h_e comprises external frictional losses $L\bar{S}_f$ and internal contraction- or expansion losses due to turbulences at channel geometry changes. L denotes the cross section distance, \bar{S}_f the representative friction slope between two sections and C the contraction or expansion coefficient.

$$h_e = L\bar{S}_f + C \left| \frac{\alpha_2 V_2^2}{2g} - \frac{\alpha_1 V_1^2}{2g} \right| \quad \text{Eq. 5.7}$$

When the cross sections are conceptualised by a single depth-averaged flow subdivision without overbanks, as it was in this case study, the velocity coefficient α is one. In cross sections with more than one flow subdivisions and highly non-uniform discharge, such as in modelling overland flow or river bends, α is larger than one. See HEC (2002 p.2-9) for the implementation of α in the 1D model.

As discussed in Chapter 3.5.5, the definition of channel subdivisions can alter the results significantly, since most common 1D model approaches assume frictionless edges of the flow subdivisions. At the relative compact cross sections of the urban Wien River, such frictionless interfaces would produce a central flow subdivision with little bed friction and a high velocity and lateral subdivisions with large friction and small velocities. This seemed not justified, so a single subdivision was defined at each cross section.

The total conveyance K is calculated from adding the conveyances K_i (Eq. 5.8) over the whole cross section. Here, n_i is the Manning's frictional coefficient, A_i the flow area and R_i is the hydraulic radius of the subdivision i . As detailed in Chapter 5.5.2, Manning's n was defined as one of the basic random variables.

$$K_i = \frac{1}{n_i} A_i R_i^{2/3} \quad \text{Eq. 5.8}$$

In case of three flow subdivisions, the mean kinetic energy head $\alpha \bar{V}^2/2g$ is obtained from flows in the left overbank l , the main channel Ch and the right overbank r by:

$$\alpha = \frac{Q_l V_l^2 + Q_{Ch} V_{Ch}^2 + Q_r V_r^2}{Q V^2} \quad \text{Eq. 5.9}$$

The frictional slope S_f in each cross section is determined as:

$$S_f = \left(\frac{Q}{K} \right)^2 \quad \text{Eq. 5.10}$$

For the river reach between two adjacent cross sections, the average friction slope of the up- and downstream section was used for hydraulic modelling.

5.5.1.2 Momentum balance and special bridge method

The momentum balance was used for calculating the water surface through the arch bridge constrictions and when the water surface passes critical depth. Disregarding the constant unit weight of water γ_w , the momentum's derivative with respect to the time reduces the momentum to the specific force SF . At cross sections with a valid sub- and a supercritical solution, the controlling flow condition is the one with the larger specific force.

Here, β is the velocity weighting coefficient, A_{flow} and A_{total} are the active flow area and the total wetted cross section area and \bar{Y} is the depth at the gravity centre of A_{total} .

$$SF = \frac{Q^2 \beta}{g A_{flow}} + \bar{Y} A_{total} \quad \text{Eq. 5.11}$$

Four cross sections characterise a bridge. Sections 2 and 3 represent the open channel geometry immediately up- and downstream the bridge, and BD and BU describe the bridge constriction elements such as deck, abutments and piers. Eq. 5.12 to Eq. 5.14 show the momentum balance through the bridge in the upstream direction. A_2 , A_{BD} , A_{BU} and A_3 are the active flow areas, A_{PBD} and A_{PBU} are the areas obstructed by the bridge arch or pier down- and upstream. \bar{Y} is the flow depth at the gravity centre of the corresponding flow area or obstructed area, F_f the external frictional force per unit weight of water and W_x the force due to the weight of water in the flow direction. C_D is the drag coefficient representing energy losses by the flow going around obstructions, by flow separations and by the resulting downstream wake.

$$A_{BD} \bar{Y}_{BD} + \frac{Q_{BD}^2 \beta_{BD}}{g A_{BD}} = A_2 \bar{Y}_2 + \frac{Q_2^2 \beta_2}{g A_2} - A_{PBD} \bar{Y}_{PBD} + F_f - W_x \quad \text{Eq. 5.12}$$

$$A_{BU} \bar{Y}_{BU} + \frac{Q_{BU}^2 \beta_{BU}}{g A_{BU}} = A_{BD} \bar{Y}_{BD} + \frac{Q_{BD}^2 \beta_{BD}}{g A_{BD}} + F_f - W_x \quad \text{Eq. 5.13}$$

$$A_3 \bar{Y}_3 + \frac{Q_3^2 \beta_3}{g A_3} = A_{BU} \bar{Y}_{BU} + \frac{Q_{BU}^2 \beta_{BU}}{g A_{BU}} + A_{PBU} \bar{Y}_{PBU} + \frac{1}{2} C_D \frac{A_{PBU} Q_3^2}{g A_3^2} + F_f - W_x \quad \text{Eq. 5.14}$$

For estimating the drag coefficient C_D , tables are available that have been established from scale tests and recalculations. In this case study, C_D was introduced as a basic random variable accounting for the unknown influence of the arch bridge constrictions (Chapter 5.5.2).

5.5.1.3 Transverse water surface inclination

By the relative large expected flow velocities and sharp bends along the river course, the cross section's water surface was expected to diverge from the horizontal position. This horizontal position is presumed by the 1D output. The ratio of centrifugal and the gravitational forces determine the transverse water surface slope:

$$\frac{dW}{dr} = \frac{V^2/r}{g} \quad \text{Eq. 5.15}$$

Here, W is the water level, r is the radius, V the flow velocity and g the gravity acceleration constant. For a mean radius \bar{r} larger than 200 meters, an average transverse inclination $\bar{\phi}$ can be approximated by the mean velocity \bar{v} (Naudascher 1992):

$$\bar{\phi} \cong \frac{\bar{v}^2}{rg}$$

Eq. 5.16

At the Wien River model domain, the largest deviation from the horizontal water surface elevation ranged up to 0.2 meters at the smallest radius of $\bar{r} = 230$ m. The mean radius was derived from a 1: 5,000 map and assigned to each cross section by using an ancillary input file. The main program of the stochastic algorithm calculated $\bar{\phi}$ from the radius and the flow velocity that was computed by HEC RAS, and it iteratively adjusted the inclined water surface to comply with the original flow area.

5.5.2 Hydraulic basic random parameters

In a hydraulic system, a number of parameters may be identified as uncertain, such as the flow quantity, the surface roughness or the river geometry. In the course of this study, it appeared possible to introduce a vast number of input parameters as basic random variates. Nevertheless, justified probability distributions were derived only for a few of these parameters which were the peak flow and energy loss coefficients.

The methods for estimating peak flow frequencies of different system states were already presented in Chapter 5.4.

For the parametric uncertainties in the channel flow model, two energy loss coefficients were introduced as basic random variables: Manning's n and the bridge drag coefficient C_D .

As calibration data for large flow events was not available, literature tables and expert judgement were used to approximate the channel roughness coefficients in most of the technical Wien River studies. But even if there was sufficient data for recalculating the frictional coefficient, there will still be a random fraction left. This was demonstrated by Plate (1992 & 1993) and Schmid (1989) for the Lower Austrian Danube River reach between Tulln and Bärndorf. They fitted a normal distribution with a five percent coefficient of variation to the Strickler frictional coefficients k_{St} (Manning's $n = 1/k_{St}$), which were recalculated from several flood events. Surprisingly, Plate (1992 & 1993) did not find a dependency of k_{St} on the discharge magnitude. As a consequence, the Monte Carlo simulations in this case study were based on a normally distributed Manning's n with a mean value of 0.02 s/m^{1/3} ($k_{St} = 50$ m^{1/3}/s) and a standard deviation of 0.001, which corresponded to a coefficient of variation of five percent.

Another source of uncertainties in this particular river was the influence of the arch bridges during very high flows, when the bridge arches obstruct the flood flows. This was conceptualised by addressing the obstruction's drag coefficient C_D in Eq. 5.14 as a basic random parameter. A lower bound was specified with $C_D = 0$ and an upper bound with the experimentally found $C_D = 2$. The lower bound would omit this loss term, the upper bound corresponds to the coefficient arising from an orthogonal flow against a plate (Naudascher 1992) and square nose piers (HEC 2002). The Monte Carlo simulations therefore based on a uniformly distributed C_D in the range of 0 and 2. In order to assign C_D to the bridge arches, these structures had to be defined as piers in the graphical user interface of HEC RAS.

In each hydraulic model run, one set of sampled basic random parameters was applied to the entire hydraulic model domain. So each cross section received the same randomly drawn frictional coefficient, and one drag coefficient was assigned to each bridge.

5.5.3 Reliability and probability of failure

The reliability and the probability of failure were derived from the stochastic hydraulic model results. These results were generated as the ratio of the simulations with a failure occurring divided by the total number of simulations (Eq. 2.6), conditional on specified average return

intervals. Those data pairs of conditional probabilities ($P_F|T, T$) were then interpolated, and an approximately continuous curve with k data points was obtained.

The procedure for calculating the probability of failure P_F from the simulated conditional data was similar to the computation of the expected annual flood losses from the scenario losses in case study 1 (Eq. 3.5 to Eq. 3.8). The k data points were interpolated at each single year on the return period axis. By that, the curve P_F/k was generated with $k = T$. Eq. 3.7 was then used for the probability estimation, and the probability of failure was computed as:

$$P_F \cong \sum^k (P_F|k)P_k \quad \text{Eq. 5.17}$$

The interpolation of P_F/k was performed by assuming the conditional probability of failure would either increase stepwise linearly with T or with $\log T$, respectively. Eq. 2.4 finally calculated the system reliability.

5.6 Loss analysis

Loss modelling in this case study focused on direct tangible flood damage to the subway system, bearing in mind that intangible and indirect consequences of an inundation would be substantial. These consequences would range from fare outage and transport delays to passenger inconvenience and the threat to human life.

5.6.1 Direct loss analysis

This chapter describes the procedure for estimating the magnitude of direct losses to the subway system. Several factors were understood as influential on the flood damage: the flooded track length, the number and vulnerability of the affected stations, the sediment load, the inundation depth and its duration, the flow velocities and the lead-time for taking emergency action. Further, the local pricing level and the construction type as an at-grade (open track) or tunnelled subway line would make a difference.

Three independent sources of information were used for the loss estimation: a compilation of subway flood incidents, literature values on construction costs and the expert judgement of engineers and the Vienna subway operator, which was part of a benefit-cost analysis (Neukirchen 1993).

Compton et al. (2004) reviewed a number of incidents and their repair costs, which were above ten million Euros in the latter four events of Table 5.4.

Table 5.4: Review of subway inundations (Compton et al. 2004)

Location, year	Event description	Source
1. New York, USA, 1992	Coastal flooding of a terminal and a tunnel	Beardsley (1993)
2. Fukuoka, Japan, 1999	Rainfall and sudden overtopping of Mikasa River	Toda and Inoue (2002)
3. Caracas, Venezuela, 1999	Subway system was shut down after flooding	Jones (1999)
4. Santiago and Valparaíso, Chile, 1999	Several days of rain caused subway system shutdown	Brandes (2000)
5. Boston, USA, 1996	Stopbank overflowing and drainage backing. Mobile barriers could not be installed on time. Inundation of several stations and 2 to 3 km track.	Brown (1996a & b), CDM (2001), Moore and Chiasson (1996)
6. Seoul, South Korea, 1998	Underwater construction wall breached after heavy rainfall. 11 stations and 11 km track inundated.	Korea Herald (1998a & b)
7. Taipei, Taiwan, 2001	425 mm rain in two days exceeding 200-year design level. Subsequent flooding of several lines, among others by a not closed construction hole in a tunnel	Chang (2001), Chuang (2001)
8. Prague, Czech Republic, 2002	500-year event at Vltava River (~ 1.4 times 100-yr.). Overflowing of banks and 1 m high barricades inundating 20 km track and 17 stations. A wall collapsed, forecasts were too optimistic, transport operation was closed down late and a steel door in the tunnel system was left open.	Krushelnicky (2002), Kikuchi and Sasaki (2002), Metrostav (2002)

In the analysis of the incidents in Table 5.4, Compton et al. (2004) found a range from 3.2 to 20 million Euros per flooded kilometre, with a most likely value around five million. Those figures were derived from the repair costs and the inundated track length (Table 5.5). The intervals in the loss magnitudes arose from different reported costs and inundation lengths. However, the available data did not allow a quantification of other influential factors, such as the number and vulnerability of the affected stations.

Although there was much uncertainty associated with these figures, the similarity of the lower and upper bound interpretations was remarkable. As far as reported, all historic events referred to subway systems in the sense of tunnelled structures. The investigated Vienna transport system, instead, also included at-grade tracks.

Further loss estimates were obtained from subway building costs for the US (Laver and Schneck 1996), for Vienna (Neukirchen 1993) and by approximations for the loss ratios.

Table 5.5: Direct losses to subway systems from the review, from building costs and from damage ratios (Compton et al. 2004)

Source		Million € per flooded km, lower & upper bounds	
Review (Table 5.4)	Boston, USA, 1996	3.3 - 20	
	Seoul, South Korea, 1998	3.2	
	Taipei, Taiwan, 2001	4.4 - 16	
	Prague, Czech Republic, 2002	3.2 - 16	
US building costs & damage ratios (Laver and Schneck 1996, Compton et al. 2004)		0.9 - 6	(At-grade)
		2.8 - 17	(Subway)
Vienna building costs & damage ratios (Neukirchen 1993, Compton et al. 2004)		5.8 - 8.1	(At-grade)
		4.4 - 16	(Subway)

Compton et al. (2004) further highlighted a number of aspects in the subway inundation incidents in Table 5.4. Human error in design, in construction execution and in emergency management played an influential role on the magnitude of losses. Flood barriers with sandbags, for instance, were reported as not successful. As far as insurance cover was stated, the Taipei system was not insured, following the high premium costs, and the Prague system was partly covered. In Fukuoka, one person was trapped and died in the underground system. Although the flood events caused many fatalities in the regions hit, the other reports did not talk about loss of life in the subway systems.

In this case study, the loss estimation was based on two assumptions. First, the numbers given by Neukirchen (1993) and Compton et al. (2004) in Table 5.5 were used, as they seemed most appropriate and allowed a distinction of two track systems. These loss magnitudes represented upper bound solutions, since the inundation depth and the other influential factors discussed above could not be considered in a loss function for a unit length of track.

Second, it was assumed that once a failure occurred, the whole investigated track length was inundated. This second upper bound solution was used, as the inundation extent in the subway system could not be quantitatively linked to the Wien River discharge.

The affected U4 stretch at-grade was estimated as 1.5 km long. The length of the tunnelled U4 track and the connected lines was approximated as 17.3 km (Figure 5.2). This track length was assumed as damaged if the mobile barriers failed (Compton et al. 2004).

5.7 Risk quantification

The computed risk expressions were based on the probability of failure P_F (Chapter 5.5.3) and the monetary loss estimates (Chapter 5.6.1). The analysed failure events were outlined in the event- and fault tree of Figure 5.5. Eq. 1.2 for computing the expected annual losses $E(L)$ was therefore reduced to:

$$E(L)_{s,t} \cong L_t P_{F,s} \quad \text{Eq. 5.18}$$

The indices s and t represent the defined scenarios (Table 5.2). The index s characterises the state of the retention schemes and the state of the floodwall. For the retention schemes, the states before and after the upgrades were analysed. For the floodwall, perfect structural reliability was assumed on one hand, and the torque equilibrium criterion was used on the other hand.

The index t denotes, if the losses were estimated for the flooded at-grade U4 track only, or if they relate to the at-grade track and the subway stretches. The former corresponded to a perfect structural and operational reliability of the mobile flood barriers. The latter assumes the barriers were not available.

6 Case study 2: Results

The results of the Wien River case study first comprise the hydrologic outcomes followed by the hydraulic findings. Then the computed reliability is presented and the results of the loss analysis and the risk quantification will be revealed. Finally, the uncertainties related to each analysis step are summarised.

6.1 Hydrologic analysis

The hydrologic analysis aimed to provide the input for the hydraulic model by estimating peak flow frequencies and by quantifying the associated uncertainty. Therefore, a reduced form of a rainfall runoff model and statistical methods were used for Monte Carlo simulations.

The results of the rainfall runoff model are presented in Table 6.1. These figures were obtained from 3,000 sampled areal design rainfall events per return interval. The corresponding peak flow frequencies are also illustrated in Figure 6.2.

Table 6.1: Mean values and coefficients of variation (CoV) of sampled design rainfall depths and generated peak flows

$T [a]$	Input: Areal design rainfall		Output: Peak flow before upgrading, pre 1998		Output: Peak flow after upgrading, after 2005	
	$\bar{P}_T [mm/6h]$	CoV	$\bar{Q}_T [m^3/s]$	CoV	$\bar{Q}_T [m^3/s]$	CoV
10	55	15 %	231	17 %	226	18 %
30	69		280	11 %	283	13 %
100	85		337	19 %	335	13 %
300	99		422	23 %	391	17 %
1,000	115		527	21 %	472	20 %
5,000	136		654	17 %	597	20 %
10,000	145		700	16 %	644	18 %

The results of the flow statistics for the gauge Kennedybrücke from the 1906 to 1997 series are presented in Table 6.2 and in Figure 6.1.

Table 6.2: Peak flow frequencies and standard errors from flow statistics of the 1906-1997 series at gauge Kennedybrücke before the retention schemes were upgraded (pre 1998)

$T [a]$	Pearson distribution			Log-Pearson distribution		
	$Q_T [m^3/s]$	$s_E [m^3/s]$	s_E / Q_T	$Q_T [m^3/s]$	$s_E [m^3/s]$	s_E / Q_T
10	128	26	20 %	122	22	18 %
30	181	33	18 %	196	42	21 %
100	238	37	18 %	302	79	26 %
300	289	55	19 %	428	134	31 %
1,000	345	70	20 %	604	225	37 %
5,000	419	91	22 %	919	424	46 %
10,000	451	100	22 %	1,088	546	50 %

Figure 6.1: Peak flow statistics at gauge Kennedybrücke from the 1906-1997 series

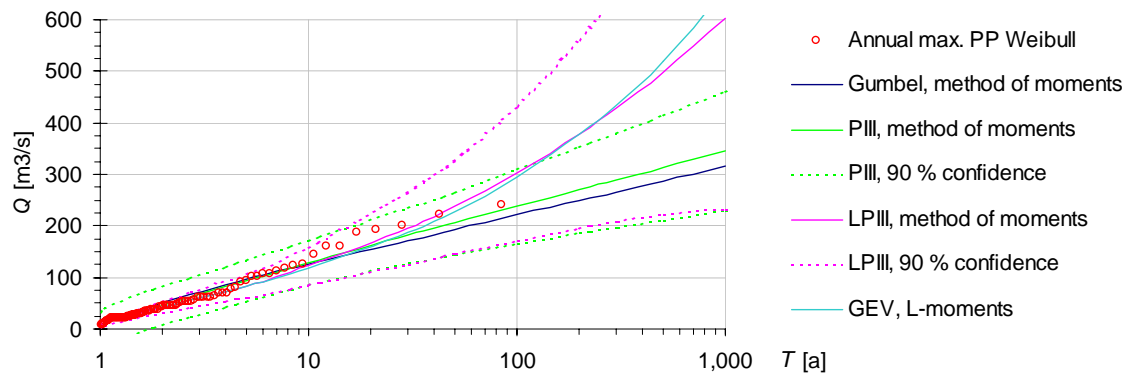
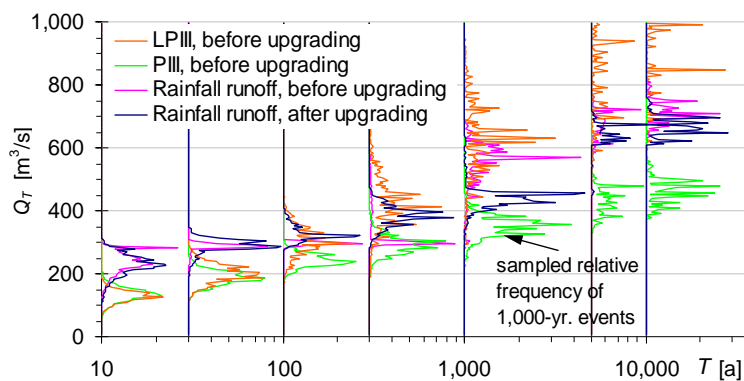


Figure 6.1 illustrates the observed annual maxima at gauge Kennedybrücke and their empirical return periods, which were determined by the plotting positions (PP) of Weibull. Larger discharges were derived by the GEV and Log-Pearson distributions, smaller by Pearson and Gumbel distribution. The Log-Pearson (LP III) and the Pearson (PIII) distributions were assessed as slightly more appropriate. For these functions, the 90 % confidence intervals are indicated.

The uncertainty estimates from both flow frequency methods provided the basis for generating the input for the hydraulic model. From the rainfall runoff model, the uncertainty in terms of the coefficient of variation (CoV) of the peak flows ranged from 11 to 23 % (Table 6.1). For the statistical data, the CoV of the peak flows was expressed as s_E / Q_T . The CoVs were found in the range of 20 % for the Pearson distribution and from 20 to about 50 % for the Log-Pearson distribution (Table 6.2).

The relative frequency of all sampled and generated peak flows is illustrated in Figure 6.2. The spikes in the curves are caused by a relative narrow Q_T -class width of 5 m³/s.

Figure 6.2: Sampled peak flow frequency from flow statistics and rainfall runoff modelling for the states before and after retention basin upgrading (frequency plots not in scale)



The alternative design rainfall events specified in Chapter 5.4.1 were not further used in this case study. The transformation of the August 2002 storm resulted in 43 mm rainfall in the western hills and in 35 mm in the eastern plains, if the largest six-hour aggregate was considered. Those figures were not critical and would correspond to up to 30-year events. The most severe aggregates in the 2002 event were those of one to two days.

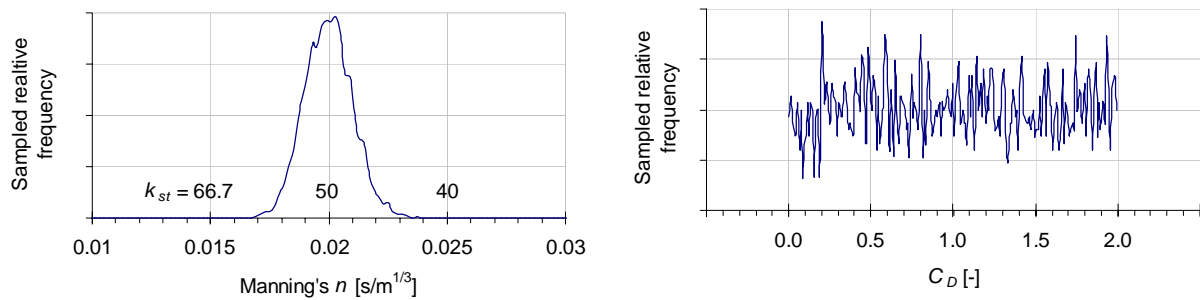
The sampled design rainfall events were well below the probable global rainfall maximum, which was estimated by Eq. 3.1 as 959 mm in six hours.

6.2 Hydraulic analysis

The results of the stochastic hydraulic modelling are first presented as the distributed character of the resistance and the load and then as the probability of failure.

The basic random variables in the channel flow process influence the load and the resistance. Figure 6.3 illustrates the relative frequencies of the basic random parameters Manning's n and the bridge drag coefficient C_D , which were obtained by 3,000 realisations.

Figure 6.3: Sampled relative frequencies of the basic random variables Manning's n and the bridge drag coefficient C_D

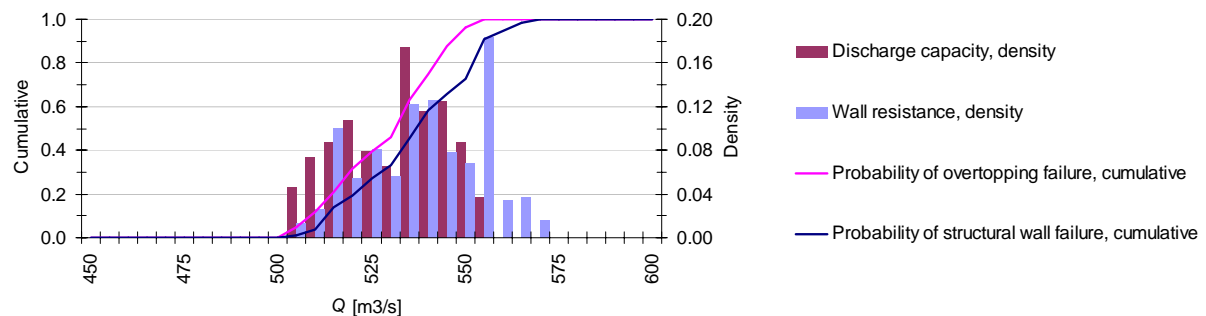


6.2.1 The resistance

The distributed character of the resistance of the river reach was first described in terms of the bankfull discharge capacity, and second by the flow magnitude at which the floodwall was loaded to its capacity (Figure 6.4). The illustrated distributions were obtained from 7,000 simulations in the critical range from 400 to 600 m³/s.

The simulations showed that discharges up to 500 m³/s could be handled by the system, but 560 m³/s almost certainly caused an overtopping of the floodwall. Structural floodwall failures occurred at slightly higher discharges. The mean values and the standard deviation of the discharge capacity were 534 and 14 m³/s, which corresponded to a coefficient of variation of 3 %. For structural floodwall failure, these figures were 541 and 16 m³/s, and again, a 3 % coefficient of variation was found.

Figure 6.4: Distribution of the resistance of the hydraulic system in terms of the bankfull discharge and the flow related to structural floodwall failure



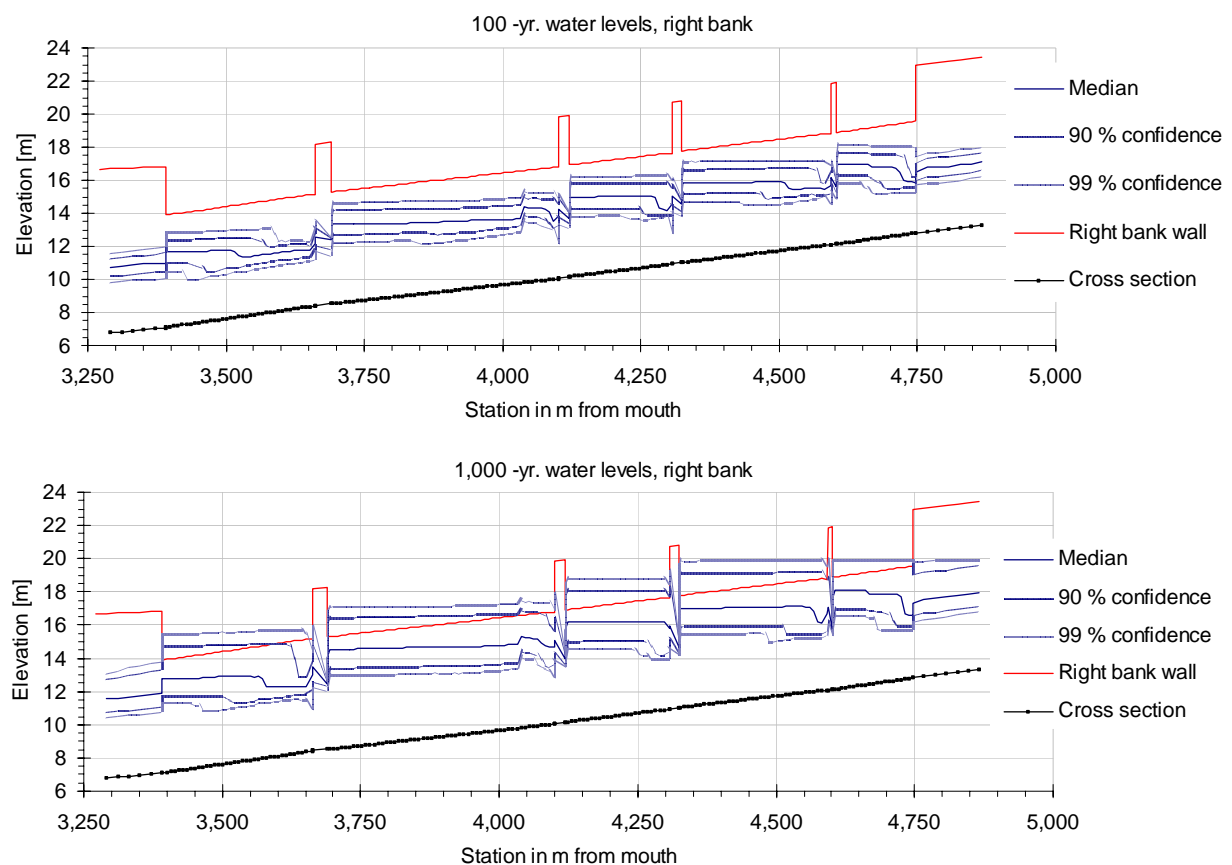
It is worthwhile mentioning, that the definition of an overtopping failure in this case study differed from deterministic analyses at Wien River. The latter were based on conservative assumptions and accounted for an additional safety height due to oscillating waves. These

two aspects were not covered in this stochastic analysis. Therefore, smaller bankfull capacities may be found in the technical documents as well.

6.2.2 The load

The distributed loads, in terms of water surface profiles, are presented by two examples in Figure 6.5. Each of them represents 3,000 Monte Carlo simulations that took about one hour on a 1.6 GHz Pentium M computer.

Figure 6.5: Distributed water levels at the right bank. Median and confidence intervals for 100- and 1,000-year events after the retention schemes were upgraded



The hydraulic Monte Carlo simulations provided plausible results and a few issues. Credible phenomena were the backwaters from the tunnel and from the arch bridge constrictions, and the supercritical flow reaches with smaller depths. These phenomena appeared as well in the deterministic water surface profile (Figure 5.11).

The results at the immediate up- and downstream ends of the bridges instead appeared as less realistic. These spiky water levels possibly originated from non-converging interim variables, where the software switched to internal boundary conditions. In a deterministic study, these results usually require a user-interpretation with due respect to the hydraulic program's warnings and error-messages.

Such interpretation of the larger depths at km 4.05 would also be appropriate. There were no channel irregularities that could cause these outcomes, and it was not clear if the computed water surfaces described a standing wave. These results were also not caused by a false format statement in the stochastic algorithm. But since other reaches were more exposed to overtopping, these doubtful results at km 4.05 did not alter the computed system reliability, and this issues was not further investigated.

6.2.3 The reliability and the probability of failure

The computed system reliability and specific failure event probabilities were computed for the Y/N switches in the event tree of Figure 5.5. The resulting probabilities are presented in Figure 6.6 for the system state after the retention schemes were upgraded. There, the system reliability appeared as 0.9991 per year. The indicated probabilities of each of the possible outcomes $P(Y)$ and $P(N)$ were derived by the interpolation of P_F over $\log T$ (Eq. 5.17).

Figure 6.6: Results of the event tree analysis for the state after upgrading the retention basins

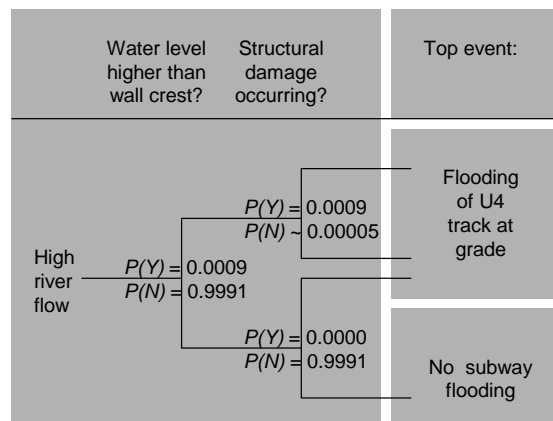


Table 6.3 comprises all outcomes of the event tree analysis for the evaluated system states. The results refer to different hydrologic analysis models and interpolation methods. The upper figures in each cell of Table 6.3 were derived by presuming a stepwise linear increase of P_F with T , the lower figures based on a stepwise linear increase of P_F with $\log T$.

Table 6.3: Event probabilities, system reliability and frequency of failure per year. The upper and lower figures base on two interpolation methods

System state, hydrologic analysis model		Probabilities of events specified in the event tree in Figure 5.5						Frequency of failure $T = 1/(1-R)$ [a]
		Water level higher than wall crest: Overtopping	Water level lower than wall crest: No overtopping	Water level higher & structural damage: Overtopping & tipping	Water level higher & no structural damage: Overtopping & no tipping	Water level lower but structural damage: No overtopping, but tipping	Water level lower & no structural damage: Reliability R	
Column no.		1	2	3	4	5	6	7
After retention schemes upgrades	Rainfall runoff	0.0008	0.9992	0.0008	~ 0.00005	0.0000	0.9992	1,254
		0.0009	0.9991	0.0009	~ 0.00005	0.0000	0.9991	1,097
Before retention schemes upgrades (Pre 1998)	Rainfall runoff	0.0017	0.9983	0.0016	0.0001	0.0000	0.9983	590
		0.0019	0.9981	0.0018	0.0001	0.0000	0.9981	524
	Pearson	0.0001	0.9999	0.0001	~ 0.00001	0.0000	0.9999	15,479
		0.0001	0.9999	0.0001	~ 0.00001	0.0000	0.9999	13,052
	Log-Pearson	0.0020	0.9980	0.0019	0.0001	0.0000	0.9980	501
		0.0022	0.9978	0.0021	0.0001	0.0000	0.9978	448

- Column 1 in Table 6.3 represents the probability of floodwaters overtopping the floodwall crest. Column 2 is its complementary.
- Column 3 details the probability of a structural wall failure if the floodwall is overtopped.
- Column 4 indicates the overtopping probability without structural damage occurring. Column 3 and Column 4 add up to column 1.
- Column 5 shows the probability of floodwall tipping when the structure is not overtopped, which surprisingly did not occur in a single model run. Therefore, column 1 in Table 6.3 represents the probability of failure.
- Column 6 finally presents the system reliability. It indicates the probability of no failure occurring within one year. The total of column 5 and column 6 equals column 2.
- Column 7 contains the average return interval of a failure.

The results showed that structural floodwall failure occurred only, if the wall was overtopped (see Page 87 for the mechanic analysis). The strengthening of the floodwall, as a technical risk management option, would therefore not change the computed results. This outcome may be discussed, as an intact floodwall would limit the inflow into the subway system, once the wall is overtopped, and it would prevent a sudden inundation of the exposed tracks.

The upgrading of the retention schemes decreased the system's probability of failure from approximately 1/550 to about 1/1,100 per year. The computed average return period of a failure event was therefore larger than the 1,000-year return period of the design load. This deviation has been discussed in Chapter 1.3 as typical for the return period-based design approach.

Table 6.3 further showed that the selection of a flow frequency analysis method could make a substantial difference to the outcomes. The results derived by the Pearson distribution seemed to overestimate the system reliability. In contrast, the similarity of the outcomes from the rainfall runoff modelling and from the Log-Pearson distribution was remarkable. The influence of the interpolation method on the results instead was not significant.

6.3 Loss analysis and risk quantification

This chapter presents the outcomes of the loss estimation and the risk quantification in common, since both results were widely overlapping.

The direct damage costs from an inundation of the at-grade track were estimated as 8.7 to 12 million Euros. Additional 77 to 278 million € of damage were estimated, if the mobile flood barriers were not available and the connected tunnelled subway stretches were flooded.

The expected annual losses (Table 6.4) were approximated as the products of these damage estimates and the probabilities of failure (column 1 in Table 6.3). The upper figures in the cells of Table 6.4 were derived by presuming a stepwise linear increase of P_F with T , the lower figures based on a stepwise linear increase of P_F with $\log T$.

Table 6.4: Intervals of expected annual losses in 1,000 € for the at-grade track and for the tunnelled subway stretches. The upper and lower figures base on two interpolation methods

State, analysis method		At-grade		Subway		At-grade + Subway	
		lower bound	upper bound	lower bound	upper bound	lower bound	upper bound
After retention schemes upgrades	Rainfall runoff	6.9	10	61	222	68	232
		7.9	11	70	254	78	265
Before retention schemes upgrades (Pre-1998)	Rainfall runoff	15	21	130	472	145	493
		17	23	146	532	163	555
	Log-Pearson	17	24	153	556	170	580
		19	27	171	622	190	649

Apparent in Table 6.4 are the wide ranges between the lower- and the upper bounds, in particular of the subway system. These intervals originated in the variability of the damage estimates per km of flooded track (Chapter 5.6.1). In comparison, the deviations caused by applying different interpolation methods were relatively small.

Although these economic losses represent barely rough estimates, the effect of upgrading the retention schemes was clearly revealed: it reduced the expected annual losses in Table 6.4 by approximately 50 %. This reduction was due to the decreased probability of failure.

Also the mobile flood barriers appeared as an effective option for risk reduction. The reliability of the mobile barriers decreased the expected annual losses by at least 90 percent. This reduction resulted from the prevented flood losses to the tunnelled subway system.

6.4 Evaluation of uncertainties

Among the hydrologic and hydraulic hazard analyses, the larger uncertainties were found in the hydrological estimation of the peak flows Q_T .

The areal design rainfall depth's coefficient of variation of 15 % resulted in an 11 to 23 % coefficient of variation of the peak flows (Table 6.1). These peak flow variations were 4 to 8 times as large as the uncertainty introduced by the channel roughness and the bridge drag coefficient. This hydraulic uncertainty was quantified by a 3 % coefficient of variation in the bankfull discharge.

The flow statistics' uncertainty, quantified by s_E/Q_T (Table 6.2), corresponded to at least the 6-fold of the uncertainty in the hydraulic system, if the results of the Pearson statistics were considered. Even larger uncertainties were associated with the Log-Pearson statistics, which corresponded to the 5- to 15-fold of the coefficient of variation in the hydraulic system.

The uncertainties in the loss estimation were verbally described. Large uncertainties were first introduced by rough assumptions for the length of the inundated track, where an upper bound solution was used. The second rough assumption was to presume, that the maximum possible losses would occur if the protection system failed. The third assumption covered the magnitude of these maximum possible losses per km of flooded track. For the at-grade track, the upper bound results were 40 % larger than the lower bound results and at the tunnelled subway system, the upper bound exceeded the lower bound results by 264 %.

7 Summary and discussion

This chapter summarises the dissertation and discusses the applied methods and the results. It is structured into hazard analysis, loss analysis, risk quantification and risk management.

In both case studies, the risk analysis expanded the understanding of the investigated systems, though the insights gained from the hazard analysis were somewhat larger than the insights into the flood losses. In both case studies, the largest uncertainties were found in the loss analysis, followed by the hydrologic analysis and the analysis of failure events. For a given flow and a defined performance of the protection system, the uncertainties inherent in the hydraulic analysis were smaller.

Although both case studies came up with a quantification of the residual risk in monetary terms, the computed losses have to be addressed as estimates rather than precise results, which corresponds to what is reported in the literature (Chapter 1.3).

7.1 Hazard analysis

The central part of the hazard analysis is the definition of scenarios and their subsequent investigation. The definition of a number of scenarios, that sufficiently cover the plausible range, is a realistic goal. A full definition of all possible scenarios instead will hardly be possible (Chapter 1.3.5). The analyses of the scenarios, which were defined in both case studies, comprised hydrologic and hydraulic methods. The hydrologic methods made use of rainfall runoff modelling and of flow statistics, and the hydraulic methods applied water surface modelling and a qualitative analyses.

Hydrologic analysis

Rainfall runoff modelling is well established for determining extreme flows. Still, the extrapolation and the variability in the available data allowed only a rather rough estimation of possible extreme events. This shall not be understood as a shortfall in the methods per se but as additional information to evaluate the preciseness of the outcomes.

In case study 1, the local precipitation characteristics had to be described by a set of different parameters instead of typical figures, since a most likely rainfall pattern could not be identified. These different precipitation scenarios resulted in a peak flow variation of up to 50 percent. So additional information and partly subjective judgement was necessary for selecting the hydrologic scenarios for the next modelling step. How far the uncertainty in the rainfall characteristics could be reduced, by considering longer time series, rain gauges outside the investigated catchment and other additional data, could not be answered. However, also former research (Apel et al. 2004) pointed at the large fraction of the computed risk expressions' variability, which was introduced by the hydrologic data.

The selected hydrologic scenarios in case study 1, that were finally used for hydraulic modelling, were a 100-year event and flows exceeding this magnitude by about 25 %, 50 % and 100 %. Those events corresponded to a 300, a 1,000 and a 5,000-year scenario, which represented a reasonably wide range of possible extreme floods at the main river. The latter scenario matched up to the catastrophic August 2002 event in some parts of Austria.

In case study 2, the rainfall was modelled by the areal precipitation depth of the storm duration, which produced the largest peak flows. As also other rainfall characteristics influence the peak flows, on one hand, accounting for one parameter may be regarded as strongly simplified. On the other hand, the stochastic modelling of different rainfall durations, varying spatio-temporal rain intensity patterns and diverse antecedent soil moisture conditions might as well be problematic, since it demands exactly for the information that

could not be derived from the available data in case study 1. Integrating all uncertainties, in modelling extreme rainfall events, into one basic random parameter may therefore be seen as a compromise: between accounting for a number of uncertain phenomena, that could not be sufficiently quantified, and the need for abstracting events in order to build a model. However, one might always detect unknown or unconsidered mechanisms behind the phenomena, which are implemented as basic random variables.

Hydraulic analysis

The hydraulic aspects in the scenario definition were based on the identified key-elements in the river- and floodplain system. Although the exhaustive qualitative hazard identification is the only way to minimise the chance to omit crucial scenarios, the scenario definition will be at least partly determined by the experience and the perception of the analyst.

Since the system performance under extreme conditions cannot be predicted, there is considerable uncertainty in the estimation of model parameters, in particular for scenarios where protection system elements fail. Large variabilities are to be expected in quantitatively describing bridge jams, levee failures, the future development of the floodplain vegetation and the river morphology.

In both case studies, the variability of a number of uncertain parameters was considered in the analysis. Most of this parametric variability was quantified from literature data, in the deterministic case study as well as in the stochastic case study. As the appropriate local observation data was not available, it had to be assumed that insights made at other rivers would apply to the case studies as well. Although this assumption is widely used, the results base on some subjective judgement, and they may be regarded as less significant in comparison with computations that are based on calibration data.

Among the modelled inundation phenomena in case study 1, levee overtopping and hinterland flows were satisfactorily reproduced. Also, the influences of road- and railway embankments, which determined the flow patterns, became apparent. Receding floods were less precisely modelled, since some details in the natural and build environment could not be resolved adequately. This also applied to a hazard that was not identified by modelling: water flowing through openings in the protection system and further into the residential areas. From these events, that were observed at a smaller flood, the fact that not all possible scenarios may be detected by modelling and by engineering practice was emphasised. Also in case study 2, some of the reviewed subway inundations were caused by unknown or overseen failure mechanisms.

In case study 2, the hydraulic and hydrologic input parameters for the stochastic model included deterministic parameters, random parameters and decision-parameters. The latter represented system properties, which may be changed by technical or operational improvements. Although there is also uncertainty in the decision parameters and in some of the parameters considered as deterministic, this parameter definition was useful by two reasons: it highlighted the alterations in the system reliability as a result of specific improvements, and it accounted for the variability in the major hydrologic and hydraulic processes.

The stochastic model produced water levels of average return periods, which were expressed by probability density functions. The results therefore comprised four dimensions, whereas state of the art hydraulic approaches consider only the former three of: the river station, the water level, the average return period and the probability distribution of the water levels for distinct return periods. However, the selected approach might be discussed, since the distributed character of the water level was not accounted for in the loss analysis, as it was proposed for instance by HEC (1998). Due to the available information, the hazard analysis and the loss analysis were linked by the probability of failure. This probability of failure was derived from integrating over the epistemic and aleatory uncertainties of the

hazard description. From this stochastic flood hazard description, one might as well obtain the system reliability in terms of a probability distribution function.

Flood hazard zones

From the case studies, four aspects appeared on the introduction of a 'residual' flood hazard zone in Austria (Chapter 1.3.1.1).

- First, mapping extreme floods larger than the 100-year event on a detailed scale is a step in the right direction as it provides important information on possible flood hazards for individuals, for communities, for planners and for the administration.
- Second, inundations behind the dikes are possible, even if flows somewhat larger than the design magnitude may be safely conveyed by the activation of structural reserves in the levee systems. The requirement for mapping such areas is already stated in the new Austrian flood hazard zoning guidelines (BMLFUW 2006b) and in comparative regulations in other countries (Kleeberg 2005).
- Third, the former 100-year floodplain in case study 1 was very similar to the inundation extents at the scenarios with levee overtopping. This finding should not be understood as a generally valid approach for a detailed delineation of residual flood hazard areas. Dikes may considerably alter the hinterland inundation patterns and retain floodwaters in the protected areas.
- And fourth, naming a hazard zone as 'residual' may be misunderstood in a way, that areas, which are not mapped, were absolutely safe from inundations. Both studies and recent observations showed that events larger than the 300-year magnitude, which shall be used for the residual hazard zone in Austria, may occur. In some areas of case study 1, where the floodplain flow was not constricted by levees, the water levels of the largest simulated flood scenario exceeded those of a 300-year event by magnitudes of half a metre and those of a 100-year event by about $\frac{3}{4}$ of a metre.

7.2 Loss analysis

The loss analysis was associated with larger uncertainties than the hazard analysis. A wide variability in the monetary flood damage to buildings was also reported from other research (Buck 1999, Merz et al. 2004a).

The most credible results were obtained for residential buildings, where data standardisation was applicable and comparative figures from ex-post analysis were available. The business, commercial and industrial sectors in case study 1 and the damage cost to the subway in case study 2 were less suitable for standardisation, mainly due to difficulties in adequately describing the object's vulnerability. Although many factors that influence the loss magnitude can be described qualitatively, there are several limitations to a quantitative and a monetary ex-ante flood loss estimation.

- First, the hazard description is incomplete, since parameters as the sediment load, the erosion and the water contamination are usually not known. This may also apply to the duration of the inundation and to the rise rate of the water level. Due to such limitations, case study 1 considered the inundation depth and the flow velocity, and case study 2 conceptualised flooding of the exposed subway system as an event, that either occurred fully or not at all.
- Second, the vulnerability estimation in terms of a damage ratio or an absolute loss magnitude is uncertain, since several properties of the elements at risk are unknown or they are not considered in the loss functions. This is typical for statistical ex-post loss analyses (Merz 2006) and it can be expected to apply also to ex-ante analyses. Also, the information on the exposed object values is limited.

- Third, there is a lack of standardised flood loss data, in particular in Austria. However, there is a potential for enhancing and for standardizing the damage data processing after a flood. Such data again provide a basis for ex-ante flood risk analyses.
- And fourth, there are methods for considering relative detailed information in the loss estimation procedure for buildings (Kraus 2004). But the application of such approaches is practically limited to smaller scales, as they require very detailed investigations and the collaboration of homeowners and managers.

Additional approaches in case study 1 to estimate potential losses in the business, commercial and industrial sectors were based on interviews and the use of statistical data. The interviews helped gaining insights into the risk mitigation strategies, which were already taken by the larger firms, such as insurance, technical measures or locating sensitive inventory to higher storeys. Still, the requested economic data were not provided in a sufficient quality and quantity. It appeared that the willingness to submit available data and the ability to estimate flood consequences in monetary terms were both limited. This might as well have been caused by the lack of well-elaborated options for managing the residual risks, so the benefits of submitting data were not that obvious.

An alternative estimation method for business interruption costs made use of national statistical data. These were the per-capita gross revenues and the net revenues of specific economic sectors, which were combined with approximations of the number of workplaces in the potentially inundated area and estimates of the duration of flood induced business interruptions. Although this approach based on rough assumptions and it employed elder data, it gave an idea about the magnitude of indirect flood losses: they might reach up to the magnitude of the direct loss estimates, if the gross revenue was considered.

Both case studies and the review in Chapter 1.3.2 unveiled uncertainties in the completeness and the preciseness of the loss estimates. The use of standard loss data requires less efforts, but it omits some aspects of the object's vulnerability. On the other hand, standardised data may be regarded as an egalitarian approach, where each building within an object class is accounted for by the one and the same value instead of a value that reflects the owner's wealthiness. However, improving the loss estimation is part of ongoing research projects, for instance the German RIMAX (Risk Management of Extreme Floods) and the European project FLOODSite, which also addresses indirect economic losses and social issues (Messner et al. 2006).

7.3 Risk quantification

The residual risk describes the risk as after implementing a protection system and contains an unknown risk fraction. This fraction originates from the limited ability to consider all scenarios and all possible consequences. Although both case studies expanded the known risk fraction, there is still an unknown rest, and a part of this rest might become known in the future.

This consideration on the residual risk applies to natural hazard risks, to health risks and to other kinds of risks, as it was discussed for instance in Merz (2006). Since the risk expressions represent a synopsis of the hazard analysis, the loss estimation and the associated uncertainties, the obtained risk quantification may therefore be addressed as limited to the covered types of losses and uncertain in its magnitude.

On one side, it may be argued that these limitations and uncertainties were too large for decision-making. On the other side it appeared from both case studies that the uncertain risk expressions were still useful in a relative sense, when risks associated with different options were compared. In case study 1, the prevention of structural or operational failures reduced the expected annual flood damages by at least one-third, and in case study 2, this reduction was estimated as 90 % and more.

The quantitative risk expression by the frequency of monetary flood losses could be derived in both case studies, at least as step-functions. The risk expressions by the expected annual losses were in both cases relatively small, and the maximum losses were very large. This drastic increase in the loss magnitudes at the larger and very seldom flood scenarios may be used to criticise the expected annual flood losses as an incomplete risk expression, since it disregards the limited ability to recover from catastrophic scenarios (Chapter 1.3.3).

In the discussion on the appropriate risk expressions, two principally different aims of the risk analysis may be detected. The analysis may focus on the risk-based decision-making or it may investigate the nature of risk itself. Risk-based decision-making will rather be linked with single-metric risk measures, such as the expected value. The nature of risk may instead be expressed in a social, an economic and an environmental dimension by risk curves and risk matrices. Integrating both risk analysis aims is a challenge for further applied and basic research, since it requires societal preferences for weighting losses and for integrating over the three dimensions of risk.

In Austria, the analysis of flood risks and residual risks is rather a new discipline and the expectations to the outcomes are manifold. Mapping and managing flood risks are also part of the proposed directive of the European Parliament and of the Council on the assessment and management of floods (Commission of the European Communities 2006). However, a monetary risk quantification will not always be necessary for managing flood risks, in particular if the number of the elements at risk is small. Such a qualitative risk analysis approach was described for instance by Hinterleitner (2002) for a polder at the Traisen River.

7.4 Risk management

The above-mentioned dramatic increase in the loss magnitudes of larger flood scenarios also reflects the design philosophy, which was applied in Austria throughout the last decades. It aimed to prevent floods up to a specified magnitude, and, only in exceptional cases, it regarded inundations and flood losses beyond that magnitude. Elements that could handle such extreme events were implemented in case study 2. Still, a successful operation of these elements is based on the on-time decision-making and on the technical reliability of the implemented systems. The review of international subway floods pointed out that this should not be taken for granted (Chapter 5.6.1).

A technical instrument to improve the control of flood hazards is the differentiation of the levees' freeboard. Case study 1 showed that without this differentiation, the levees at the industrially used left riverbank and at the agriculturally used right bank were overtopped at the same discharge. The design considerations for the freeboard shall therefore be based on the consequences of its exceedance. This approach is already stated in the new technical guidelines for the Federal River Engineering Administration (BMLFUW 2006a). Further recommendations for the design of the freeboard and for the implementation of overflow section in dikes have been elaborated (Nachtnebel and Klenkhart 2004). These overflow sections reduce the likelihood of levee failures and of uncontrolled inundations in the hinterland.

The role of flood risk analysis in the design and the evaluation of flood protection schemes may be summarised as:

- In a normative design approach with mainly a 100-year design target, a risk analysis may be applied to determine the residual risk and to evaluate the effectiveness and the benefits of particular risk management options. The outcomes of the analysis may also be used to communicate flood risks to the general public. Further, it is worthwhile mentioning, that a general critique on the normative design approach for technical flood protection schemes cannot be derived from the case studies, *if* the residual flood risks were sufficiently covered.

- Within a risk-based approach, that optimises the design magnitude for instance by minimizing the total of the expected residual economic losses and the costs for construction and maintenance of a protection scheme, a monetary risk analysis will be inevitable.
- Approaches that consider economic, social and environmental risks may base on a monetary quantification of all relevant effects, on a cost-effectiveness model or on methods of multi-criteria decision-making.

7.5 Deterministic and stochastic approaches

In the discussion of deterministic and stochastic approaches, computational limitations that may shift in the future, the available input data and the number and the kind of output parameters deserve major attention. Two more relevant aspects are the capability to integrate stochastic results in the decision-making process and the ability to present and communicate distributed outputs. This especially applies for end products as animations, for data to be imported into a GIS and when the variability ranges in the order of magnitude of the output parameter itself.

Numerical stochastic modelling in flood risk analysis requires either a rather simple process or a higher degree of model abstraction. For instance, 2D unsteady flows are deterministically modelled and used for Monte Carlo simulations in a reduced form (Apel et al. 2004).

The efforts to integrate a hydraulic model into Monte Carlo simulations depend to a high degree on the programming skills, like case study 2 outlined. Many of today's hydrologic and hydraulic models are developed and sold as deterministic applications, so eventually the source-codes will either be highly complex or they will not be available.

Case study 2 showed further, that although many uncertain input parameters were identified, just a few could be characterised by justified input data distributions, as a subjective estimation of the distribution functions was avoided. However, if distributed input data are available, if the output shall be characterised by a probability distribution function and if the resources for preparing a stochastic solution are accessible, Monte Carlo simulations can be recommended.

8 Conclusions

Conclusions and suggestions from this work were drawn on the flood risk analysis, on the definition and investigation of flood scenarios, on the quantification of risk, on the uncertainties and on further research.

Flood risk analysis

The analysis of flood risks helps to gain insights into a system of sensitive values, technical elements and flood hazards. The risk definition in this work therefore combined scenarios of possible flood hazards, their probabilities and their consequences. Different risk definitions are also found, for instance in the new Austrian guidelines for the Federal River Engineering Administration (BMLUW 2006a). In these guidelines, risk is defined as the occurrence probability of a specific flood scenario within a specified time period. In Austria, the last decades' approach to flood risk has focused on the analysis and the control of flood hazards and less attention was paid to the analysis and the reduction of flood losses and the residual risk.

The common understanding of risk, which results in the definition of quantitative or qualitative risk expressions, represents the basis for a flood risk analysis. It is suggested to express flood risks by risk curves or by risk matrices in addition to the expected annual flood losses.

Scenarios

The key tasks in the analysis of flood hazards and their probabilities are the definition and the subsequent investigation of flood scenarios. In this work, the scenarios were defined to cover a wide range of possible hydrologic and hydraulic conditions. These conditions included discharges and the performance of the main elements within the system of the river, the floodplains and the technical structures. Those scenarios were analysed by either running a set of deterministic computations with different hydrologic and hydraulic input parameters, or by Monte Carlo simulations, which were based on probability-distributed input parameters.

It may remain in discussion how seldom the largest considered scenario should be, since even phenomena like the estimated probable maximum flood and the probable maximum precipitation have been exceeded (Merz 2006 p.104). Based on the case studies in this work, it is suggested to consider two kinds of events in the definition of the largest scenario: 1,000-year or larger events and the occurrence of structural and operational failures. Considerations on the return periods of flood scenarios should account for longer time horizons than the one-year period, which is related to the well-known probability estimates. In a 50-year period, the probability of experiencing at least one 300-year event amounts to 15 percent, which may be regarded as considerably high. Analysing flood risks by 300-year events was suggested by BMLFUW (2006a & b).

Risk quantification

From the elaboration of both case studies, it is suggested to use the results of a monetary risk analysis in a relative context, namely by comparing risk expressions that are associated with different options. Absolute risk measures instead are linked with much uncertainty, and some subjective judgement may be necessary to quantify the uncertainty. Beside these uncertainties, there are two more reasons why the residual flood risk can be estimated, but it cannot be precisely quantified: the hazard analysis will be limited to a number of scenarios and the loss analysis will be restricted to a fraction of all possible consequences.

Uncertainties

Among the hydrologic analyses, the hydraulic analyses and the loss analyses, the largest uncertainties in both case studies emerged from the quantification of monetary flood losses. The flood losses were in addition overlaid by indirect losses, which could only be roughly estimated, and by not quantified intangible effects. Somewhat smaller were the uncertainties in the hydrologic estimation of the flow frequencies and in the hydraulic analysis of failure scenarios. The uncertainties in the channel flow processes and in the inundation modelling were relatively small. These findings showed the need to consider the uncertainties, which are introduced in the risk analysis by the imperfect knowledge of the system under study.

Further research

This work showed that the methods applied for risk analysis are partly well-established, but further research is necessary, in particular for the loss estimation: on the aspects of risks that are not quantified easily and on the incorporation of uncertainties in the quantitative risk estimates.

Two kinds of approaches for analysing flood risks seem promising:

- Basic research approaches to the nature of risk, which consider the economic, the social and the environmental dimension of risk.
- Pragmatic approaches for risk quantification, which are based on standardised procedures for flood risk analysis. Manuals, as they were used for case study 1, would be helpful to foster the use of risk analyses in the Austrian river engineering practice. As the monetary analysis has some limitations, these manuals should be completed by a set of qualitative indicators and by recommendations on handling uncertainties.

9 References

- Abbott, M. B.; Ionescu, F. (1967): On the numerical computation of nearly-horizontal flows. *Journal of Hydraulic Research* 5, 97-117.
- Aigner, H.; Hanten, K. P.; Stania, K.; Stiefelmeyer, H. (2002): Ausweisung von Naturgefahren – Gefahrenzonenplanung. *Österreichische Wasser- und Abfallwirtschaft* 54 (7-8), 105-109.
- Ale, B. J. M. (2002): Risk assessment practices in The Netherlands. *Safety Science* 40, 105-126.
- Ang, A. H.-S.; Tang, W. H. (1975): Probability Concepts in Engineering Planning and Design: Volume 1-Basic Principles. New York: John Wiley & Sons.
- Apel, H.; Thieken, A. H.; Merz, B.; Blöschl, G. (2004): Flood risk assessment and associated uncertainty. *Natural Hazards and Earth System Sciences* 4, 295-308.
- Auer, I.; Böhm, R.; Mohnl, H. (1989): Klima von Wien: Eine anwendungsorientierte Klimatographie. Beiträge zur Stadtforschung, Stadtentwicklung und Stadtgestaltung: Band 20. Wien: Magistrat der Stadt Wien.
- Bauer, J. (2004): Naturgefahren und Raumplanung in Bayern. In: ÖWAV-Symposium: Raumordnung und Hochwasserschutz, 21.-22. Juni 2004. Wien: ÖWAV, 1-2.
- Bauer, S.; Hausperger, M.; Mader, H.; Oberhofer, A. (1993): Hochwasserrückhalteanlagen für den Wienfluss: wasserwirtschaftlich-ökologisches Gesamtkonzept der Stadt Wien. *Österreichische Wasserwirtschaft* 24 (9-10), 242-257.
- Beardsley, C. (1993-02-01). Simple solutions. (preventing the flooding problem of the Hudson River tubes). Mechanical Engineering-CIME 115 (2), 4.
<http://www.highbeam.com/doc/1G1-13472993.html> (2001-10-13).
- Bergström, S. (1992): The HBV Model – its structure and applications; SMHI Reports Hydrology, No. 4. Norrköping.
- BMLF (1980): Vorläufige Richtlinie für die Durchführung von Kosten-Nutzen-Untersuchungen im Flussbau. Wien: Bundesministerium für Land- und Forstwirtschaft, Sektion IV.
- BMLF (1994a): Richtlinien für die Bundeswasserbauverwaltung: RIWA-T. Wien: Bundesministerium für Land- und Forstwirtschaft, Sektion IV – Wasserwirtschaft und Wasserbau.
- BMLF (1994b): Richtlinien für die Gefahrenzonenabgrenzung. Wien: Referat VC8a, Forsttechnischer Dienst für Wildbach- und Lawinenverbauung.
- BMLFUW (2005a-08-25): Hochwasserereignis 21. bis 25. August 2005 in Österreich: Erste Einschätzung der Jährlichkeiten der aufgetretenen Hochwasserscheitel.
<http://www.wassernet.at/filemanager/download/12124/> (2006-05-30).
- BMLFUW (2005b): Hydrologischer Atlas Österreichs: 2. Lieferung. Wien: BMLFUW.
- BMLFUW (2006a-06-30): Technische Richtlinien für die Bundeswasserbauverwaltung: RIWA-T gemäß § 3 Abs. 2 WBFG: Fassung 2006. Wien: BMLFUW.
<http://wasser.lebensministerium.at/filemanager/download/16583/> (2006-09-12).
- BMLFUW (2006b-06-23): Richtlinien zur Gefahrenzonenausweisung für die Bundeswasserbauverwaltung: Fassung 2006. Wien: BMLFUW.
<http://www.wassernet.at/filemanager/download/16584/> (2006-09-12).
- Bohnenblust, H. (1988): Risk-based decision making in the transportation sector. In: Jorissen, R. E.; Stallen, P. J. M. (eds.): Quantified Societal Risk and Policy Making. Dordrecht: Kluwer Academic Publishers, 14.

- Booyesen, H. J.; Viljoen, M. F.; Villiers, G. T. (1999): Methodology of the calculation of industrial flood damage and its application to an industry in Vereeniging. *Water SA* 25, 41-46. http://www.wrc.org.za/archives/watersa_archive/1999/January/jan99_p41.pdf (2005-05-30).
- Brandes, H. (2000-06): The Venezuela Flash Floods and Debris Flows of 15-16 December 1999. *Landslide News* 13, 5-7. <http://www.landslide-soc.org/publications/l-news/13/1305.htm> (2001-10-13).
- Brown, L. (1996a-10-23): MBTA damage may top \$10M. *Boston Herald*. <http://pqasb.pqarchiver.com/bostonherald/access/17337594.html?dids=17337594:17337594&FMT=ABS&FMTS=ABS:FT&date=Oct+23%2C+1996&author=LAURA+BROWN&pub=Boston+Herald&edition=&startpage=006&desc=MBTA+damage+may+top+%2410M> (2001-10-13).
- Brown, L. (1996b-11-16): MBTA acts to bring flood-damaged Green Line up to speed. *Boston Herald*. <http://pqasb.pqarchiver.com/bostonherald/access/17343995.html?dids=17343995:17343995&FMT=ABS&FMTS=ABS:FT&date=Nov+16%2C+1996&author=LAURA+BROWN&pub=Boston+Herald&edition=&startpage=006&desc=MBTA+acts+to+bring+flood-damaged+Green+Line+up+to+speed> (2001-10-13).
- Buck, W. (1999): Auswertung der HOWAS-Datenbank: HY 98/15. Karlsruhe: Institut für Wasserwirtschaft und Kulturtechnik, Universität Karlsruhe.
- Bureau of Reclamation (2004-07-19): Glossary. <http://www.usbr.gov/library/glossary/> (2006-10-29).
- BUWAL (1999a): Risikoanalyse bei gravitativen Naturgefahren. Fallbeispiele und Daten. Umwelt-Materialien 107/II Naturgefahren. Bern: BUWAL. <http://www.umwelt-schweiz.ch/buwal/shop/files/pdf/php01As2z.pdf> (2006-05-30).
- BUWAL (1999b): Risikoanalyse bei gravitativen Naturgefahren. Methode. Umwelt-Materialien 107/I Naturgefahren. Bern: BUWAL. <http://www.umwelt-schweiz.ch/buwal/shop/files/pdf/phpAy8rtB.pdf> (2006-05-30).
- BWG (2001): Hochwasserschutz an Fließgewässern: Wegleitungen des BWG. Biel: BWG. <http://www.bwg.admin.ch/themen/natur/d/pdf/wlhwsg.pdf> (2006-05-30).
- BWG (2002): Hilfe-Assistent zum Excel-Tool MethodeBWG für die Abschätzung des Schadenpotentials Überschwemmung und Übermürung: Version 1.2. Biel: BWG. <http://www.bwg.admin.ch/service/download/d/schapo/schapoah.pdf> (2006-05-30).
- BWW; BRP; BUWAL (1997): Berücksichtigung der Hochwassergefahren bei raumwirksamen Tätigkeiten: Empfehlungen 1997, Naturgefahren. Biel: BWW; BRP; BUWAL. <http://www.bwg.admin.ch/themen/natur/d/pdf/empfhwg.pdf> (2006-05-30).
- CDM (2001-12): Draft Environmental Impact Report (DEIR): EOE #11865. Muddy River Restoration Project. Boston. <http://www.muddyriverproject.org/DEIR/index.htm> (2006-11-06).
- Chang, C. C. (2001): Managing Taiwan's Catastrophic Risk. In: 2001 Annual Convention of The Actuarial Institute of The Republic of China, 13 November 2001. Taipei.
- Chuang, J. (2001-10-25). Mayor Ma questioned over Nari. *Taipei Times*. <http://www.taipeitimes.com/News/front/archives/2001/10/25/108603> (2003-01-14).
- Commission of the European Communities (2006): Proposal for a Directive of the European Parliament and of the Council on the assessment and management of floods. http://ec.europa.eu/environment/water/flood_risk/pdf/com_2006_15_en.pdf (2006-05-30).

- Compton, K.; Ermolieva, T.; Linnerooth-Bayer, J. (2002): Integrated Flood Risk Management for Urban Infrastructure: Managing the Flood Risk to Vienna's Heavy Rail Mass Rapid Transit System. In: Second Annual IIASA-DPRI Meeting: Integrated Disaster Risk Management: Megacity Vulnerability and Resilience, 29-31 July 2002. Laxenburg, 1-20. <http://www.iiasa.ac.at/Research/RMS/dpri2002/Papers/Compton.pdf> (2006-11-05).
- Compton, K. L.; Faber, R.; Ermolieva, T.; Linnerooth-Bayer, J.; Nachtnebel, H.-P. (2004): Development of a Catastrophe Model for Managing the Risks of Urban Flash Flooding in Vienna: Interim Report IR-04-xx. Laxenburg: International Institute for Applied Systems Analysis.
- Chow, V. T.; Maidment, D. R.; Mays, L. W. (1988): Applied Hydrology. McGraw-Hill.
- CUR (1990): Probabilistic design of flood defences: CUR TAW report 141. Rotterdam: Balkema.
- Darlington, R. A.; Lambert, K. B. (2001): Comparing the Hurricane Disaster Risk of U.S. Coastal Counties. *Natural Hazards Review* 2 (3), 132-142.
- Debene, A.; Nachtnebel, H.-P. (2005): Abflussanalyse Donau-Traisen: Endbericht. Wien: IWHW-BOKU.
- DHI (2004a): MIKE 11: A Modelling System for Rivers and Channels. Reference Manual. DHI. Software. Hørsholm: DHI.
- DHI (2004b): MIKE FLOOD: 1D-2D Modelling. User Manual. DHI Software. Hørsholm: DHI.
- DIN (1996): Wasserwesen, Begriffe. DIN-Taschenbuch 211: Beuth.
- DVWK (1984): Arbeitsanleitung zur Anwendung von Niederschlag-Abfluß Modellen in kleinen Einzugsgebieten, Teil II: Synthese. Regeln zur Wasserwirtschaft, Heft 113. Parey Hamburg.
- DVWK (1991): Hydraulische Berechnung von Fließgewässern. Merkblätter 220. Parey Hamburg.
- DVWK (1999): Statistische Analyse von Hochwasserabflüssen. Merkblätter 251. Parey, Hamburg.
- DWD (1997): KOSTRA – Starkniederschlagshöhen für Deutschland. Deutscher Wetterdienst, Abteilung Klimatologie – Referat Hydrometeorologie. Offenbach am Main: Selbstverlag des Deutschen Wetterdienstes.
- Egli, T. (2002): Hochwasservorsorge: Maßnahmen und ihre Wirksamkeit. Koblenz: IKSR. http://iksr.de/uploads/media/RZ_iksr_dt.pdf (2003-01-16)
- Egli, T. (1996): Hochwasserschutz und Raumplanung. Schutz vor Naturgefahren mit Instrumenten der Raumplanung – dargestellt am Beispiel von Hochwasser und Murgängen. Zürich: vdf Hochschulverlag.
- Eikenberg, C. (1998): Journalistenhandbuch zum Katastrophenmanagement. 5. Auflage. Bonn: Deutsches IDNDR-Komitee für Katastrophenvorbeugung.
- Faber, M. H.; Stewart, M. G. (2003): Risk assessment for civil engineering facilities: critical overview and discussion. *Reliability Engineering and System Safety* 80, 173–184.
- Faber, R.; Compton, K.; Ermolieva, T.; Bayer, J.; Nachtnebel, H.-P. (2003): Flood Risk Assessment and Management for Vienna's Subway. Facing Uncertainties and Temporal Changes. In: Third DPRI-IIASA International Symposium on Integrated Disaster Risk Management (IDRM-2003), 3-5 July 2003. Kyoto, 1-17.

- Faber, R.; Hinterleitner, G.; Kiesenhofer, L.; Nachtnebel, H.-P. (2004a): Überprüfung und Bewertung der neuen Richtlinien für die Erstellung von Gefahrenzonenplänen am Beispiel des unteren Kamp und der Schwechat: Workpackage (WP) Naturgefahren Bundeswasserbauverwaltung (BWV) Teilprojekt (TP) 04a. In: BMLFUW (ed.): Analyse der Hochwasserereignisse vom August 2002 – Flood Risk. Wien: BMLFUW, CD-ROM: 05_WP-Naturgefahren_BWV\WP_Naturgefahren_BWV_TP04a.pdf.
- Faber, R.; Nachtnebel, H.-P.; Rabacher, C.; Hinterleitner, G. (2004b): Operative Maßnahmen Donau: Workpackage (WP) Donau Teilprojekt (TP) 05. In: BMLFUW (ed.): Analyse der Hochwasserereignisse vom August 2002 – Flood Risk. Wien: BMLFUW, CD-ROM: 04_WP-Donau\WP_Donau_TP05.pdf.
- Faber, R.; Leroch, K.; Nachtnebel, H.-P. (2005): Risikoanalyse des bestehenden Hochwasserschutzes der Stadt Gleisdorf und Umgebung. Wien: IWHW-BOKU.
- Fritzsche, A. F. (1986): Wie sicher leben wir? Risikobeurteilung und –bewältigung in unserer Gesellschaft. Köln: TÜV Rheinland.
- Fuchs, M. (1998): Modeling Snowmelt Runoff in an Alpine Watershed. Diploma thesis at the University of Natural Resources and Applied Life Sciences, Vienna.
- Fuchs, M. (2005): Auswirkungen von möglichen Klimaänderungen auf die Hydrologie verschiedener Regionen in Österreich. Dissertation an der Universität für Bodenkultur Wien.
- Gutknecht, D.; Reszler, C.; Blöschl, G. (2002-08-30): Jahrtausend-Hochwasser am Kamp? TU Wien: Forschungshomepage. <http://www.tuwien.ac.at/forschung/nachrichten/a-kamp.htm> (2006-05-30).
- GVL (2004): Hochwasserschutz: Beschreibung und Quantifizierung von Schadenbildern. Biel: BWG. <http://www.bwg.admin.ch/themen/natur/d/pdf/modschad.pdf> (2006-05-30).
- Haan, C. T. (2002): Statistical Methods in Hydrology: Second Edition. Ames: Iowa State Press.
- Habersack, H.; Bürgel, J.; Petraschek, A. (2004): Synthesebericht. In: BMLFUW (ed.): Analyse der Hochwasserereignisse vom August 2002 – Flood Risk. Wien: BMLFUW, CD-ROM: 00_Synthesebericht\Synthesebericht - FloodRisk.pdf.
- Habersack, H., Moser A. (eds. 2003): Plattform Hochwasser: Ereignisdokumentation Hochwasser August 2002. Wien: ZENAR – BOKU. http://zenar.boku.ac.at/PDF-Files/Hochwasser_2002_Gesamt.PDF (2006-05-30).
- Haidvogel, G.; Seebacher, F.; Pinka, P.; Gabriel, H.; Fraiss, B.; Küblbäck, G.; Kusebauch, G. (2004): Raumordnung und Hochwasserschutz am Beispiel der Traisen – Siedlungsentwicklung und Schadensanalyse: Workpackage (WP) Naturgefahren Bundeswasserbauverwaltung (BWV) Teilprojekt (TP) 07. In: BMLFUW (ed.): Analyse der Hochwasserereignisse vom August 2002 – Flood Risk. Wien: BMLFUW, CD-ROM: 05_WP-Naturgefahren_BWV\WP_Naturgefahren_BWV_TP07.pdf.
- Haimes, Y. Y. (1998): Risk Modeling, Assessment, and Management: Wiley Series in Systems Engineering. New York: John Wiley & Sons.
- Hammerl, C.; Lenhardt, W.; Steinacker, R.; Steinhauser, P. (eds. 2001): Die Zentralanstalt für Meteorologie und Geodynamik 1851 – 2001: 150 Jahre Meteorologie und Geophysik in Österreich. CD-ROM: ÖKLIM: Digitaler Klimaatlas Österreichs: Eine interaktive Reise durch die Vergangenheit, Gegenwart und Zukunft des Klimas. Graz: Leykam.
- HEC (1996-08-01): Engineering and Design - Risk-Based Analysis for Flood Damage Reduction Studies. Washington DC: Hydrologic Engineering Centre, US Army Corps of Engineers. <http://www.usace.army.mil/publications/eng-manuals/em1110-2-1619/entire.pdf>

- HEC (1998): HEC-FDA. Flood Damage Reduction Analysis: User's Manual. Davis: Hydrologic Engineering Centre, US Army Corps of Engineers. <http://www.hec.usace.army.mil/software/hec-fda/documentation/toc.pdf> (2003-01-14).
- HEC (2001): HEC-RAS. River Analysis System: Version 3.0.1. Davis: Hydrologic Engineering Centre, US Army Corps of Engineers.
- HEC (2002): HEC-RAS. Hydraulic Reference Manual. Davis: Hydrologic Engineering Centre, US Army Corps of Engineers. <http://www.hec.usace.army.mil/software/hec-ras/documents/hydref/index.html> (2006-10-27).
- Helm, P. (1996): Integrated Risk Management for Natural and Technological Disasters. Tephra 15 (1), 5-19. Wellington: Ministry of Civil Defence and Emergency Management. [http://www.mcdem.govt.nz/MEMWebsite.nsf/Files/tephra96/\\$file/tephra96.pdf](http://www.mcdem.govt.nz/MEMWebsite.nsf/Files/tephra96/$file/tephra96.pdf) (2006-05-30).
- Hershfield, D. M. (1961): Estimating the probable maximum precipitation. *Journal of the Hydraulics Division* (American Society of Civil Engineers) 87, 99-106.
- Hershfield, D. M. (1965): Method for estimating probable maximum rainfall. *Journal American Water Works Association* 57, 965-972.
- Hinterleitner, G. (2002): Restrisikobetrachtungen bei bestehenden Hochwasserschutzsystemen. *Österreichische Wasser- und Abfallwirtschaft* 54 (7-8), 99-103.
- Hinterleitner, G. (2006): Risiko und Restrisiko in der Schutzwasserwirtschaft. In: ÖWAV-Symposium: Naturgefahr Wasser – Wahrnehmung und Management, 22.-23. Februar 2006. Wien: ÖWAV, 1-10.
- Hollenstein, K. (2005): Reconsidering the risk assessment concept: Standardizing the impact description as a building block for vulnerability assessment. *Natural Hazards and Earth System Sciences* 5, 301–307.
- Hydrotec (2001-12): Hochwasser-Aktionsplan Lenne: Teil I: Bericht und Karten. Hagen: Staatliches Umweltamt. http://www.stua-ha.nrw.de/map/p/hwlenne/main/07_Bericht/tr/bericht.pdf (2006-05-30).
- Hydrotec (circa 2002): Hochwasser-Aktionsplan Sieg - Gemeinschaftsprojekt der Länder Nordrhein-Westfalen und Rheinland-Pfalz. Siegen: Staatliches Umweltamt. <http://www.stua-si.nrw.de/sieg/b1/index.htm> (2006-05-30).
- IKSR (2001): Rheinatlas. Wiesbaden-Bierstadt: Ruiz Rodriguez + Zeisler + Blank, GbR. <http://www.rheinatlas.de/> (2006-05-30).
- IWHW; Gruppe Wasser (1988): Retentionsuntersuchung Wienfluss. Wien: Magistratsabteilung 45 - Wasserbau.
- Jones, B. (1999-12-17): Torrential rains paralyse Venezuela. *The Columbian*. http://nl.newsbank.com/nl-search/we/Archives?p_action=list&p_topdoc=11 (2001-10-13).
- Jonkman, S. N.; van Gelder, P. H. A. J. M.; Vrijling, J. K. (2003): An overview of quantitative risk measures for loss of life and economic damage. *Journal of Hazardous Materials* A99, 1-30.
- Kaplan, S.; Garrick, B. J. (1981): On the quantitative definition of risk. *Risk Analysis* 1 (1), 11-27.
- Kelman, I. (2003): Defining Risk. FloodRiskNet Newsletter, Issue 2, 6-9. <http://www.ilankelman.org/abstracts/kelman2003frn.pdf> (2006-10-28).

- Kemmerling, W.; Kaupa, H. (1988): Informationsbericht zur Durchführung von Kosten-Nutzen-Untersuchungen in der Schutzwasserwirtschaft und in der Lawinenverbauung. Wasserwirtschaft und Wasserversorgung: Planungen und Untersuchungen. Wien: BMLF.
- Kienholz, H.; Krummenacher, B.; Kipfer, A.; Perret, S. (2004): Aspects of Integral Risk Management in Practice – Considerations with Respect to Mountain Hazards in Switzerland. *Österreichische Wasser- und Abfallwirtschaft* 56 (3-4), 43-50.
- Kikuchi, R.; Sasaki, A. (2002): Report on Preliminary Study of the Elbe River Floods. Infrastructure Development Institute, IFNet Preparatory Unit, "Water in Rivers". http://www.internationalfloodnetwork.org/04/rep_02eurPS.pdf (2003-01-14).
- Kite, G.W. (1988): Frequency and Risk Analysis in Hydrology. Littleton: Water Resources Publication.
- Kleeberg, H.-B. (ed. 2005): Hochwasser-Gefahrenkarten. Forum für Hydrologie und Wasserbewirtschaftung, Heft 08.05. München: Universität für Bundeswehr.
- Kling, H. (2002): Development of Tools for a Semi-Distributed Runoff Model. Diploma thesis at the University of Natural Resources and Applied Life Sciences, Vienna.
- Korea Herald (1998a-05-04): Online article. (2002).
- Korea Herald (1998b-06-16): Online article. (2002).
- Krainer, R. (2003): Möglichkeiten und Grenzen des Hochwasserschutzes - Risikoabschätzung und -bewertung am Beispiel von Hochwasserrückhaltebecken. Dissertation an der Technischen Universität Graz.
- Kranewitter, H. (2002): Liegenschaftsbewertung. 4. Auflage. Wien: GESCO.
- Kraus, D. (2004): Wirtschaftlichkeit und Priorisierung von Schutzmaßnahmen vor Wildbächen, Erosion und Lawinen: IAN Report 94: Workpackage (WP) Naturgefahren Wildbach- und Lawinenverbauung (WLV) Teilprojekt (TP) 03. In: BMLFUW (ed.): Analyse der Hochwasserereignisse vom August 2002 – Flood Risk. Wien: BMLFUW, CD-ROM: 06_WP-Naturgefahren_WLV\WP_Naturgefahren_WLV_TP03.pdf.
- Kreibich, H.; Thieken, A. H.; Pertow, T.; Müller, M.; Merz, B. (2005): Flood loss reduction of private households due to building precautionary measures – lessons learned from the Elbe flood in August 2002. *Natural Hazards and Earth System Sciences* 5, 117-126.
- Kreps, H., Schimpf, H. (1965): Starkregen und Starkregenstatistik. In: BMLF (ed.): Mitteilungsblatt des Hydrographischen Dienstes in Österreich. Nr. 42. Wien: BMLF, 1-44.
- Krushelnicky, A. (2002-08-24): Officials try to shift blame as Prague's metro floods. Telegraph. <http://www.telegraph.co.uk/news/main.jhtml?xml=/news/2002/08/24/wflood24.xml> (2006-05-30).
- Laver, R. S.; Schneck, D. C. (1995): The Transit Capital Cost Price Index Study: MD-90-7001-01. Washington DC: Federal Transit Administration.
- Lazowski, W.; Zuckerstätter, C. (circa 2001): Der neue Wienfluß. Natur und Technik im Einklang. Wien: Magistrat der Stadt Wien – MA 45.
- Leavesley, G. H. Restrepo, P. J.; Markstrom, S. L.; Dixon, M.; Stannard, L. G. (1996): The Modular Modelling System (MMS): User's guide. Denver: U.S. Geological Survey.
- Lehmann, B. (2005): Empfehlungen zur naturnahen Gewässerentwicklung im urbanen Raum unter Berücksichtigung der Hochwassersicherheit. Mitteilungen des Instituts für Wasser und Gewässerentwicklung, Bereich Wasserwirtschaft und Kulturtechnik, der Universität Karlsruhe (TH), 230. Karlsruhe.

- LFI-RWTH; ProAqua GmbH; Pflügner, W. (2001): Potentielle Hochwasserschäden am Rhein in NRW. Aachen. <http://www.proaqua-gmbh.de/hws/hwsnrw/hws/index.htm> (2006-05-30).
- Lorenz, P.; Skoda, G. (2000): Bemessungsniederschläge kurzer Dauerstufen ($D \leq 12$ Stunden) mit inadäquaten Daten. In: BMLFUW (ed.): Mitteilungsblatt des Hydrographischen Dienstes in Österreich. Nr. 80. Wien: BMLFUW, 1-24.
- Merz, B. (2006): Hochwasserrisiken: Grenzen und Möglichkeiten der Risikoabschätzung. Stuttgart: Schweizerbart.
- Merz, B.; Apel, H.; Gocht, M. (2004): Entwicklung eines probabilistischen Ansatzes zur Bestimmung des Deichversagen durch Überströmen. In: Merz, B. and Apel, H. (eds.): Risiken durch Naturgefahren in Deutschland: Abschlussbericht des BMBF-Verbundprojektes Deutsches Forschungsnetz Naturkatastrophen (DFNK). Potsdam: 77-84. <http://bib.gfz-potsdam.de/edoc/get/5569/0/1c3be7021ddfd1a3affb3b195e3f461b/0401.pdf> (2006-05-30).
- Merz, B.; Kreibich, H.; Thieken, A.; Schmidtke, R. (2004): Estimation uncertainty of direct monetary flood damage to buildings. *Natural Hazards and Earth System Sciences* 4, 153-163.
- Merz, B.; Thieken, A. (2004): Flood Risk Analysis: Concepts and Challenges. *Österreichische Wasser- und Abfallwirtschaft* 56 (3-4), 27-34.
- Messner, F.; Penning-Rowsell, E.; Green, C.; Meyer, V.; Tunstall, S.; van der Veen, A. (2006): Guidelines for Socio-economic Flood Damage Evaluation. Wallingford. http://www.floodsite.net/html/partner_area/project_docs/T9_06_01_Flood_damage_guidelines_D9_1_v1_0_p01.pdf (2006-09-12).
- Metrostav (2002-10-07): Metrostav unambiguously disclaim their responsibility for flood in the Prague Metro. Praha: Metrostav. http://www.metrostav.cz/en/news/press_releases/detail?id=254 (2003-01-16).
- Mock, R. (2001-04-19): Moderne Methoden der Risikobewertung komplexer Systeme. Netzwerk Stadt und Landschaft, Eidgenössische Technische Hochschule Zürich. <http://www.nsl.ethz.ch/index.php/en/content/download/365/2315/file/> (2006-05-30).
- Moore, S.; Chiasson, G. (1996-12-04): The Green Line Flood of 1996. <http://members.aol.com/netransit8/flood/flood.html> (2003-01-16).
- Morgan, M. G.; Henrion, M. (1990): Uncertainty: A Guide to Dealing with Uncertainty in Quantitative Risk and Policy Analysis. Cambridge: Cambridge University Press.
- Müller, M.; Kreibich, H.; Thieken, A.; Merz, B. (2005): Hochwasservorsorge bei Unternehmen – Befragungsergebnisse nach der Flut. In: 5. Forum Katastrophenvorsorge, 14. Oktober 2004 in Mainz: Naturgefahren im Focus der Wissenschaft – Strategien der Sensibilisierung und der räumlichen Vorsorge. Schriftenreihe des DKKV 31: 37-40.
- Nachtnebel, H.-P.; Baumung, S.; Lettl, W. (1993): Abflußprognosemodell für das Einzugsgebiet der Enns und der Steyr (Handbuch). Wien: IWHW-BOKU.
- Nachtnebel, H.-P.; Fürst, J.; Fuchs, M.; Brantner, E. (1999): Abflussprognosemodell Enns: Analyse der bisherigen Ergebnisse. Anpassung der Modellparameter. Endbericht. Wien: IWHW-BOKU.
- Nachtnebel, H.-P. (2003): Integriertes Risikomanagement bei Hochwässern. In: ÖWAV-Symposium: Die Hochwasserkatastrophe 2002: Auf dem Weg zu einem integralen Management von Hochwasserrisiken, 11.-13. März 2003. Wien: ÖWAV, 1-5.
- Naudascher, E. (1992): Hydraulik der Gerinne und Gerinnebauwerke. 2. Auflage. Wien: Springer.

- Neukirchen (1993): Hochwasserrückhalteanlagen für den Wienfluss: Kosten-Nutzen-Untersuchung. Wien: Magistratsabteilung 45 - Wasserbau.
- Neukirchen (1995): Wienfluss: Flussgebietsmodell. Wien: Magistratsabteilung 45 - Wasserbau.
- Neukirchen (2000): Wienfluss: Neugestaltung. Bauabschnitt 01 Einreichprojekt. Wien: Magistratsabteilung 45 - Wasserbau.
- Neukirchen, H.; Rosinak, W.; Schügerl, W.; Rezabek, R. H. (1985): Wienfluss: Wasserbautechnische Variantenuntersuchung. Wien: Magistratsabteilung 45 - Wasserbau.
- Niekamp, O. (2001): Hochwasserschäden. In: Patt, H. (ed.): Hochwasser-Handbuch: Auswirkungen und Schutz. Berlin: Springer, 441-459.
- NOAA Coastal Service Centre (2006-06-13): Glossary.
<http://www.csc.noaa.gov/vata/glossary.html> (2006-10-29).
- Nobilis, F., Lorenz, P. (1997): Flood trends in Austria. In: Leavesley, G. H.; Lins, H. F.; Nobilis, F. et al. (eds.): Destructive Water: Water-Caused Natural Disasters, their Abatement and Control. Wallingford: IAHS Press, 77-81.
- NÖ. LR. (1985): Auswertung der Niederschlagsreihe 1901-1980. Wien: Niederösterreichische Landesregierung. In: Neukirchen (1995): Wienfluss Flussgebietsmodell. Wien: Magistratsabteilung 45 - Wasserbau.
- Pekarek, W. (1998): Analyse der Starkniederschläge im Juli 1997. In: BMLFUW (ed.): Mitteilungsblatt des Hydrographischen Dienstes in Österreich. Nr. 76. Wien: BMLFUW, 47-50.
- Penning-Rowsell, E. C.; Johnson, C. L.; Tunstall, S. M.; Tapsell, S. M.; Morris, J.; Chatterton, J. B.; Coker, A. M.; Green, C. H. (2003): The benefits of flood and coastal defence: techniques and data for 2003. Enfield: Middlesex University Flood Hazard Research Centre.
- Petak, W. J.; Atkisson, A. A. (1982): Natural Hazard Risk Assessment and Public Policy: Anticipating the Unexpected. New York: Springer.
- Petraschek, A. (2004a): Gefahren- und Risikozonierung unter Berücksichtigung der Raumplanung in der Schweiz. In: ÖWAV-Symposium: Raumordnung und Hochwasserschutz, 21.-22. Juni 2004. Wien: ÖWAV, 1-5.
- Petraschek, A. (2004b): Beeinflussung der Risiken und des Schadenverlaufs. In: OoCC (Organe consultatif sur les changements climatiques, Beratendes Organ für Fragen der Klimaänderung): Extremereignisse und Klimaänderung. Bern, 34-37.
http://www.proclim.ch/Products/Extremereignisse03/PDF_D/1-06.pdf (2006-11-16).
- Plate, E. J. (1992): Stochastic design in hydraulics: Concepts for a broader application. Proceedings. In: Sixth IAHR Internat. Symposium on Stochastic Hydraulics. Taipei, 1-9.
- Plate, E. J. (1993): Statistik und angewandte Wahrscheinlichkeitslehre für Bauingenieure. Berlin: Ernst & Sohn.
- Plate, E. J. (2002): Flood Risk and Flood Management. *Journal of Hydrology* 267, 2-11.
- Plate, E. J.; Merz, B. (eds. 2001): Naturkatastrophen: Ursachen, Auswirkungen, Vorsorge. Stuttgart: Schweizerbart.
- Puwein, W.; Scheiblecker, M.; Sinabell, F.; Smeral, E. (2003): Volkswirtschaftliche Stellungnahme zu den Schäden des Hochwassers vom August 2002. In: Habersack, H.; Moser, A. (eds.): Plattform Hochwasser: Ereignisdokumentation Hochwasser August 2002. Wien: ZENAR – BOKU, 117-122. http://zenar.boku.ac.at/PDF-Files/Hochwasser_2002_Gesamt.PDF (2006-05-30).

- Rodriguez, R. + Zeisler; geomer GmbH; PlanEVAL; Haskoning (2001): Übersichtskarten der Überschwemmungsgefährdung und der möglichen Vermögensschäden am Rhein. Abschlußbericht: Vorgehensweise zur Ermittlung der hochwassergefährdeten Flächen, Vorgehensweise zur Ermittlung der möglichen Vermögensschäden. Wiesbaden: IKSR.
- Sackl, B. (1995): Hydrologische und hydraulische Berechnungen: RHB – Gleisdorf. In: Turk, A. (1995): Hochwasserschutz Stadt Gleisdorf und Umgebung: Detailprojekt 1995. Gleisdorf
- Saurer, B.; Baumann, N. (1992): Hochwasserrückhalteanlagen: Planung, Bau und Betrieb. Steiermark-Information 16. Graz: Amt der Steiermärkischen Landesregierung, Landesbaudirektion, Fachabteilung III a, Wasserwirtschaft.
- Sayers, P.; Hall, J.; Meadowcroft, I. (2002): Towards risk-based flood hazard management in the UK. *Civil Engineering* 150 (5), 36-42.
- Schimpf, H. (1970): Untersuchungen über das Auftreten beachtlicher Niederschläge in Österreich. *Österreichische Wasserwirtschaft* 22 (5-6), 121-125.
- Schmid, B. (1989): Zum Problem der stationären Fließbeiwertrechnung: Grundlagen, Methodik und Anwendung am Beispiel des Donauabschnittes zwischen Bärndorf und Tulln. In: BMLF (ed.): Mitteilungsblatt des Hydrographischen Dienstes in Österreich. Nr. 60. Wien: BMLF, 1-8.
- Schmidtke, R. F. (1981): Monetäre Bewertung wasserwirtschaftlicher Maßnahmen: Systematik der volkswirtschaftlichen Nutzenermittlung. München: Bayerisches Landesamt für Wasserwirtschaft.
- Schmidtke, R. F. (1982): Kompendium Nutzen-Kosten-Untersuchungen in der Wasserwirtschaft. Wien: Universität für Bodenkultur.
- Schmidtke, R. F. (2000): Klimaveränderung – sozioökonomische Konsequenzen. Karlsruhe: Landesanstalt für Umwelt, Messungen und Naturschutz Baden-Württemberg (LUBW), 269-276. <http://www.kliwa.de/download/symp2000/vortrag23.pdf> (2006-05-30).
- Sivapalan, M.; Blöschl, G. (1998): Transformation of point rainfall to areal rainfall: Intensity-duration-frequency curves. *Journal of Hydrology* 204, 150-167.
- Skoda, G.; Weilguni, V.; Haiden, T. (2003): Konvektive Starkniederschläge. In: BMLFUW (ed.): Mitteilungsblatt des Hydrographischen Dienstes in Österreich. Nr. 82. Wien: BMLFUW, 83-98.
- Slovic, P. (2001): The risk game. *Journal of Hazardous Materials* 86, 17-24.
- Smith, K; Ward, R. (1998): Floods - Physical Processes and Human Impacts. Chichester: John Wiley & Sons.
- Society for Risk Analysis (2004-12-01): Glossary of Risk Analysis Terms. http://sra.org/resources_glossary.php (2006-10-29).
- Sönnichsen (2003): Hochwasser-Aktionsplan Werre: Erläuterungsbereich. Minden: Staatliches Umweltamt. <http://www.stua-mi.nrw.de/hwap/Erlaeuterungsbericht-HWAP-Werre.pdf> (2006-05-30).
- Stapel, S.; Pasanen, J.; Reinecke, S. (2004): Kaufkraftparitäten und abgeleitete Wirtschaftsindikatoren für EU, Beitrittskandidaten und EFTA. Statistik kurz gefasst: Wirtschaft und Finanzen 37/2004. Luxembourg: Eurostat. http://www.eds-destatis.de/de/downloads/sif/nj_04_37.pdf (2006-05-30).
- Statistik Austria (2005a): Ausgewählte Kennziffern der Volkswirtschaftlichen Gesamtrechnung. Wien: Statistik Austria. http://www.statistik.at/statistische_uebersichten/deutsch/pdf/k00t_4.pdf (2006-05-30).
- Statistik Austria (2005b): Arbeitsstättenzählung vom 15. Mai 2001: Gemeinde Gleisdorf. Wien: Statistik Austria. <http://www.statistik.at/blickgem/az1/g61713.pdf> (2006-05-30).

- Statistik Austria (2005c): Wirtschaftskennzahlen der Unternehmen aus der Leistungs- und Strukturstatistik 2003. Wien: Statistik Austria.
http://www.statistik.at/unternehmen/lse3_05.pdf (2006-05-30).
- Stedinger, J.; Vogel, R.; Foufoula-Georgiou, E. (1992): Frequency analysis in Extreme Events. In: Maidment, D. R. (ed): Handbook of Hydrology. McGraw-Hill, 18.1-18.66.
- Steinhauser, F.; Eckel, O.; Sauberer, F. (1957): Klima und Bioklima von Wien: Eine Übersicht mit besonderer Berücksichtigung der Bedürfnisse der Stadtplanung und des Bauwesens. II. Teil. Wien: Österreichische Gesellschaft für Meteorologie.
- Stubenvoll, H. (1994): Hydrologisches Gutachten: Raab bis Rabnitzbach in Gleisdorf. Graz: Amt der Steiermärkischen Landesregierung, Fachabteilung IIIa, Wasserwirtschaft. In: Sackl, B. (1995): Hydrologische und hydraulische Berechnungen: RHB – Gleisdorf. Graz.
- Swiss National Bank (2005): Devisenkurse. Zürich.
http://www.snb.ch/d/publikationen/monatsheft/aktuelle_publication/pdf/statmon_DF/G1_Devisenkurse.pdf (2005-11-28).
- Thaller, G. (2002-10-25): Hochwasserschutz an der Raab (Gleisdorf, Albersdorf-Prebuch, Ludersdorf-Wilfersdorf). Graz: Amt der Steiermärkischen Landesregierung, Abteilung 19 - Wasser und Abfallwirtschaft.
<http://www.wasserwirtschaft.steiermark.at/cms/beitrag/10007278/4579558/> (2005-03-02).
- Tibet, W.; Paar, A. (2005): Hochwasser vom 21.8.2005: Aktenvermerk 19.9.2005. Gleisdorf: Stadtgemeinde Gleisdorf, Wirtschaftshof.
- Toda, K.; Inoue, K. (2002): Characteristics of recent urban floods in Japan and countermeasures against them. In: Wu, B. S.; Wang, Z. Y.; Wang, G. Q. et al. (eds.): Flood Defence '2002. Volume II. New York: Science Press, 1365-1371.
- Tung, Y.-K. (2002-08-30): Risk-based design of flood defence systems. In: Second International Symposium on Flood Defence (ISFD '2002), 10-13 September 2002, Beijing, 71-81. <http://www.cws.net.cn/cwsnet/meeting-fanghong/v10107.pdf> (2006-11-19).
- Turk, A. (1996): Hochwasserschutz Stadt Gleisdorf und Umgebung: Detailprojekt 1995. Gleisdorf: Amt der Steiermärkischen Landesregierung, Fachabteilung IIIa, Wasserwirtschaft.
- Turk, A. (1997): Hochwasserschutz Stadt Gleisdorf und Umgebung: Detailprojekt 1997. Gleisdorf: Amt der Steiermärkischen Landesregierung, Fachabteilung IIIa, Wasserwirtschaft.
- UNDHA (1992): Internationally Agreed Glossary of Basic Terms Related to Disaster Management. Geneva: UN DHA.
- USEPA (2006-03-08): Glossary of IRIS Terms. <http://www.epa.gov/iris/gloss8.htm> (2006-10-29).
- van Manen, S. E.; Brinkhuis, M. (2005): Quantitative flood risk assessment for Polders. *Reliability Engineering and System Safety* 90, 229-237.
- Vrijling, J. K. (2001): Probabilistic design of water defence systems in The Netherlands. *Reliability Engineering and System Safety* 74, 337-344.
- Vrouwenvelder, T.; Lovegrove, R.; Holicky, M.; Tanner, P.; Canisius, G. (2001): Risk Assessment and Risk Communication in Civil Engineering. In: International Conference of Safety, Risk and Reliability Trends in Engineering, 21-23 March 2001. Malta, 885-890.

10 Index of tables

Table 1.1: Typology of flood damages with examples (Messner et al. 2006, Penning-Rowsell et al. 2003, Smith and Ward 1998)	17
Table 1.2: Aims of this dissertation in the context of flood risk management	25
Table 1.3: Objectives for applying the methodology to the case studies	27
Table 3.1: Maximum observed daily precipitation (BMLFUW 2005b)	36
Table 3.2: Scenario overview	38
Table 3.3: Rain gauges used for extreme value statistics	40
Table 3.4: Selected hydrologic scenarios	43
Table 3.5: Flood intensity classes for loss estimation (BWW et al. 1997)	52
Table 3.6: Loss functions for the flood intensity classes (in €)	52
Table 3.7: Ex-ante (a) and ex-post (p) building losses for accuracy evaluation of the applied loss functions	53
Table 3.8: Risk Matrix (Adapted from BUWAL 1999b)	55
Table 4.1: Rainfall intensity patterns of the 21 analysed events	57
Table 4.2: Extrapolated 100 and 1,000-year point design rainfall depths in mm	59
Table 4.3: Overview of the modelled hydrographs of River Raab	61
Table 4.4: Selected rainfall runoff events for hydrodynamic modelling	65
Table 4.5: Inundation process with increasing flow at Raab River	66
Table 4.6: Cross section at km 65.915: Flows under the current conditions (2005, row 1) and flow changes due to different vegetation scenarios	69
Table 4.7: Number of affected buildings	72
Table 4.8: Risk matrix: Cumulated direct losses to buildings, estimated by two methods	73
Table 4.9: Average direct losses to buildings, estimated by two methods	73
Table 4.10: Flood impacts and direct losses to roads and railway lines	74
Table 4.11: Input data for expected annual loss calculation	76
Table 4.12: Expected annual losses derived by different interpolation methods	76
Table 4.13: Simplified benefit-cost analysis for the flood protection system	77
Table 4.14: Failure scenarios and expected annual losses	79
Table 5.1: Maximum observed daily precipitation from west to east (BMLFUW 2005b)	82
Table 5.2: Scenario overview	86
Table 5.3: Rainfall runoff data for the rural and the urban Wien River catchment obtained by modelling and approximations*	91
Table 5.4: Review of subway inundations (Compton et al. 2004)	98
Table 5.5: Direct losses to subway systems from the review, from building costs and from damage ratios (Compton et al. 2004)	99
Table 6.1: Mean values and coefficients of variation (CoV) of sampled design rainfall depths and generated peak flows	101

Table 6.2: Peak flow frequencies and standard errors from flow statistics of the 1906-1997 series at gauge Kennedybrücke before the retention schemes were upgraded (pre 1998)	101
Table 6.3: Event probabilities, system reliability and frequency of failure per year. The upper and lower figures base on two interpolation methods	105
Table 6.4: Intervals of expected annual losses in 1,000 € for the at-grade track and for the tunnelled subway stretches. The upper and lower figures base on two interpolation methods	107

11 Index of figures

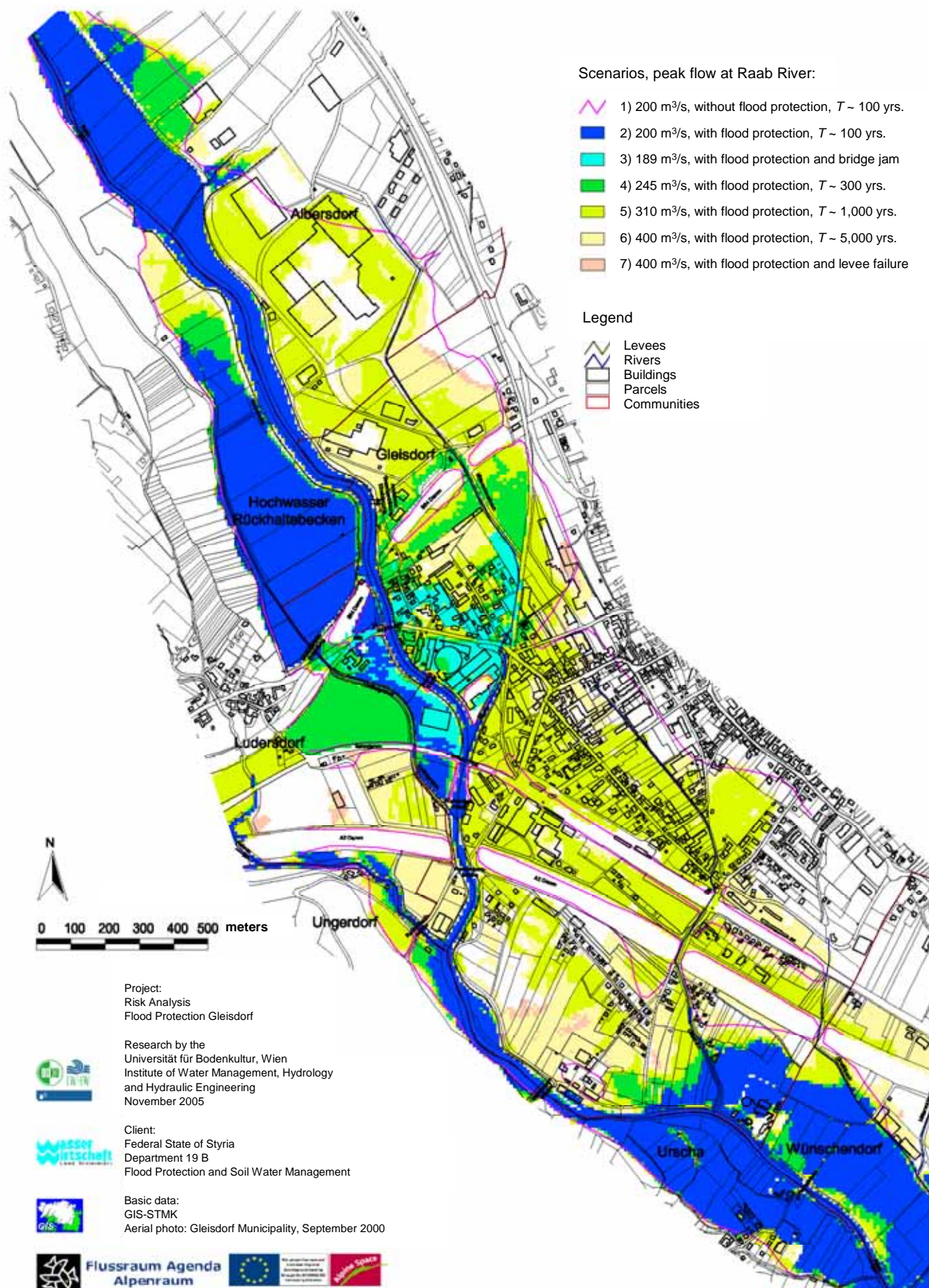
Figure 1.1: One-hour design rainfall data for Wien, Hohe Warte	16
Figure 1.2: Safety targets for societal risks in The Netherlands compared to a specific hazard or activity (Adapted from Faber and Steward 2003)	20
Figure 1.3: Main focus of this dissertation in the context of risk assessment (Adapted from Mock 2001)	26
Figure 1.4: Overview of the objectives of this dissertation	26
Figure 2.1: Flood intensity classes for loss estimation and hazard zones defined by the inundation depth and the flow velocity	30
Figure 2.2: Definition and modelling of scenarios in the deterministic approach (Adapted from Fuchs 2005)	31
Figure 2.3: Modelling of flood losses in the stochastic approach	32
Figure 2.4: Example for determining P_F from the basic random variables r and s	33
Figure 3.1: Raab River basin and gauging stations (BMLFUW 2005b)	35
Figure 3.2: The Gleisdorf model domain, the former 100-year floodplain and the technical flood protection system	36
Figure 3.3: Areal reduction factors ARF for a large and a moderate rainfall reduction	41
Figure 3.4: 10-metre elevation grid and river cross sections from the 2005 survey and from planning documents	46
Figure 3.5: 1D river (l.), links with 2D cells and breach location.....	47
Figure 3.6: Weirs in Gleisdorf. The downstream Gliederwehr (l.) and the upstream Felberwehr during low flow in January 2005.....	48
Figure 3.7: Cross sections for analysing vegetation scenarios	49
Figure 3.8: Loss estimation procedure	51
Figure 4.1: Cumulative and partial distribution of rainfall intensities over the rainfall duration	58
Figure 4.2: Seven-day antecedent rainfall of 21 analysed events.....	58
Figure 4.3: Observed hourly rainfall, seven-days antecedent rain and the definition of the antecedent soil moisture conditions 'Wet' and 'Dry'	58
Figure 4.4: Lag time of 21 analysed flood events.....	59
Figure 4.5: Average extrapolated 100 and 1,000-year point design rainfall depths	60
Figure 4.6: Six-hour point- and areal design rainfall depths at gauge Laßnitzhöhe	61
Figure 4.7: Peak flows at Raab River for different rainfall durations	62
Figure 4.8: Data for probability estimation of Raab River peak flows.....	63
Figure 4.9: Annual peak flow statistics for gauge Takern II.....	64
Figure 4.10: Raab and Rabnitzbach hydrographs of selected rainfall runoff events.....	65
Figure 4.11: Inundations without (l.) and with jammed bridges. The exposed B 65 Bridge is marked (r.).....	67
Figure 4.12: Cross section at km 65.915: Homogenous flow subdivisions with higher plants and areas without higher vegetation	69

Figure 4.13: Discharge at the Raab River and the inflow into the retention basin over the lateral weir according to the 1995 project (Sackl 1995, Turk 1996) and to the scenario results.....	70
Figure 4.14: Frequency of cumulated direct losses, estimated by two methods.....	72
Figure 4.15 Interpolation and numeric integration of expected annual losses: the frequency of losses a), the losses weighted by the probability b) and the cumulated weighted losses c)	77
Figure 4.16: Expected annual losses split up according to average return intervals	78
Figure 5.1: Wien River basin, gauging stations and land cover (BMLFUW 2005b)	81
Figure 5.2: Vienna subway system, the model domain at the Wien River and the mobile stop log barriers (Map: MetroPlanet 2002)	82
Figure 5.3: Schematic Wien River cross section in the model domain (Adapted from Neukirchen 1993).....	83
Figure 5.4: Wien River upstream the gauge Kennedybrücke during dry conditions and the 1975 flood (Photos: MA 45 – Wasserbau & BMLFUW)	84
Figure 5.5: System model of subway flooding at Wien River	86
Figure 5.6: Flowchart of the stochastic algorithm.....	88
Figure 5.7: Six-hour point- and areal design rainfall in the Wien River basin.....	90
Figure 5.8: Six-hour point- and areal design rainfall data in the Wien River basin and the definitions for rainfall sampling.....	90
Figure 5.9: Sampled relative frequency of six-hour areal rainfall for several average return intervals (Frequency curves not in scale).....	91
Figure 5.10: Annual peak flow series at gauge Kennedybrücke (Data Source: G. Schenekl, personnel comment, 2006-02-27)	92
Figure 5.11: Deterministic hydraulic model with a water surface profile at 300 m ³ /s	93
Figure 6.1: Peak flow statistics at gauge Kennedybrücke from the 1906-1997 series.....	102
Figure 6.2: Sampled peak flow frequency from flow statistics and rainfall runoff modelling for the states before and after retention basin upgrading (frequency plots not in scale)....	102
Figure 6.3: Sampled relative frequencies of the basic random variables Manning's n and the bridge drag coefficient C_D	103
Figure 6.4: Distribution of the resistance of the hydraulic system in terms of the bankfull discharge and the flow related to structural floodwall failure.....	103
Figure 6.5: Distributed water levels at the right bank. Median and confidence intervals for 100- and 1,000-year events after the retention schemes were upgraded.....	104
Figure 6.6: Results of the event tree analysis for the state after upgrading the retention basins.....	105

12 Appendix: Inundation maps of case study 1

For the Gleisdorf case study, the following six maps show the inundation extends and the maximum depths of the investigated scenarios. The first map compiles the affected areas, and the following maps display the maximum flow depth in each scenario.

Inundation areas of the modelled scenarios



Inundation map, scenario 2a

Assumptions for scenario 2a:

No structural and operational failure

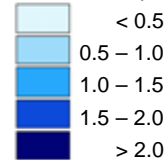
Flows:

Raab 200 m³/s (= design magnitude)

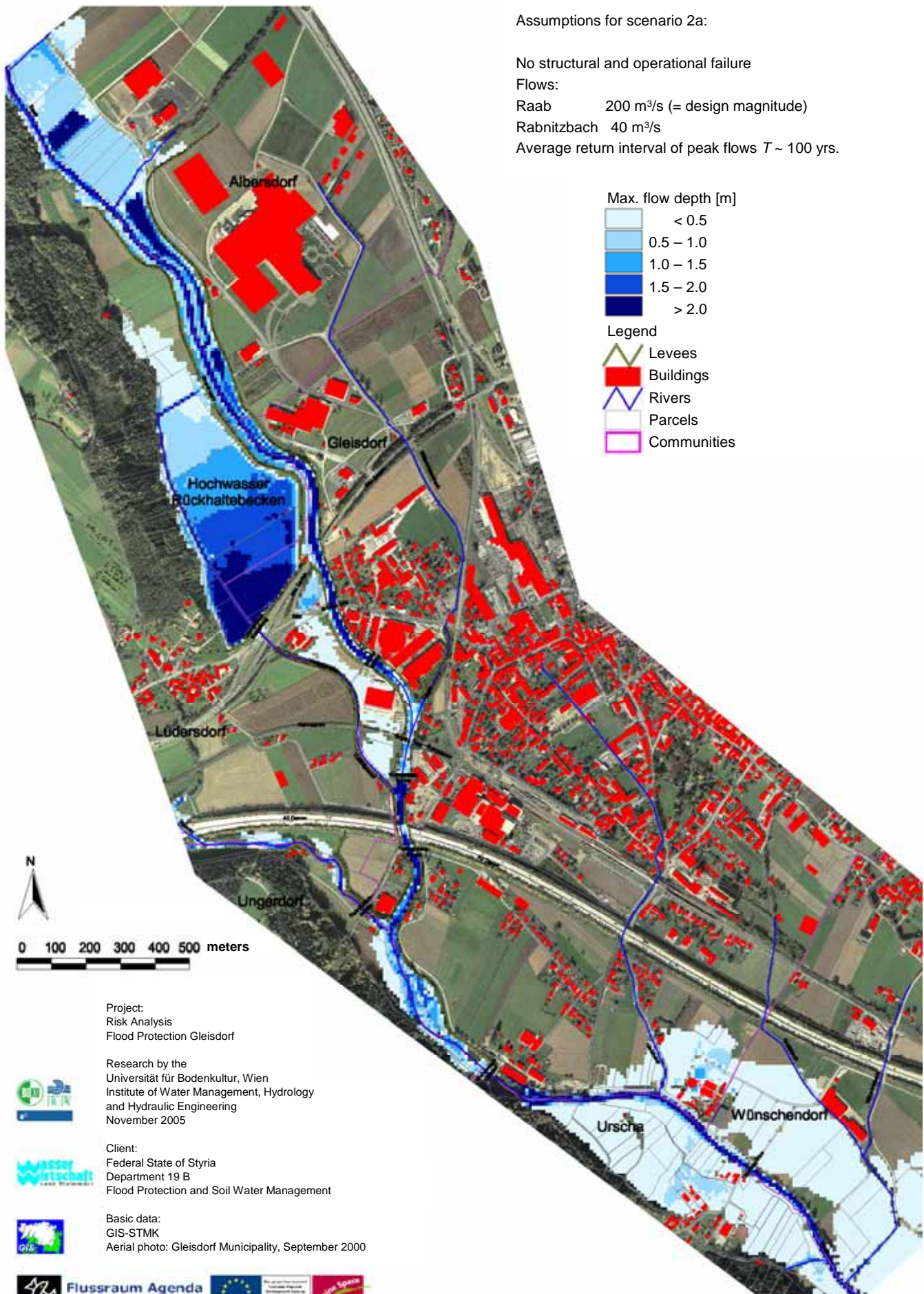
Rabnitzbach 40 m³/s

Average return interval of peak flows $T \sim 100$ yrs.

Max. flow depth [m]



Legend



Project:
Risk Analysis
Flood Protection Gleisdorf



Research by the
Universität für Bodenkultur, Wien
Institute of Water Management, Hydrology
and Hydraulic Engineering
November 2005



Client:
Federal State of Styria
Department 19 B
Flood Protection and Soil Water Management



Basic data:
GIS-STMK
Aerial photo: Gleisdorf Municipality, September 2000



Flussraum Agenda
Alpenraum



Inundation map, scenario 3

Assumptions for scenario 3:

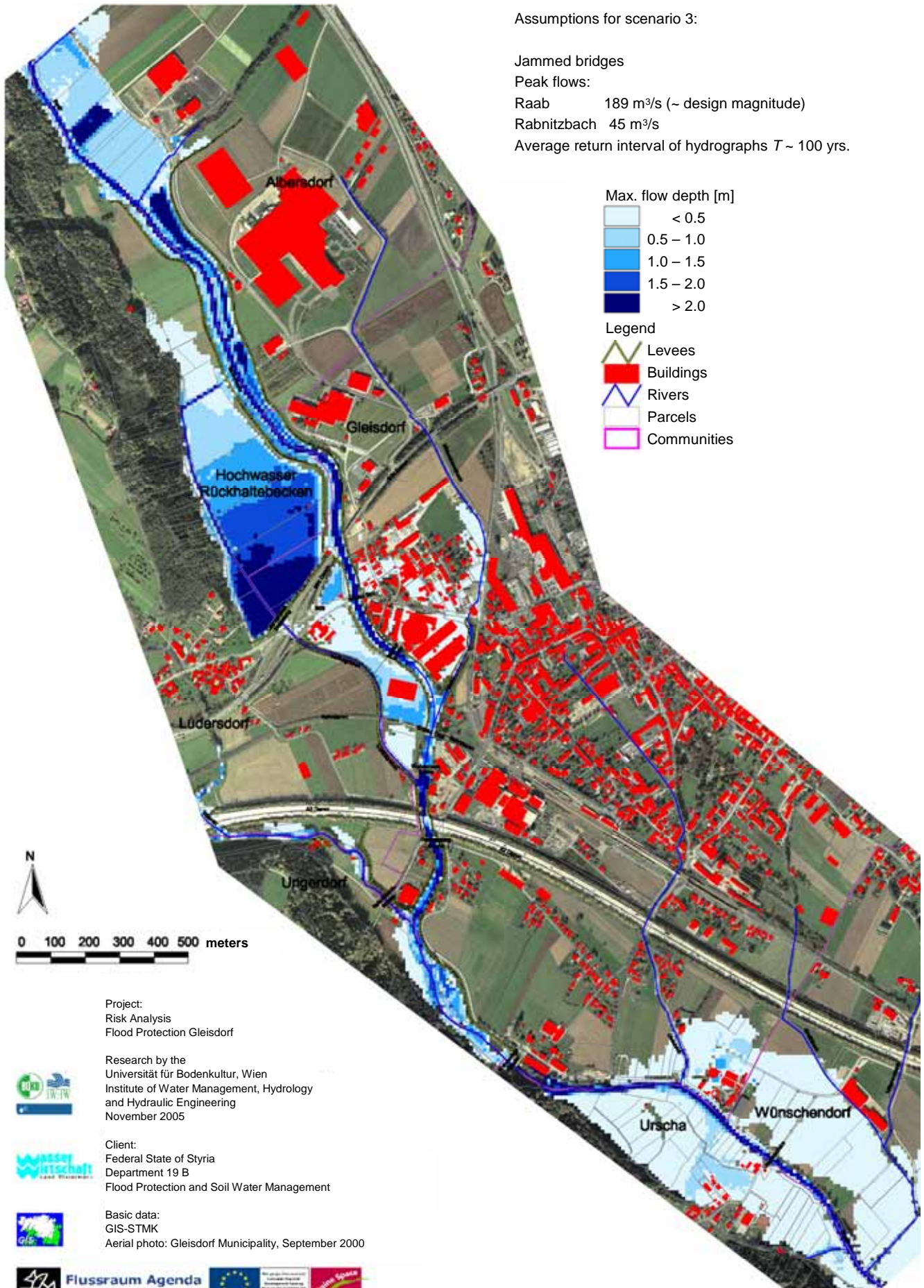
Jammed bridges

Peak flows:

Raab 189 m³/s (~ design magnitude)

Rabnitzbach 45 m³/s

Average return interval of hydrographs $T \sim 100$ yrs.



Inundation map, scenario 4

Assumptions for scenario 4:

No structural and operational failure

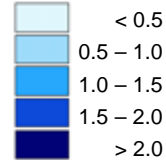
Peak flows:

Raab 245 m³/s (~ 1.25-fold design magnitude)

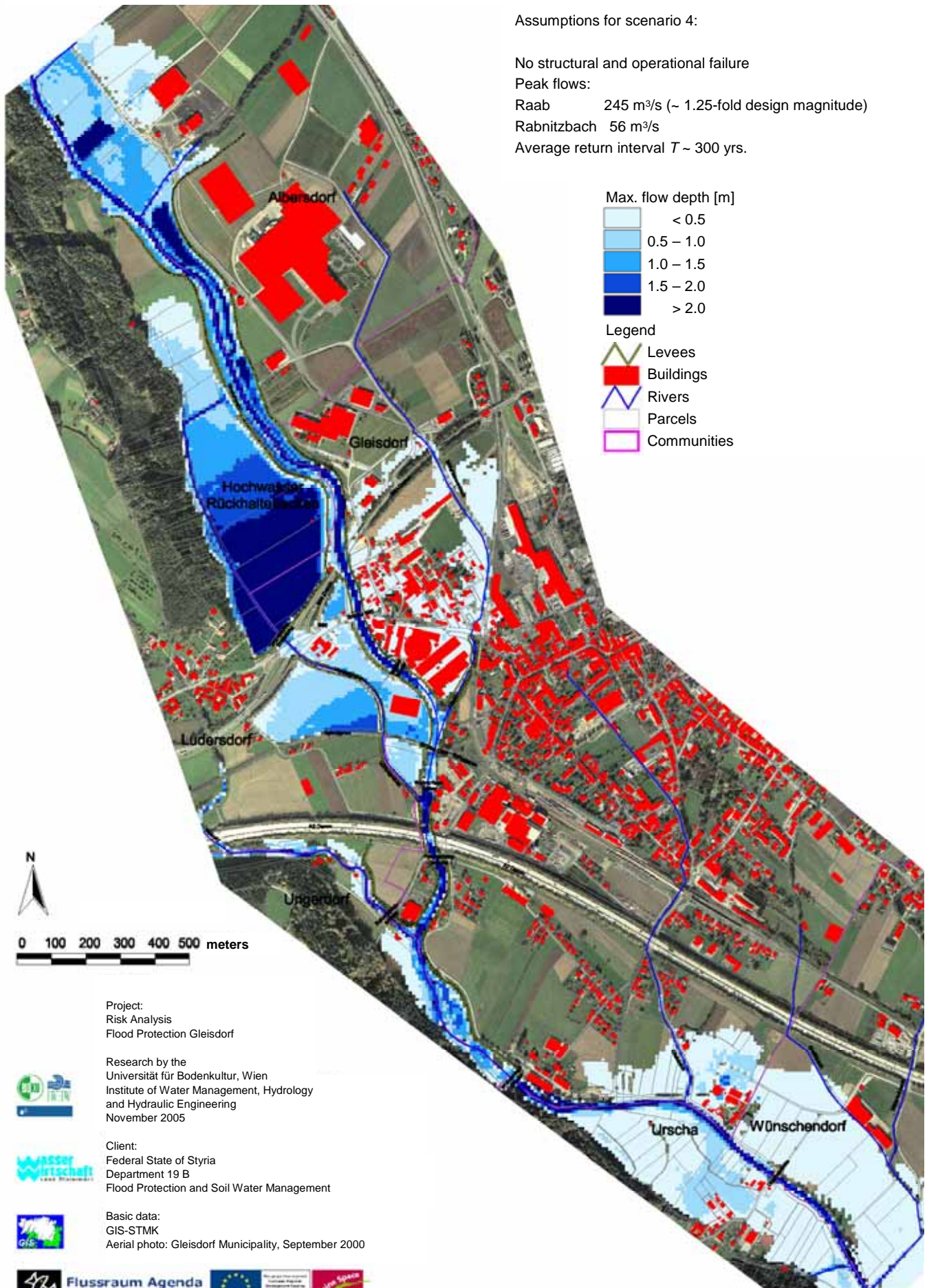
Rabnitzbach 56 m³/s

Average return interval $T \sim 300$ yrs.

Max. flow depth [m]



Legend



Project:
Risk Analysis
Flood Protection Gleisdorf



Research by the
Universität für Bodenkultur, Wien
Institute of Water Management, Hydrology
and Hydraulic Engineering
November 2005



Client:
Federal State of Styria
Department 19 B
Flood Protection and Soil Water Management



Basic data:
GIS-STMK
Aerial photo: Gleisdorf Municipality, September 2000



Flussraum Agenda
Alpenraum



European Union
Regional Development
Funding the Future



Inundation map, scenario 5

Assumptions for scenario 5:

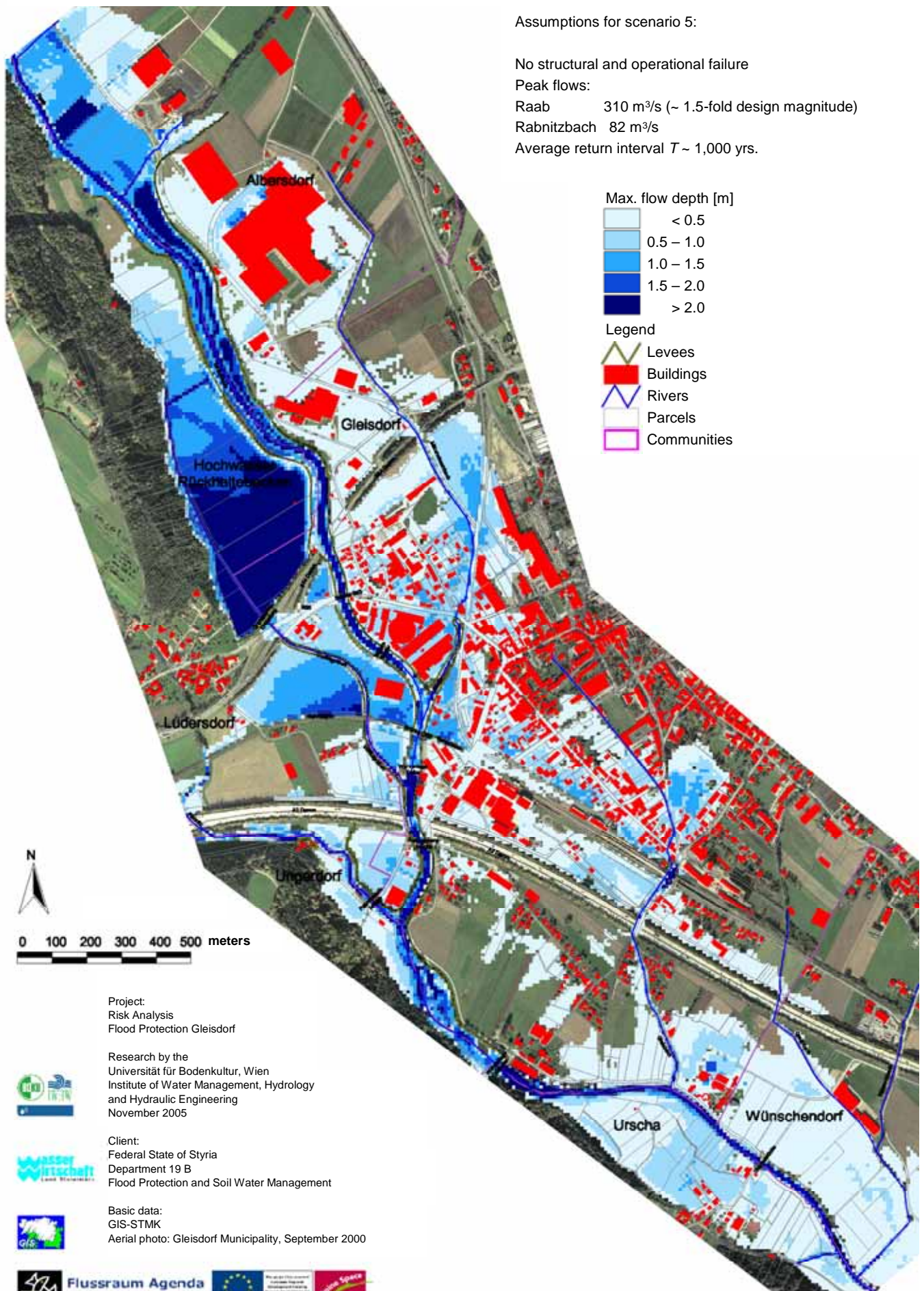
No structural and operational failure

Peak flows:

Raab 310 m³/s (~ 1.5-fold design magnitude)

Rabnitzbach 82 m³/s

Average return interval $T \sim 1,000$ yrs.



Project:
Risk Analysis
Flood Protection Gleisdorf



Research by the
Universität für Bodenkultur, Wien
Institute of Water Management, Hydrology
and Hydraulic Engineering
November 2005



Client:
Federal State of Styria
Department 19 B
Flood Protection and Soil Water Management



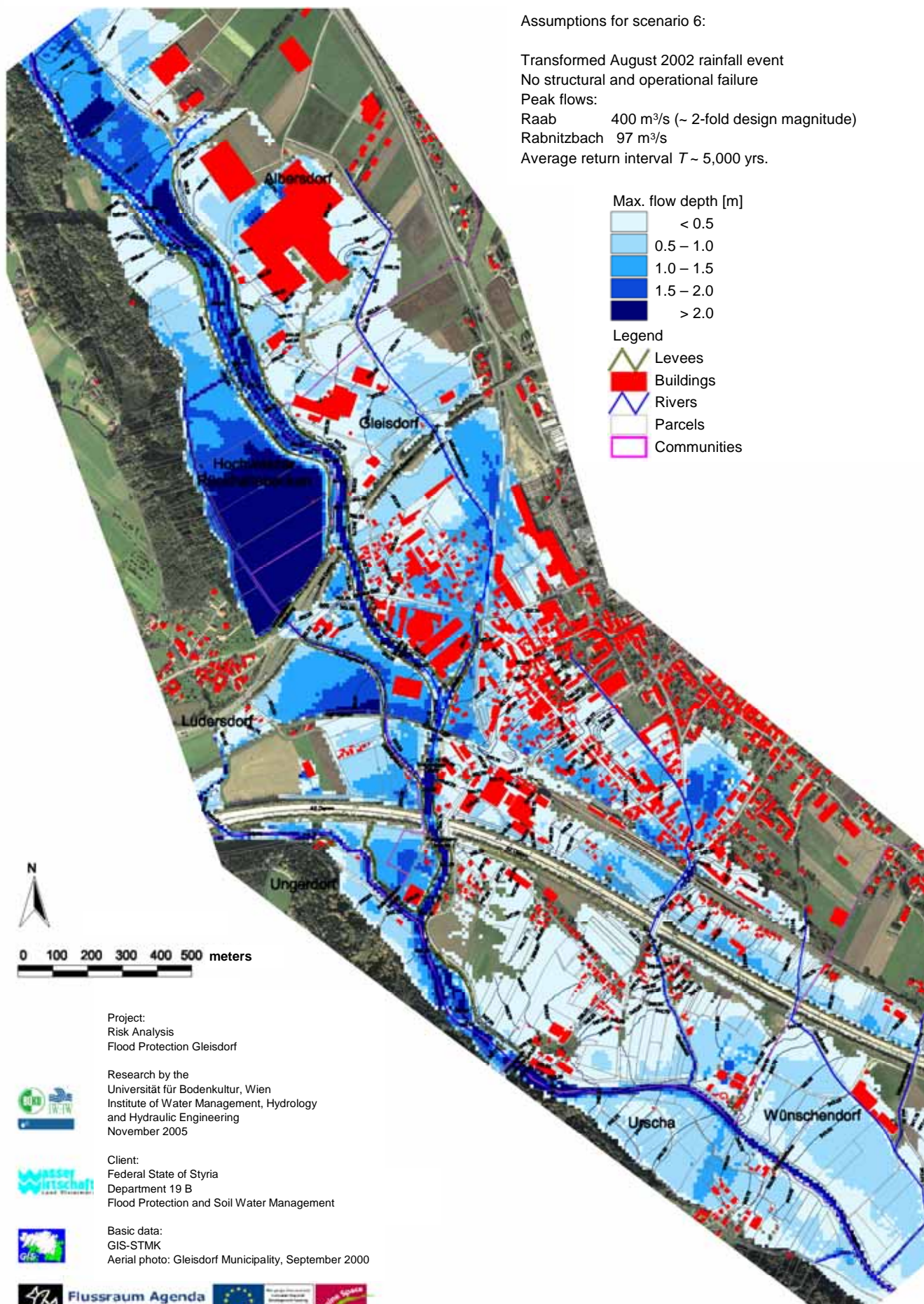
Basic data:
GIS-STMK
Aerial photo: Gleisdorf Municipality, September 2000



Flussraum Agenda
Alpenraum



Inundation map, scenario 6



13 Table of abbreviations and variables

1D	One-dimensional surface water flow model
2D	Two-dimensional surface water flow model
A	Area, specified in m ² or km ²
BMLF	Bundesministerium für Land- und Forstwirtschaft (Federal Ministry of Agriculture and Forestry), since 2000: BMLFUW
BMLFUW	Bundesministerium für Land- und Forstwirtschaft, Umwelt und Wasserwirtschaft (Federal Ministry of Agriculture, Forestry, Environment and Water Management)
BOKU	Universität für Bodenkultur Wien (University of Natural Resources and Applied Life Sciences, Vienna)
BRP	Bundesamt für Raumplanung (Swiss Federal Office for Urban and Regional Planning)
BUWAL	Bundesamt für Umwelt, Wald und Landschaft (Swiss Federal Office for Environment, Forestry and Landscape)
BWG	Bundesamt für Wasser und Geologie (Swiss Federal Office for Water and Geology)
BWW	Bundesamt für Wasserwirtschaft (Swiss Federal Office for Water Management)
CDM	Camp Dresser & McKee Incorporated
CoV	Coefficient of variation
c_s	Skewness of a sample
CUR	Civieltechnisch Centrum Uitvoering Research en Regelgeving (Centre for Civil Engineering Research and Codes)
D	Duration of a rain event or precipitation aggregate
DHI	Danish Hydraulic Institute
DIN	Deutsches Institut für Normung (German Institute for Standardization)
DVWK	Deutscher Verband für Wasserwirtschaft und Kulturbau (German Association for Water, Wastewater and Waste)
DWD	Deutsche Wetterdienst (German National Meteorological Service)
$E(L)$	Expected value of losses
EOEA	Executive Office of Environmental Affairs
$f(.)$	Function of ...
GVL	Gebäudeversicherung des Kantons Luzern (Building Insurance of the Canton of Lucerne in Switzerland)
H	Flow depth
HEC	Hydrologic Engineering Center
HQ_T	T -year flood
IAN	Institut für Alpine Naturgefahren
IKSR	Internationale Kommission zum Schutze des Rheins (International Commission for the Protection of the Rhine)
IRIS	Integrated Risk Information System

IWHW	Institut für Wasserwirtschaft, Hydrologie und konstruktiven Wasserbau (Institute of Water Management, Hydrology and Hydraulic Engineering at BOKU)
K	Statistic frequency factor or Conveyance
k_{St}	$= 1/n$ Frictional loss coefficient according to Strickler, in $m^{1/3}/s$
LFI-RWTH	Lehr- und Forschungsgebiet Ingenieurhydrologie-Rheinisch-Westfälische Technische Hochschule (Section of Engineering Hydrology at Aachen University)
$L(x), L_j$	Consequences, losses due to the hazard magnitude x , or the scenario j
MBTA	Massachusetts Bay Transportation Authority
n	Sample size or frictional loss coefficient according to Manning in $s/m^{1/3}$. $n = 1/k_{St}$
NOAA	National Oceanic and Atmospheric Administration
NÖ LR	Niederösterreichische Landesregierung (Provincial Government of Lower Austria)
NRW	Nordrhein-Westfalen
O_i	Object at risk, number i
P	Probability or precipitation depth in mm
P_F	Probability of failure per year
P_T	Precipitation depth in mm assigned to the average return interval T
P_u	Probability of a magnitude being not exceeded
$p(x)$	Probability density function of a hazard with the magnitude x occurring in a year
Q	Flow in m^3/s
Q_{max}	Peak flow in m^3/s
Q_T	Flow in m^3/s assigned to the average return interval T
R	Hydraulic Radius
R	$= 1 - P_F$. Reliability: Probability that a system does not fail within one year
r	$= x^*$. Design magnitude of the natural hazard protection system
SF	Specific force
S_j	Scenario number j
S_f	Frictional slope
s	$= x$. A specified magnitude of the hazard
s_E	Standard error
s_x, s_y	Standard deviation of a sample
T	Average return interval of an extreme event, specified in years
UNDHA	United Nations Department of Humanitarian Affairs
USEPA	United States Environmental Protection Agency
V, v	Flow velocity
W	Water level in m above a reference altitude, e.g. sea level
W_j	Scenario weight according to its occurrence probability

W_T	Water level in m above a reference level assigned to the average return interval T
X	Parameter describing possible natural hazard
x	A specified magnitude of the hazard X
x^*	Design magnitude of the natural hazard protection system
Y	Depth
Z	Channel invert elevation in m above a reference altitude, e.g. sea level
ZAMG	Zentralanstalt für Meteorologie und Geodynamik (Central Institute for Meteorology and Geodynamics)
z	= $r-s$. Safety margin
ZENAR	Zentrum für Naturgefahren und Risikomanagement (Centre of Natural Hazards and Riskmanagement) at BOKU

14 Curriculum vitae



Personal data

Name Rudolf Faber
 Birth November 16, 1973, Salzburg, Austria
 Nationality Austria
 University University of Natural Resources and Applied Life Sciences Vienna
 e-mail [rudolf.faber\(at\)boku.ac.at](mailto:rudolf.faber(at)boku.ac.at)
 Education 2001-2006: Doctoral studies on flood risks

2006: Guest at the National Institute of Water and Atmospheric Research, Christchurch, New Zealand

1993-2001: Diploma studies of Land and Water Management and Engineering at BOKU, awarding the degree Diplom - Ingenieur

1998: One semester Erasmus study exchange at Chalmers Technical University, Gothenburg, Sweden

1992: School leaving examination (Matura), Salzburg

1980-1992: Elementary and secondary school, Salzburg

Professional experience 2001 till 2006: Research assistant at BOKU – IWHW Vienna, working on current and completed projects:

Preparatory study on the water management in inundation areas, Upper Austria

Risk analysis: Flood protection Gleisdorf, Austrian state of Styria

URBEM Urban River Basin Enhancement Methods. Project with 12 European partners coordinated by HR Wallingford. Funded by the EC under the 5th Framework Programme

FloodRisk – Evaluation of the Danube River flood protection in Austria

FloodRisk – Evaluation of the proposed modifications on the Austrian flood hazard zoning guidelines

The Management of Catastrophic Risk with a focus on Urban Disaster Risk: Flood Risk Assessment and Management in Urban Areas. Joint research with IIASA-RMS

2001: BOKU, Institute of Sanitary Engineering and Water Pollution Control: Assistant on EU-Life project on scale modelling and real time monitoring of Danube River bank filtration for water provision purposes in Vienna

1996-2000: Internships in several public and private consulting and management organizations in the water sector in Salzburg

1992-1993: Civilian service as hospital nurse assistance at the Salzburg State Hospital

Vienna December 2006